IMPROVEMENT OF ADHESION BETWEEN POLYURETHANE COMPOSITES AND TOP COAT BY MEANS OF THE IN-MOLD COATING WITH VINYL ESTER METHOD

NATCHA PRAKYMORAMAS

A THESIS SUBMITTED IN PARTIAL FULFILLMENT

OF THE REQUIREMENT FOR THE DEGREE OF

MASTER OF ENGINEERING IN AUTOMOTIVE ENGINEERING

(INTERNATIONAL PROGRAM)

INTERNATIONAL COLLEGE

KING MONGKUT'S INSTITUTE OF TECHNOLOGY LADKRABANG

2011

KMITL-2011-IC-M-004-003

TOPIC OF THESIS	Improvement of Adhesion Between Polyurethane Composites and Top Coat by Means of The In-Mold Coating with Vinyl Ester Method
NAME OF STUDENT	Natcha Prakymoramas
STUDENT CODE	50061902
DEGREE	Master of Engineering
MAJOR	Automotive Engineering (International Program)
ADVISOR	Asst. Prof. Dr. Surat Areerat
CO-ADVISOR	Dr. Wuttipong Ruangseesantivanon
CO-ADVISOR	Prof. Dr. Isao Satoh
CO-ADVISOR	Assoc. Prof. Dr. Takushi Saito

ABSTRACT

This study is aimed to improve the adhesion between polyurethane composite and top coat by in-mold coating of vinyl ester onto the mold surface prior to the molding of polyurethane composite. Later this treated polyurethane composite is over coated with the top coat. By this manner, the surface energy of polyurethane composite is increased and hence the adhesion between polyurethane composite and top coat becomes improved, in one step. In the preliminary, the effect of processing temperature on heat distortion temperature, flexural propreties and microstructure was investigated. It was found that 60 $^{\circ}$C was the optimum mold temperature, which was used in the following study. After that the optimal formula of polyurethane composite is investigated by heat distortion temperature test, which was determined by the service temperature at 100 $^{\circ}$C. It was found that optimal formulation consists of polyurethane matrix with the density of 1.0 g/cm^3 containing 30 % glass fiber. This polyurethane composite was then manufactured by in-mold coating process with vinyl ester. In-mold coating was performed by

spraying vinyl ester onto the mold cavity preloaded with glass fiber prior to pouring the mixture of polyol and isocyanate. The thin layer of vinyl ester is then readily applied onto the surface of polyurethane composite. Afterwards the sample was coated with top coat. The interfacial adhesion between polyurethane composite in-mold coated and top coat was examined by means of pull off test, cross cut test, digital microscope and attenuated total reflection-infrared spectroscopic method. It was found that the treatment of polyurethane composite with vinyl ester resulted in improved adhesion. The increase in adhesion strength associates with contact angle value, which decreases by in-mod coating with vinyl ester. The decrease in contact angle values on the coated polyurethane composite surface can be explained by the creation of polar functional groups (C=O, C-O) and increasing of surface roughness.

ACKNOWLEDGMENTS

This thesis could not be completed without the assistance of many persons to whom I would like to express my sincere appreciation.

First, I would like to express my appreciation to my advisors, Asst. Prof. Dr. Surat Areerat, Dr. Wuttipong Rungseesantivanon, Prof. Isao Satoh and Assoc.Prof. Takushi Saito who have given me many helpful and valuable advises.

I would also like to thank Mr. Dumrong Thanomjit and Miss Bongkot Hararak for their help during the experiments, then time and device in this research.

Moreover, I would like to show gratitude to National Metal and Materials Technology Center (MTEC), especially the Plastic tech laboratory for providing the high performance machine as well as financial support.

I am grateful to National Science and Technology Development Agency (NSTDA), which provided the full scholarship for studying in the master program.

Finally, I am very grateful to my family for all love, caring, understanding and motivation throughout my life.

Natcha Prakymoramas

CONTENTS

CONTENTS (CONT.)

Page

CONTENTS (CONT.)

Page

CONTENTS (CONT.)

Page

CONTENTS (CONT.)

Page

LIST OF TABLES

LIST OF FIGURES

LIST OF FIGURES (CONT)

Figure Page

LIST OF FIGURES (CONT)

Figure Page

CHAPTER 1

INTRODUCTION

1.1 Background

Polyurethanes are versatile materials that can be used in many industries, for instance, automotive, furniture, construction, thermal insulation and footwear. Polyurethane results from the exothermic reaction between polyisocyanate and polyol by stepwise polymerization (also called condensation) [1-2].

Reaction injection molding, RIM, is one of the methods in producing polyurethane parts from monomer or oligomers. RIM was first developed in Germany from polyurethane rigid foam technology used to produce integral- skin, rigid urethane foam for automotive and furniture[1]. Most commercial RIM products are filled with reinforcing materials such as mica, glass flakes, chopped glass and continuous fibers. The addition of reinforcing agents can improve dimensional stability and mechanical properties [1]. However, the disadvantages of polyurethane composites are difficulties to get a "Class A" surface.

In order to acquire a smooth surface and to reduce or eliminate porosities, In-mold coating (IMC) is implemented [3-4]. There have been several researches focusing on in-mold coating process to enhance a surface part as follows:

1.1.1 In-mold Coating of Sheet Molding Compound

Sheet molding compound (SMC) is a continuous sheet of ready to mold composite materials that contains fibers and mineral fillers dispersed in a thermosetting resin. However, parts molded with sheet molding compound usually have porosities, waviness and sink [3-4]. In order to improve the part surface property, in-mold coating is used with SMC process. This method uses a liquid coating material which is cured and bonded to provide paint-like coating after being injected onto the SMC part surface. As a result, IMC is considered as an integral part

of the molding when producing SMC exterior automotive body panels. Figure 1.1 shows in-mold coating of SMC compression molding process [4].

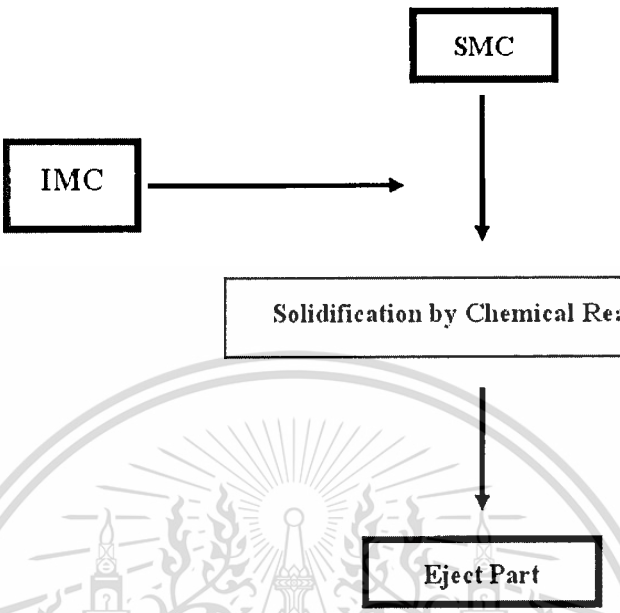

Figure 1.1 Addition of In-Mold Coating into SMC compression molding process [4]

1.1.2 In-mold Coating of Injection Molded Thermoplastic Parts

In automotive industry, thermoplastics are used to produce both interior and exterior parts which have low surface energy. Therefore, it is difficult to paint these surfaces. The IMC of a thermoplastic is studied by injecting a low viscosity liquid thermoset material onto these surfaces. The coating material has been developed by OMNOVA Solutions INC. Akron, USA which is injected onto the substrate, while the part still remains in the mold. Through compression during the filling stage it flows to cover the whole part surface. The thermoplastic integrated with coating material by IMC process is shown in Figure 1.2 [4].

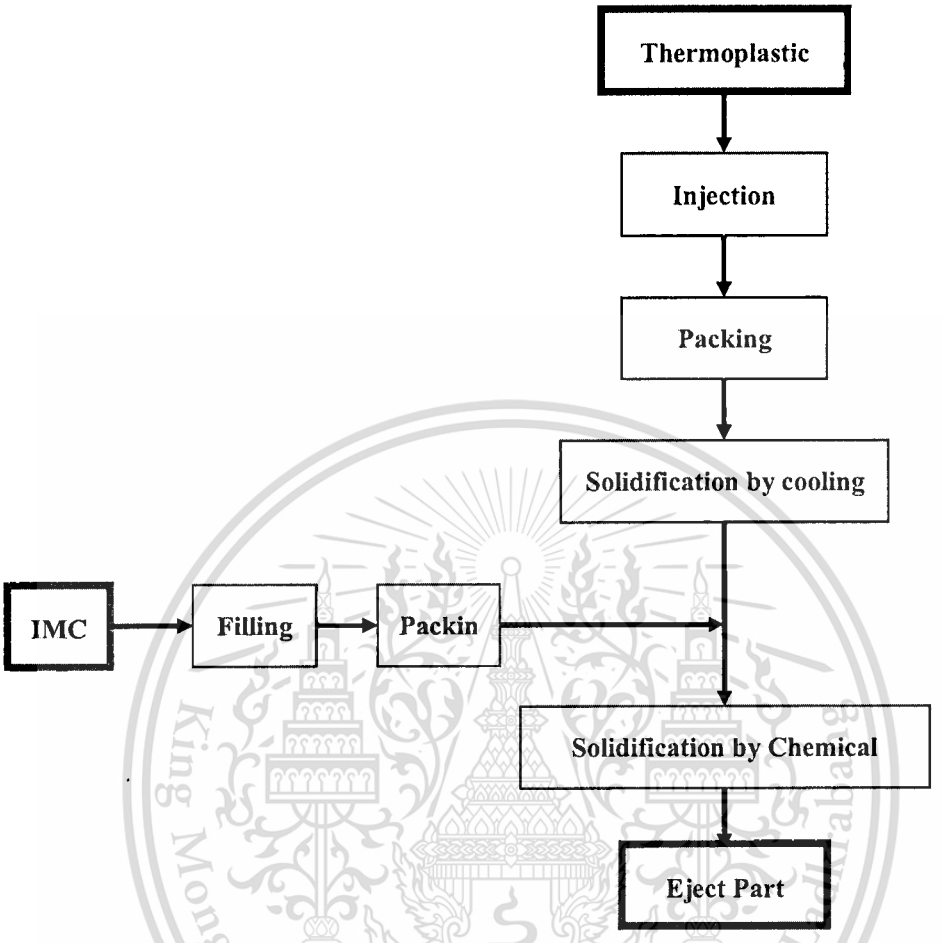

Figure 1.2 Addition of In-Mold Coating into Injection Molding process [4]

1.2 Objectives

1.2.1 To investigate the effect of processing temperature on mechanical and thermal properties and morphological

1.2.2 To investigate the optimum polyurethane composite formulation for in-mold coating process

1.2.3 To improve adhesion between the optimum polyurethane composite in-mold coated with vinyl ester prepared by in-mold coating and PLANITTO #250 (top coat)

1.2.4 To study the adhesion between of top coat and the optimum polyurethane composite in-mold coated with vinyl ester prepared by in-mold coating

1.3 Scopes of Research

1.3.1 The first study was aimed to investigate the effect of the mold temperature on mechanical and thermal properties and microstructure of polyurethane. Polyurethane was prepared by reaction between polyether polyol and 4, 4'diphenylmethane diisocyanate (MDI) in the ratio of 1:2 with target density of 1.0 g/cm^3. The flexural strength and modulus and the heat deflection temperature of polyurethane samples produced by using reaction molding in a preheated aluminum mold at 40, 50 and 60°C were investigated. In addition, the microscopic structure of polyurethane was observed by using the scanning electron microscopy (SEM), and then the SEM photographs were analyzed by image processing program.

1.3.2 The second study was to find the optimum polyurethane composite formulation which can later be coated. In this study, different amounts of glass fiber ranging from 0 to 40 % by volume/density were added into the mold before. Then, the mixture of polyol and isocyanate in the ratio of 1:2 in order to obtain polyurethane matrix having densities ranging from 0.8 to 1.0 g/cm^3 were poured into the mold. The production of this was carried out at the optimum mold temperature resulted from the first study. After that, heat deflection temperature of polyurethane samples was measured. Besides, the microscopic structure of polyurethane composite samples was observed by using the scanning electron microscopy (SEM), and then the SEM photographs were analyzed by image processing program.

1.3.3 In the third study, the contact angle, surface roughness and attenuated total reflectance Fourier transform infrared (ATR-FTIR) studies were carried out to characterize the surface properties of polyurethane composite before PLANITTO # 250 being coated. Then, the adhesion of sample coated with PLANITTO # 250 is investigated by the cross cut test and pull off test. After that fracture of coating film and sample after pull off test were examined by ATR-FTIR and the optical microscope image analysis was performed on fracture surface to get some information on interaction behavior of materials at the interface.

1.4 Research methodology

1.4.1 To study material, formulations, properties and processing of polyurethane composites

1.4.2 To study coating material and method of In-mold coating process

1.4.3 To study literature reviews

1.4.4 To research and develop the suitable formula for polyurethane composites

1.4.5 To research in-mold coating process for using polyurethane composites

1.4.6 To test adhesion between polyurethane composite layers and coating layers

1.5 Expected Benefits

1.5.1 The suitable formula of polyurethane composite for in-mold coating process

1.5.2 Preliminary study could be extending to the application in automotive industries or more advance application.

CHAPTER 2

LITERATURE REVIEWS

2.1 Semi-rigid polyurethane

The formation of semi-rigid polyurethane foam is based on several components for example functional isocyanates of diphenylmethane disiocyanate (MDI), polyether polyol, water, physical blowing agent, catalyst and surfactants. [5]

2.1.1 Reaction of isocyanates

The formation of polyurethane involves in three principal reactions

(1)Reaction of isocyanate with polyol to form urethane

$$\left[R{-}OH\right]_n + \left[R'{-}N{=}C{=}O\right]_n \longrightarrow \left[R{-}CO{-}O{-}NH{-}R'\right]_n \qquad (2.1)$$

Polyol Isocyanate Polyurethane

This reaction is exothermic. The rate of the polymerization reaction depends upon the structure of both isocyanate and polyol [2, 5-8].

(2) Reaction of isocyanate with water leading to carbomic acid, which can be break down to carbon dioxide and an amine [2, 5-8]

$$R{-}N{=}C{=}O + H_2O \rightarrow R{-}NH{-}CO{-}CH \rightarrow R{-}NH_2 + CO_2 \qquad (2.2)$$

Isocyanate Water Carbomic acid Amine Carbon dioxide

The reaction of isocyanate with water is the most exothermic reactions that will take place during the foaming process, a process that occurs under almost adiabatic conditions because the foam produced is an excellent thermal insulator. The carbon dioxide generated diffuses to nucleation sites, at which carbon dioxide gas cells begin to grow by accretion of additional liberated carbon dioxide and by thermal expansion. The nucleation sites are believed to be small air bubbles entrained in the liquid mixture during intensive mixing of the formation, and stabilized by surfactant [5].

(3) Reaction of amine with isocyanate to form a urea linkage [2, 5-8]

$$R-NH_2 + R'-N=C=O \longrightarrow R-NH-CO-NH-R' \qquad (2.3)$$

Amine Isocyanate Urea

The reaction of diisocyanates with primary and secondary amine compounds is the most important reaction in polyurethane. Diamines are used as chain–extending and curing agents in polyurethane manufacture. The effect of selected diamines addition is to increase the reactivity of the reaction mixture and the resulting polyurea segments in the polymer increase the potential for the both primary (covalent) and secondary or hydrogen-bonded, cross-linking. The reaction of unhindered isocyanates with primary amines, at room temperature in the absence of catalysts, is about 100 to 1000 times faster than the reaction with primary alcohols. The reactivity of amines increases with the basicity of the aromatic amines. Substantial reductions in the reactivity of aromatic amines, useful in elastomer formulation, result from steric hindrance by substituent, such as ethyl groups, ortho to the amine group or from the presence of electron with drawing groups, such as chlorine, in the molecule. Tertiary amines, as they contain no active hydrogen atoms, do not react with isocyanates, but are powerful catalytsts for many other isocyanate reactions [5].

2.1.2 Secondary reaction of isocyanates [2, 5-7]

Isocyanate can react with the active hydrogen atoms of the urethane and urea linkage to form biuret and allophanate, respectively. Both reactions are crosslinking reaction. The isocyanate with urea groups is significantly faster and occurs at a lower temperature than that with urethane group.

$$\left[R-NH-CO-NH-R'\right]_n + \left[R'-N=C=O\right]_n \leftrightarrow \left[R-N(HN-R')-CO-O-NH-R'\right]_n \qquad (2.4)$$

Urea Isocyanate Biuret

$$\left[R-CO-O-NH-R'\right]_n + \left[R'-N=C=O\right]_n \leftrightarrow \left[R-N(HN-R')-CO-COO-R'\right]_n \qquad (2.5)$$

Urethane Isocyanate Allophanate

2.1.3 Isocyanates polymerization reactions [2, 5-6,9]

Isocyanates become uretidinediones, dimers, and isocyanurate, trimer, especially in the presence of basic catalyst. Dimer formation arises only from aromatic isocyanates and it is inhibited by ortho substituents. Thus 2,4- and 2,6- TDI do not form dimmers at normal temperatures but 4,4′-diphenylmethane diisocyanate (MDI) dimerises slowly when left standing at room temperature. At higher temperature insoluble polymeric material are formed.

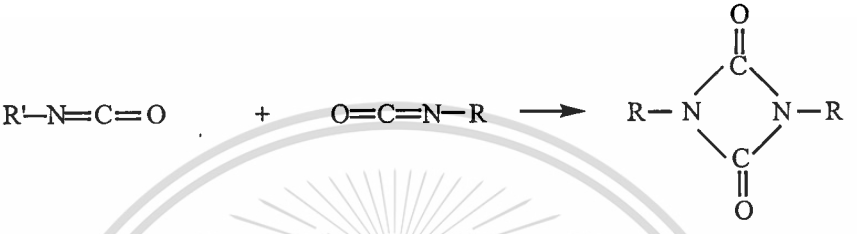

(2.6)

Aromatic isocyanate Uretidinedione

Isocyanurates (see equation 2.7) are formed on heating either aliphatic or aromatic isocyanates. The reaction is accelerated by basic catalysts. Isocyanurates formation in polyurethane manufacture gives very stable branch points as, unlike the uretidinedione, biuret, allophanate and urethane, the reaction is not easily reversed. Isocyanurate foams from both MDI and TDI show little degradation below 270 °C.

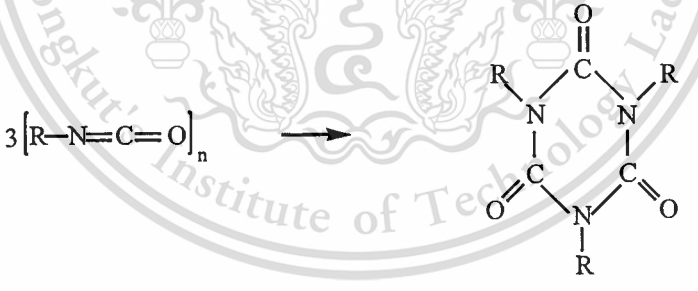

(2.7)

Isocyanate —— Trimerisation ——Isocyanurate

2.1.4 Isocyanates [2, 5]

Isocyanates are significant monomers for formation of polyurethane, which have two types as follows:

(1.) Toluene diisocyanate (TDI) is the most commonly used diisocyanate on a worldwide basis (in 1997 about 715,000 metric tons) [5]. TDI is mainly used as a 80:20 mixture

of the 2,4 and 2,6 – isomers, which are shown in Figure 2.1 and less commonly as 65:35 mixture and sometimes as the pure 2,4 compound. It is highly reactive with melting points of 21.8 and 8.5 °C for the 2, 4 and 2, 6 – isomers, respectively and in the range 5 to 15 °C for the mixtures [2, 8]. TDI serves mostly for the production of flexible polyurethane foams.

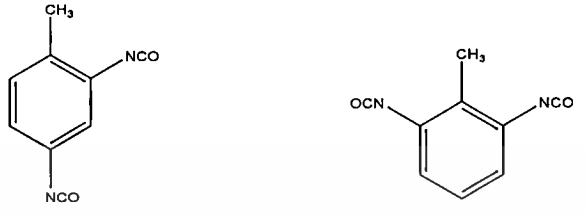

2, 4-TDI 2, 6-TDI

Figure 2.1 TDI isomers [2, 5]

(2.) Methylene diphenylene diisocyanate (MDI) is the second most commonly used aromatic polyisocyanate produced from aniline, formaldehyde and catalyst (hydrochloric). The condensation of aniline with formaldehyde does not lead to the single product, 4, 4′- diamino – diphenylmethane (MDA), but to a mixture which also contain the 2, 4′-and 2, 2′- isomers and also to condensation products which contain more than two aromatic rings in the molecule such as three and higher ring compounds. MDI consists of many chemical species. It is offered in a wide variety of products which include, besides the pure 4, 4′- two ring products, a great variety of so-called polymeric MDI type for the different application area, which are shown in Figure 2.2.

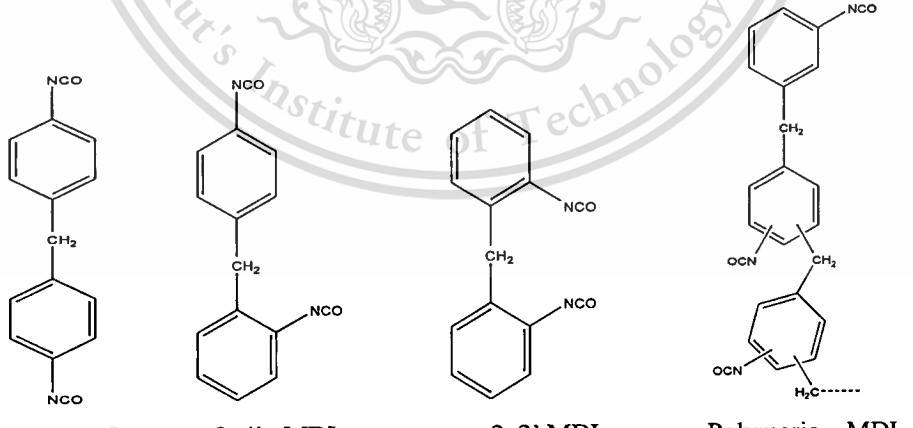

4, 4'-MDI 2, 4' –MDI 2, 2' MDI Polymeric – MDI

Figure 2.2 MDI isomers [2, 5-8]

Pure MDI is a white to pale yellow crystalline solid which can be used in liquid state at ambient temperature [5].

The pure 4, 4'-MDI isomer is preferably used for the manufacture of high performance polyurethane elastomers. The mixtures consist of higher three-ring and polymeric MDI. Polymeric MDI is the basis for most rigid foam formulations. On the other hand, certain MDI types, specifically those which contain higher 2, 4'- isomer contents, can also be used for flexible polyurethane foam [5]. In this study uses MDI that is supported by BASF Thailand, Ltd.

Isocyanates are considered hazardous. Expose to atmospheric moisture must be avoided. Thermal degradation of isocyanates occurs above 175 °C. Relatively low concentration of isocyanates irritates the respiratory system and the toxicity of isocyanates when inhaled or in contact with the skin differs considerably. TDI has a high volatility of 142 mg/m^3 at 20 °C with a concentration of the saturated vapor whereas that volatility of MDI is 0.8 mg/m^3. For this reason, MDI is considered safer than TDI. However, all isocyanates require careful handling [5].

2.1.5 Polyol [2, 5]

The soft phase of polyurethane is a functional alcohol or polyol phase [4]. Properties of polyurethane are determined by polyol compounds with several hydroxyl functions in the molecule. Polyols can be divided into two types; polyethers and polyesters. Commercially, about 90% of polyols used in polyurethane manufacture are polyether polyols [2] Polyether polyol used in rigid polyurethane foams are produced by addition of 1,2-propylene oxide to the hydroxyl or amino groups of low molecular weight molecules, usually by an anionic chain mechanism (reaction in Equation 2.8 to 2.10).

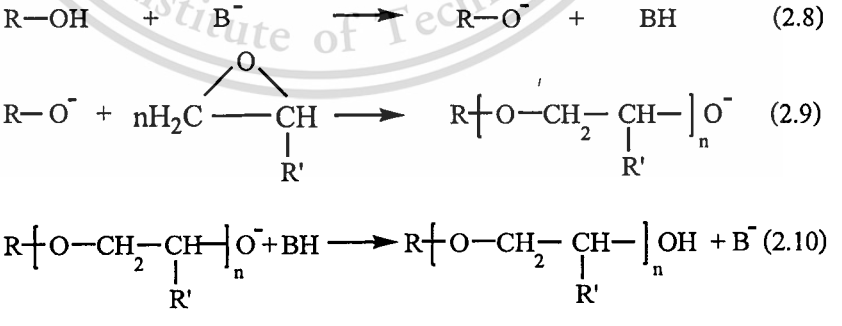

Where B^- is anion catalyst

Equation 2.10: Preparation of polyether polyols by an anionic chain mechanism

The initiating hydroxyl compounds are treated with potassium hydroxide or other bases, forming a starting mixture that reacts exothermically with the alkoxide. More basic

aliphatic amines require no additional catalysts. Ethylene oxide and propyleneoxide can be added. If ethylene oxide is terminal, it produces primary hydroxyl groups rather than the secondary hydroxyls formed from terminal propylene oxide. After completion of the alkoxide addition, the polyol is neutralized, filtered and otherwise purified. Antioxidants such as butylated hydroxytoluene are added to inhibit peroxide formation [2, 5].

The functionality and equivalent weight of polyether polyols can be widely varied. This is a notable advantage of polyether polyols over polyester polyols, and, for this reason, polyether polyols are used for producing various polyurethanes, e.g., rigid, flexible and semi-flexible foams, elastomers, coatings, adhesives, and resins [2].

Polyester polyols for urethane and related polymer foams include: (a) aliphatic polyesters prepared by the reaction of dibasic acids, such as adipic acid, phthalic acid, and sebacic acid, with glycols such as ethylene glycol, propylene glycol, diethylene glycol, 1,4- butanediol and 1,6-hexanediol; (b)aliphatic polyesters prepared by the ring-opening polymerization of lactones, e.g., epsilon-caprolactone; and (c) aromatic polyesters prepared by the transesterification of reclaimed polyethylene terephthalate or distillation residues of dimethylterephthalate. The polyesters (a) and (b) are used for making flexible foams, elastomers, coatings and adhesives, and (c) are used for producing rigid urethane foams and urethane-modified isocyanurate foams [2, 5].

2.1.6 Water [2, 5]

Water is similar to chemical blowing agent and reacts with an isocyanate group resulting in a primary amine and carbon dioxide. The water content influences both the cell structure and the solid-state morphology of the foam. Higher water contents typically result in foams with lower density due to the increased blowing reaction.

2.1.7 Blowing agent [6]

Thermosetting foams are produced by using blowing agent, which can be divided into two types; i.e., chemical and physical blowing agents

In the case of chemical blowing agents, the conventional gas-generation reaction for flexible urethane foams is the water-isocyanate reaction. The blowing agents used include the following compounds (a) enolizable compounds such as nitroalkanes (nitroethane, nitropropane)

aldoximes (acetaldoximes), nitrourea, acid amides (formamide,acetamide), active methylene-containing compounds, (acetylactone, ethyl acetoacetate), and (b) boric acid.

Furthermore, physical blowing agent, e.g., water, physical blowing agents have the following advantages: (a) the exothermal reaction is removed in part by the evaporation of the physical blowing agents, and the resultant foams have reduced discoloration, scorching and fire risk; (b) the system viscosity is lowered, and pour-in-place foaming is facilitated; (c) some physical blowing agents(e.g., CFC-11) provide higher thermal insulation properties in foam formation than those of water-blown foams. Physical blowing agents may be classified as CFCs (chlorofluorocarbons), HCFCs (hydrochlorofluorocarbons), HFCs (hydrofluorocarbon ethers) and non-fluorine-containing organic liquids. These fluorinated blowing agents can also be used in foaming polyisocyanurate foams, polyoxazolidone foams, and polyurea foams [6].

2.1.8 Catalyst [2]

A number of catalysts can be used for the reaction of isocyanates, polyol with water. These include aliphatic and aromatic tertiary amines, organometallic compounds and tin compounds Alkali metal salts of carboxylic acids, phenols and symmetrical triazine derivatives are used to promote the polymerization of isocyanates [2].

2.1.9 Surfactant [6]

A surfactant is a major raw material for polyurethane foams. Surfactants play an important role in obtaining required cell structures, e.g., fine cells, coarse cells, closed cells, and opened cells, that greatly influence foam properties. Surfactants for urethane and related polymer foams are usually silicone-surfactants. These surfactants generally are copolymers of poly (dimethylsiloxane) [-Si(CH,),-O-l, oxyalkylene chains, e.g., polyethylene oxide chain (EO), and polypropyene oxide chains, (PO),. The copolymers can be linear, branched or pendant types. The surfactants have different functions, i.e., emulsifying, foam stabilizing and cell-size control [6].

2.1.10 Reinforcement [1-2, 7-8]

The main objective of add reinforcement is to improve modulus and higher heat distortion temperature. Conversely, thermal expansion can reduce [1]. For many applications, polyurethane materials are filled with many type of reinforced, for instance, mica, Flake glass,

and milled and continuous glass fiber. Several studies have been reported that polyurethane foam reinforced with glass fiber have the best mechanical properties [7].

Glass Fibers are the oldest form of strong fibers used in composite structural materials. Continuous fibers are made by a gravity extrusion process. Molten glass is place into a drawing furnace and is formed into fibers by passing though small-diameter orifice. After, cooling, a protective, lubricating finish or size is applied to protect the fibers from self-abrasion and improve handle ability. Glass strand are made by bundling together hundreds of tiny filament with an adhesive [1]. Most reinforcing glass is made from E glass, which has a low alkaline content and serves as a good electrical insulator .If more stiffness is required, S glass providing a 20% improvement over E glass is preferable, but is more costly to process. The major constituents of the different glasses are summarized in the Table 2.1 [8]. The properties of the reinforcing glass fibers are summarized in Table 2.2.

Table 2.1 The constituents of the different type glass reinforcement [8]

Glass fiber types	Component Material, Weight %								
	SiO_2	Al_2O_3	CaO	MgO	NA_2O, K_2O, Li_2O	B_2O_3	ZnO	TiO_2	Fe_2O_3
E	52.4	14	17.2	4.6	0.8	10.6	-	-	0.4
A	72	1.2	10	2.5	14.2	-	-	-	0.3
S	64.4	25	-	10.3	-	-	-	-	-
ECR	58.4	11	22	2.2	0.9	0.09	3	2.1	0.26

E glass = electrical grade; excellent electrical properties and durability

A glass = high alkali content; especially good for reinforcement good chemical resistance

S glass = high strength; noted for high tensile strength and high thermal stability

ECR glass = E glass modified for high chemical resistivity; good electrical properties

Table 2.2 The properties of the reinforcing glass fibers [8]

Glass Type	Density (g/cm^3)	Single fiber Tensile strength (GPa)	Single fiber Modulus (GPa)
S	2.49	4.5	86.0
E	2.56	3.6	76.0
A	2.45	3.1	72.0
ECR	2.60	3.4	73.0

2.1.11 Mold Release agent [2]

A release agent is necessary in order to easily and quickly remove the foam from the mold. Product based on wax, soaps and oil are injected by air pressure into the open mold. The effectiveness of the release agent depends less on the amount than on the uniformity of the coating. The force per area being necessary to open the mold can be used as scale for the release effectiveness. The basic knowledge of the polyurethane system and the kind of mold material, surface quality and form geometry are necessary in order to select the most suitable release agent [2].

2.2 Fundamental principles of foam formation [9]

The following three steps can be distinguished in the foam production process.

2.2.1 Bubble formation

Bubble formation occurs as soon as the reactants have been mixed. Then the mixture starts increasing in volume. At this step two sub stages are apparent: First, the period in which the evolving blowing gas dissolves in the mixture until saturation. Next, the period in which once gas saturation has been achieved, with the participation of the dissolved air, micronuclei of bubble and the mixture starts to look like a cream [9].

2.2.2 Bubble growth

Bubble growth results primarily from which begins with a visible increase in volume of the reactant mixture attains the highest possible volume [9].

2.2.3 Stabilization

Stabilization is the liquid component of the reactant mixture become a solid polymer and acquires an acceptable strength [9].

2.3 Vinyl ester [10-11]

Polyester resins have been used widely in composite products in various commercial and industrial markets for many years. Applications include boat structures, automobile panels, building panels, and corrosion resistant tanks and pipes. Recent pressure to obtain higher performance composites at a lower cost has motivated interest in vinyl-ester systems because they possess superior corrosion resistance and mechanical properties compared to polyesters (in some cases they approach epoxy properties) while maintaining similar ease of processing characteristics, especially in liquid molding processes. The components of a typical vinyl ester resin are illustrated in Figure 2.3.

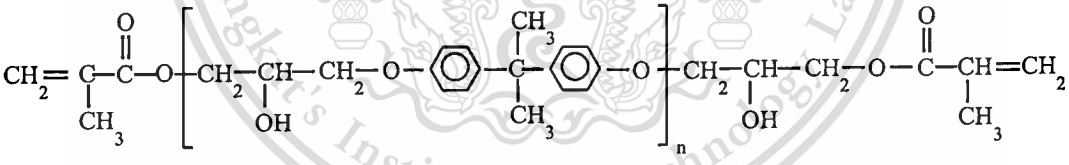

Figure 2.3 Vinyl ester resin monomeric components [10]

Vinylesters (VE) are chemically closely related to both unsaturated polyesters and epoxies and in most respects represent a compromise between two. They are like unsaturated polyester resins, which can be cured and crosslinked by means of free radical mechanisms, in the presence or absence of unsaturated monomers, such as styrene. Their low room temperature viscosity coupled with rapid curing rate and relatively low cost also makes them suitable for various molding processes like the conventional unsaturated polyester resins. In addition, the cured vinyl ester resins possess excellent mechanical strength, as well as chemical and solvent resistance, which are not found in most unsaturated polyester resins. The excellent properties of vinyl ester resins can be attributed to the hybrid molecular structure of epoxies and polyesters. In vinyl ester

resins, the aromatic rings provide good mechanical properties. The ether linkage contributes to good chemical resistance. The ester groups and two C=C double bond linkages are located at the end of the polymer chains, which lead to the high reactivity of the terminal unsaturation of vinyl ester resins.

For curing of vinyl ester resins, the commonly used initiators are organic peroxides and hydroperoxides including methyl ethyl ketone peroxide, benzoyl peroxide and cumene hydroperoxide, etc. Rapid decomposition of initiators may occur under heat or by the use of promoters, such as tertiary amines and salts of metals like cobalt octoate or naphthenate, at low temperatures [10].

2.4 Density of foamed polymer [9]

The apparent density, which characterizes the relative contents of solid and gas phase in a material, is the fundamental morphological parameter of foamed polymer and is related to the properties of foamed plastics such as strength, thermophysical properties and electrical properties.

In general, the density is determined by the densities of solid and gas phase. It is related to the porosity of the foam as in Equation 2.7

$$Q = Q_s(1-G) + Q_g \tag{2.7}$$

Where Q_s the true density of the solid is phase and is equal to the ratio of the total material mass to the difference between the total volume of the material and the cell volume

Q_g is the gas density in the cells

G is the porosity of the foam, which equal to the ratio of the cell volume to the total material volume.

In practice, the density of plastic foam is calculated as the ratio of sample weight M to geometrical volume V_0 as follow Equation 2.8.

$$Q = \frac{\mathrm{M}}{V_0} \tag{2.8}$$

Where the density is given in g/cm^3 or kg/m^3 [9].

2.5 Cell size of foamed polymer [9]

The size of the cell and cell size distribution depend on process condition for foaming. The number of cells per unit volume of foam (N_c) is an important parameter, especially in estimating the effectiveness of the microstructure throughout the bulk of the sample. The parameter N_c is a function of cell size and density of plastic foam as in Equation 2.9

$$N_c = \frac{\left|1 - Q/Q_p\right|}{10^{-4} d} \tag{2.9}$$

Where N_c is the number of cells per unit volume of foam

Q is the density of the foam in g/cm^3

Q_p is the polymer matrix density in g/cm^3 and d is the mean cell size in mm.

The density and the ratio of the number of opened/closed cells are the fundamental morphological parameters of foam plastics [9].

2.6 Cell size and physical properties [9]

The cell size can have a significant influence on the properties of plastics foam. For example, the coefficient of thermal conductivity of foams increases with an increase in cell size, because there are more paths for the heat transfer by radiation and convection. Young's modulus of both flexible and rigid plastic foam decreases when the cell size increases. The compressive strength and Young's modulus of phenol-formaldehyde plastic foams with small cells, cell diameter less than 0.2-0.3 mm, increase more markedly with an increase in cell size than foams with larger cells. Shoutov found that the tensile strength and ultimate elongation of many flexible foams increase as the cell size decrease. Blair reported that the compressive strength of plastic foam under high compressive loads decreases, when the cell size increases [9].

2.7 Crosslinking reaction mechanisms [12]

2.7.1 Free radical polymerization

The basic steps in free radical polymerization are initiation, propagation, chain transfer, and termination [12].

Initiation

Initiation can be achieved by adding a small amount of a chemical that decomposes easily to form free radicals. Initiators can be monofunctional and form the same radical or they can be multifunctional and form different radicals by following Equation 2.10 .

$$I_2 \xrightarrow{k_o} 2I \qquad (2.10)$$

For monofunctional initiators the reaction sequence between monomer *M* and initiator *I* is in Equation 2.11.

$$I + M \longrightarrow R_1 \qquad (2.11)$$

Propagation

The propagation sequence between a free radical R_1 with a monomer unit is in Equation 2.12

$$R_j + M \xrightarrow{k_p} R_{j+1} \qquad (2.12)$$

The specific reaction rates k_p are assumed to be identical for the addition of each monomer to the growing chain. This is usually an excellent assumption once two or more monomers have been added to R_1. The specific reaction rate k_i is often taken to be equal to k_p.

Chain transfer

The transfer of a radical from a growing polymer chain can occur in the following ways:

1. Transfer to a monomer as follow Equation 2.13:

$$R_j + M \longrightarrow P_j + R_1 \qquad (2.13)$$

Here a *live* polymer chain of *j* monomer units transfer (R_j) its free radical to the monomer to form the radical R_1 and a *dead* polymer chain of *j* monomer units (Pj).

2. Transfer to another species in Equation 2.14:

$$R_j + C \xrightarrow{k_c} P_j + R_1 \qquad (2.14)$$

3. Transfer of the radical to the solvent by following Equation 2.15:

$$R_j + S \xrightarrow{k_s} P_j + R_1 \qquad (2.15)$$

The specific reaction rates in chain transfer are all assumed to be independent of the chain length. It also notes that while the radicals R_1 produced in each of the chain transfer steps are different, they function in essentially the same manner as the radical R_1 in the propagation step to form radical R_2.

Termination

Termination to form dead polymer occurs primarily by two mechanisms:

1. Addition (coupling) of two growing polymers as follows Equation 2.16:

$$R_j + R_k \xrightarrow{k_{ta}} P_j + K \qquad (2.16)$$

2. Termination by disproportionation as Equaiton 2.17:

$$R_j + R_k \xrightarrow{k_{td}} P_j + P_k \qquad (2.17)$$

2.8 Adhesion theory [13]

The mechanism of adhesion has been investigated for many years. Several theories have been proposed in an attempt to provide an explanation for adhesion phenomena. However, no single theory explains adhesion in a general, comprehensive way. The bonding of an adhesive to an object or a surface is the sum of a number of mechanical, physical, and chemical forces that overlap and influence one another. As it is not possible to separate these forces from one another, the mechanical interlocking causes by the mechanical anchoring of the adhesive in the pores and the uneven parts of the surface, electrostatic forces as regard to the difference in electronegativities of adhering materials, and the other adhesion mechanisms dealing with intermolecular and chemical bonding forces that occur at the interfaces of heterogeneous systems. This chemical adhesion mechanism is explained in the case of the intermolecular forces by the adsorption theory and in the case of chemical interactions by the chemisorption theory. The processes that play a role in the bonding of similar types of thermoplastic high-polymer materials,

e.g. homogeneous systems, can be determined with the diffusion theory [13].

2.8.1 Mechanical interlocking

The mechanical interlocking theory of adhesion states that good adhesion occurs only when an adhesive penetrates and locks into the pores, holes, cavities and other irregularities of the adhered surface of a substrate and locks mechanically to substrate. The enhancement of adhesion can be attributed to increase surface roughness. The adhesive must not only wet the substrate, but also have the right rheological properties to penetrate pores and openings in a reasonable time. This theory explains a few example adhesions such as, rubber bonding to textiles and paper can occur good adhesion between smooth adhered surfaces as well, it is clear that while interlocking helps promote adhesion, it is not really a generally applicable adhesion mechanism [13].

2.8.2 Electrostatic theory

The basis of the electrostatic theory of adhesion is the difference in electonegativities of adhesing materials. Adhesive force is attributed to the transfer of electrons across the interface creating positive and negative charges that attract one another. For example, when an organic polymer is brought into contact with metal, electrons are transferred from metal into the polymer, creating an attracting electrical double layer (EDL) [13].

2.8.3 Adsorption theory or thermodynamic theory

The thermodynamic model of adhesion attributed to Sharpe and Schonhorn that is the most widely used approach at present science. This theory is based on the belief that the adhesive will be adhere to the substrate by van der waals forces and acid-base interactions at interface. The magnitude of these forces can be related to fundamental thermodynamic quantities for example, surface free energies of both adhesive and adhered.

Wetting equilibrium may be defined from the profile of a sessile drop a planar solid surface in a solid-liquid system. According to Young's equation, the surface tensions (γ) of materials at three phrase contacts are related to the equilibrium contact angle.

$$\gamma_{SV} = \gamma_{SL} + \gamma_{LV} \cos\theta \tag{2.10}$$

γ_{SV} : Surface free energy of a solid-vapor interface

γ_{SL} : Surface free energy of a solid-liquid interface

γ_{LV} : Surface free energy of a liquid-vapor interface

The surface free energy of a solid–vapor interface is sometimes lower than the surface free energy of the solid in vacuum. This decrease is explained as the spreading pressure π $(\pi = \gamma_S - \gamma_{SV})$ of the vapor onto the solid surface. In most case, in particular when dealing with polymer materials,¶ could be neglected therefore γ_S is used in place of γ_{SV} in wetting analyses. A range of wetting is indicated by contact angle θ. The contact angle becomes zero so that the liquid will spread.

The equilibrium spreading coefficient S defined as follow Equation 2.11 and 2.12:

$$\gamma_{SV} \geq \gamma_{SL} + \gamma_{LV} \tag{2.11}$$

or

$$S = \gamma_s - \gamma_{SV} - \gamma_{LV} \geq 0 \tag{2.12}$$

Normally, good adhesion of liquid to a substrate can be achieved when the contacts angle them is zero or close to zero

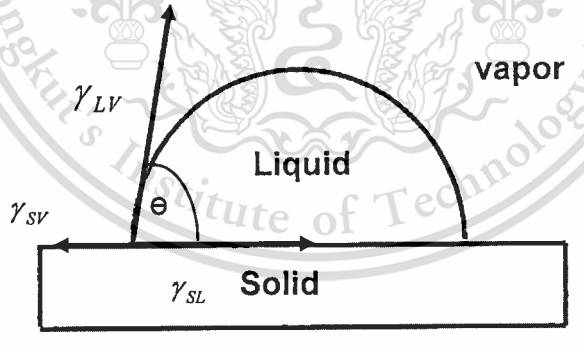

Figure 2.4 the three phase boundary of sessile drop on a solid surface [14]

According to the Young – Dupre′ Equation (2.13), the adhesion work is also given by

$$W_a = \gamma_L(\cos\theta + 1) \tag{2.13}$$

Where W_a and γ_L are the adhesion work and surface tension of water (78.2 mJ m^{-2}), respectively.

2.8.4 Diffusion theory

The diffusion theory is based on the assumption that is to reciprocate diffusion of macromolecules across the interface, so that creating an interdiffusion such as a liquid adhesive may diffuse into the substrate material. Generally, adhesive molecules are polymeric. They have limited compatibility with substrate molecules or the chain movement of the polymer is constrained by it's highly crosslinked, crystalline structure, when it is below its glass transition temperature, therefore the interdiffusion layer was thickness about 0.5 -10 nm. Additionally, in case where the compatibility is high, the interdiffused layer has been found to be as much as10 μm thick.

Factors that influence the diffusion process are contact time, temperature, molecular weight of polymers and physical form (liquid, solid). Polarity generally increases adhesion.

Some evidence may demonstrate that the interdiffusion phenomenon exists in mobile and compatible polymers and may promote the intrinsic adhesion. The diffusion theory, however, has found limited application where the polymer and adherent are not soluble or the chain movement of the polymer is constrained by its highly crosslinked, crystalline structure, or when it is below its glass transition temperature [13].

2.8.5 Chemical bonding theory

The chemical bonding mechanism is suggested that chemical bonds from across the (adhesive-substrate) interface. Chemical bonds are strong and make a significant contribution to the intrinsic adhesion in some cases.

For example, primary bond, covalent bond has energy about 100-1000 KJ/mol which is compared higher than secondary bond (Van der Waals forces) has energy about 0.08-50 KJ/mol. The formations of chemical bonds depend on reaction of both adhesive and substrate [13].

2.9 Principles of absorption spectroscopy [12, 14]

The absorption spectroscopy process associates with absorption and transmission of radiation, as a function of frequency or wave length due to its interaction with a sample. Absorption spectroscopy is used as an analytical chemistry tool to determine the presence of a

particular substance in a sample and to quantify the amount of the substance present. Infrared and ultraviolet-visible spectroscopies are almost employed in analytical application. There are wide ranges of experimental approaches to measuring absorption spectra. The most common arrangement is to direct a generated beam of radiation at a sample and detect the intensity of the radiation that passes through it [12].

The transmitted energy can be used to calculate the adsorption.

2.9.1 Beer-Lambert law

Beer-Lambert law is used to relate the amount of light transmitted by a sample to the thickness of the sample. The absorbance of a solution is directly proportional to the thickness and the concentration of the sample following Equation 2.14. When monochromatic radiation passes through a sample, the intensity of the emitted radiation depends upon the thickness and concentration of the sample [12, 14].

$$A = \varepsilon CL \tag{2.14}$$

Where A is the absorbance of the solution, C is the concentration, L is the length of the radiation path through the sample and ε is the extinction coefficient.

The absorbance is equal to the difference between the logarithms of the intensity of the light the sample (I_o) and the intensity of the light transmitted (I) by the sample [14].

$$A = \log I_o - \log I \tag{2.15}$$

$$A = \log\left(\frac{I_o(\lambda)}{I(\lambda)}\right) \tag{2.16}$$

$$A = \log\left(\frac{I_o(\lambda)}{I_o(\lambda)e^{-\mu L}}\right) \tag{2.17}$$

$$A = \log\left(e^{\mu L}\right) \tag{2.18}$$

$$A = \mu L \log e \tag{2.19}$$

$$A = 0.4343\mu L \tag{2.20}$$

This definition includes both absorption and scattering. A further definition is the extinction coefficient ε [14].

$$\varepsilon = 0.4343\delta \tag{2.21}$$

So

$$\mathrm{A} = \varepsilon CL \tag{2.22}$$

Absorbance is therefore dimensionless. Transmittance is defined as follows [14]:

$$T = \left(\frac{I}{I_o}\right) \tag{2.23}$$

The percentage transmittance ($\%T$) is

$$\%\ T = \left(\frac{I}{I_o}\right) \tag{2.24}$$

2.10 Literature Reviews

The correspondence articles are as follows:

Kamal and co-worker [15] revealed significant information on the microstructure and some processing variables. Shot time and nucleation level are the variables that affect the microstructure significantly, while mold temperature has a little or no effect. It was found that high shot size and low nucleation level reduce the bubble size and flatten the bubble size distribution. A high shot size and a low nucleation level are utilized, the overall tensile strength is higher than in the others. The tensile properties as well as the impact properties can be correlated to the bubble size and number distribution.

Kim et al. [16] studied the effect of glass fiber on cell structure, density, thermal conductivity, mechanical and thermal properties of composite foam, rigid polyurethane foam. In the term of cell structure, it is observed that the foams contain the spherical and polyhedral shape where the cell size generally decreases as the glass fiber content increases. The amount cells around the glass fiber content increases. It is specifically small, indicating that cell growth is hindered by fibers. In addition, bubble rise and growth are also physically hindered by the presence of glass fibers. The closed cell fraction linearly decreases with the glass fiber content. Foam density increased with increasing amount of glass fiber in accordance with the decrease cell size which is due to the decreased interface energy of the foam. In addition, the thermal conductivity of the composite foam is increased due to the high thermal conductivity of glass fiber and decreased due to the decreased cell size. Moreover, compression strength, tensile

strength and modulus increased with the addition of glass fibers incorporated into the polymer matrix. The increase glass fiber reinforcement was also in accordance with the increased foam density.

Takemori [17] found that the addition of glass fibers leads to significant rise in modulus as well as increased values for the heat distortion temperature.

Hatchetta and co-worker [18] proposed that the density and the modulus decrease as a function of increasing processing temperature. The densities of the polyurethane foam samples with identical volumes were processed at 25 °C, 45 °C and 85 °C. The results have revealed that the density of polyurethane foam processed at 25 °C was the highest with values density of 0.147 g/cm^3, with a relative standard deviation of 2 %. It was found that higher than the target density of 0.100 g/cm^3. On other hand, less density of polyurethane foam are acquired at the processing temperature of 45 °C (0.124 g/cm^3) and 85 °C (0.110 g/cm^3) with relative standard deviation of 3 and 2 %, respectively. The percent decrease in density for the polyurethane foams processed at 45 °C and 85 °C is on the order of 16% and 25 % respectively. The result indicated that processing the polyurethane foam samples can influence the increased thermal activity of the polyurethane foam at higher temperatures and a decrease in chemical cross-links in the material. In addition, the modulus depend on the processing temperature with a regression coefficient of R = 0.998. The magnitude change was noticed at 45 °C and 85 °C with a decrease in modulus by 7 and 20 %.

Esmacinlnezhad et al. [19] examined the mechanical properties of rigid polyurethane foam and the microstructures of the foam. The results indicated that the rigid polyurethane foam with the smallest cell size and the narrowest cell size distribution has the highest mechanical properties.

Yang and co-worker [20] investigated the effect of content of SiO_2 and fibers and the effect of length of fibers on the mechanical properties of the polyurethane composite foam. The results showed that the tensile strength of the polyurethane composite foam is optimal when the content of SiO_2 and glass fiber is 20 and 7.8 %.

Mirabedini et al. [21] demonstrated the effect of microwave irradiation on the surface characteristic of polypropylene. Contact angle measurements, SEM and ATR-FTIR technique were used to study the changes in the surface of the samples. The pull-off test method was employed to evaluate the adhesion strength of an acrylic lacquer on the treated polypropylene

samples. A relative increase in the surface free energy of the treated PP was observed. The surface became hydrophilic on exposure to microwave irradiation for 120 s. SEM revealed a slightly pitted structure on the surface of PP due to the treatment. ATR-FTIR analysis of treated surface showed some chemical changes evident from presence of carbonyl group and also formation of carbon double bonds. The adhesion measurement tests on bonded joints demonstrated an increase in performance as showed by a change in the locus of failure from adhesive to cohesive failure within the bond line.

Shojaei et al.[22] studied the performance of the radiation grafting technique as a chemically based surface pretreatment method to adhesion modification of polyethylene surfaces toward the metallic layer. Gamma irradiation over a dose range of 4-10 kGy is used for grafting of vinyl monomers including acrylamide (AAm) and 1-vinyl-2-pyrrolidone (NVP) onto the surface of three different polyethylenes including low density polyethylene and two kinds of high density polyethylenes, namely HDPE-1 and HDPE-2. The grafting yield is evaluated based on the weight increase of the samples. It is found that the grafting yield is dominated by the crystallinity of the polyethylene, so that lower crystalline percent of polyethylene leads to higher grafting yield. Additionally, lower irradiation dose rate causes higher grafting efficiency. The polyethylene samples are also hydroxylated by exposing to gamma rays in water at dose level of 100 kGy to make the surfaces hydrophilic. Moreover, the surface of the polyethylenes is subjected to the conventional surface treatment methods including chemical etching and mechanical abrasion. Surface characterization is performed by contact angle measurements and scanning electron microscope before and after the surface modification. A copper layer with nominal thickness ranging 3–10 μm is deposited on the surface of treated and treated substrates using both the electroless plating and magnetron sputtering processes. The adhesion of the metallic layer is investigated by the cross-cut and the pull-off tests. It is shown that radiation grafting of AAm monomer on polyethylene surfaces always leads to an excellent adhesion toward copper layer irrespective of metallization process, probably due to strong chemical complexes between AAm monomers and copper atom. However NVP-grafted surfaces show poor adhesion which may be due to hindrance effect of the nitrogen functionality in NVP. The mechanical roughening shows a slight positive effect on the adhesion, but the maximum bonding strength achieved in this case is 1 MPa in the sputtering process. In addition, maximum bonding strength belongs to LDPE treated by radiation grafting of AAm, so that no failure is observed in the pull

off test. The results also indicate that the bonding strength of the radiation grafting depends on the content of grafted AAm, while it seems that the adhesion strength in chemical etching method is dominated by both the chemical and physical interactions. Eventually, it is shown that the radiation grafting is an efficient surface treatment method for metalizing the polyethylene surfaces.

CHAPTER 3

EXPERIMENTAL PROCEDURES

3.1 Materials

In this study, Polyurethane foam Elastoflex®E3552/100 supplied by BASF was prepared using, polyether polyol and 4, 4'-diphenylmethane diisocyanate (MDI). Densities of the diisocyanate and the polyether polyol were 1.23 g/cm^3 and 1.1 g/cm^3 at 25 $^{\circ}$C, respectively. Glass fiber, density 2.506 g/cm^3, was of woving Spay Up 2004 type. Gel coat (Vinylester resin) and methyl ethyl ketone peroxide (MEKP) were supplied by Neotech inspection & chemical Co., Ltd. Bangkok, Thailand. Mold release was supplied by supervac co.Ltd.

3.2 Experimental Procedures

The overall experimental procedures in this work can be divided into three parts. Firstly, the mechanical, thermal and microstructure were examined as a function of processing temperature (40 $^{\circ}$C, 50°C and 60 $^{\circ}$C). Secondly, thermal property (Heat distortion temperature (HDT)/deflection temperature under load (DTUL)) was investigated to obtain the optimum polyurethane composite formulation in order to use in in-mold coating process with vinyl ester. In addition, microstructure was examined and discussed. Thirdly, the adhesion between polyurethane composite in-mold coated by in-mold coating process with vinyl ester and PLANITTO # 250 was determined and compared with the adhesion between polyurethane composite molded without using the in-mold coating process and PLANITTO # 250. The methodology is explained in detail later.

3.2.1 The Effect of Processing Temperature on Mechanical and Thermal properties and Microstructure

The polyurethane foam was synthesized by one shot method. Polyether polyol and 4, 4′diphenylmethane diisocyanate (MDI) were mixed to produce polyurethane foam with the target density of 1.00 g/cm^3, which correlates with volume mold of the ratio of 1:2. The

components were first put into a mixing cup, mixed thoroughly at 1,500 rpm by a mechanical stirrer, at room temperature for 20 seconds and poured into the opening cavity mold, then kept reaction time about 30 minutes. The influence of processing temperature on mechanical, thermal properties and morphological were examined. Mold release was first applied to the mold help the mold releasing. Three sets of samples were processed at controlled temperature of 40 °C, 50°C and 60 °C for a period of 30 minutes. The polyurethane foam samples were characterized by flexural test and heat distortion temperature test. Moreover, the microstructure of polyurethane foam was inspected using the scanning electron microscopy (SEM) and then the SEM micrographs were evaluated by image processing program.

3.2.2 Investigation of the optimum formula of polyurethane composites for in-mold coating process

In this study, the optimum formula of polyurethane composite was investigated for in-mold coating process. The temperature at which the materials can be survived in an oven coating/painting of PLANTTO# 250 set to 100 °C was defined as the criteria. Therefore, the effects of the following variables in the polyurethane composite on its heat distortion temperature were studied: (1) Polyurethane density 0.8, 0.9, 1.0 g/cm^3 (2) content of glass fiber: 0, 10, 20, 30, and 40 %. Other factors in the foam formulation, such as catalyst, surfactant and isocyanate index were kept constant. In addition, study of the microstructures of sample was conducted relative to previous study.

3.2.3 Investigations of the adhesion between the coating layer (PLANITTO #250) and the optimum polyurethane composite during the in-mold coating with vinyl ester

The optimum polyurethane composite obtained from section 3.2.2 was used in in-mold coating with vinyl ester. The experimental procedures in this work are shown in Figure 3.1. Initially, the vinyl ester was mixed with 2% MEKP and sprayed with the thickness of 50 μm onto the aluminum plaque-plated mold. Then the glass fibers were evenly manually distributed in the mold. Polyol and diisocyanates were mixed and poured into the preloaded mold. The mold was then closed with the holding pressure of 6 MPa. After 30 minutes, the specimen was demolded. In addition, the specimens were prepared by the conventional process in order to compare the adhesion with those prepared by in-mold coating process. The measurement of the contact angle

was carried out to evaluate the wettability of the both surfaces. Subsequently, both specimens were coated with top coat (PLANITTO# 250(2- component: acryl resin paint / isocyanate)) from CH INDUSTRY CO., LTD. In the final step, Adhesion test method can be investigated by two measuring techniques such as pull-off adhesion test and cross cut test. The importance of foaming reaction for adhesion or cohesion was investigated by fourier transform infrared attenuated total reflectance (ATR -FTIR) spectroscopy.

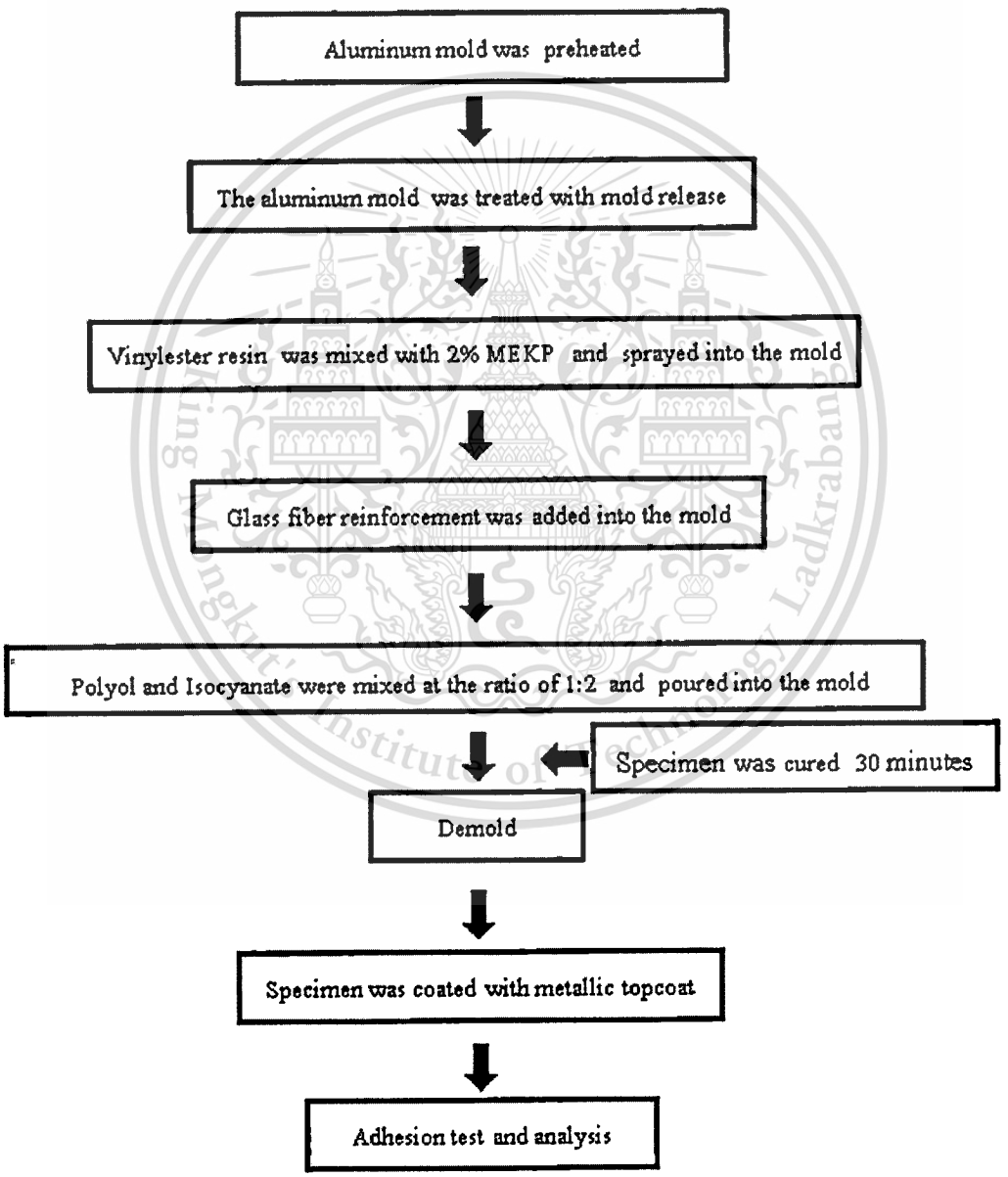

Figure 3.1 Flow chart of study of in-mold coating of polyurethane composite

3.3 Testing of Properties

3.3.1 Physical properties

3.3.1.1 Density

The measurement of density was done based on the Archimedes principle. This corresponds to the standard test method (ASTM D 1622). The density can be calculated using Equation. 3.1.

$$\rho = \frac{(M_a \times \rho_w)}{(M_w - M_a)} \tag{3.1}$$

Where ρ = the density of test specimen (g/cm^3)

M_a = mass of test specimen in the air (g)

M_w = mass of test specimen in water (g)

ρ_w = the density of water at the measuring temperature (g/cm^3)

In the second study, the density of polyurethanes and polyurethane composites were measured and averaged of at least five measurements by electronic densimeter MD-2005 (see Figure 3.2).

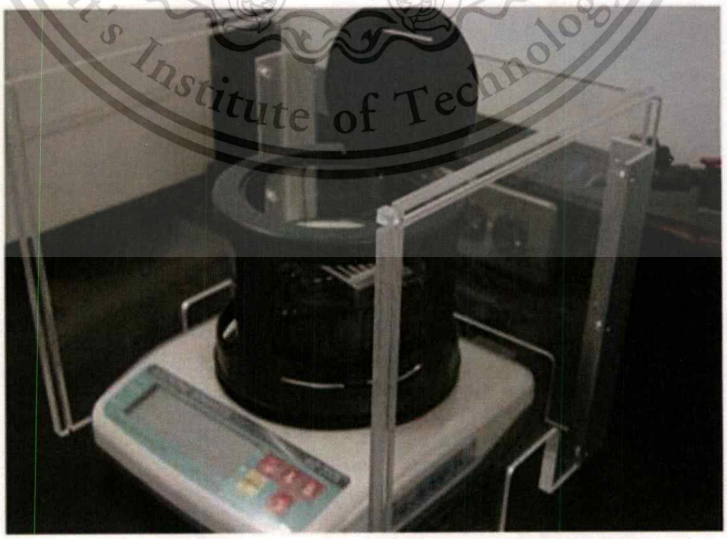

Figure 3.2 Electronic densimeter MD-2005

3.3.1.2 Microstructure

The characterization of the cellular structure of the specimens was observed using the scanning electron microscopy (SEM) JEOL JSM-5410 in Figure 3.4. First, the samples were freeze-fractured in liquid nitrogen. The fracture surface were gold coated to make them conducting by using JEOL JFC-1200 fine coater in Figure 3.3. The cell size and bubble size distribution of the polyurethane were defined by means of the polarized light microscope.

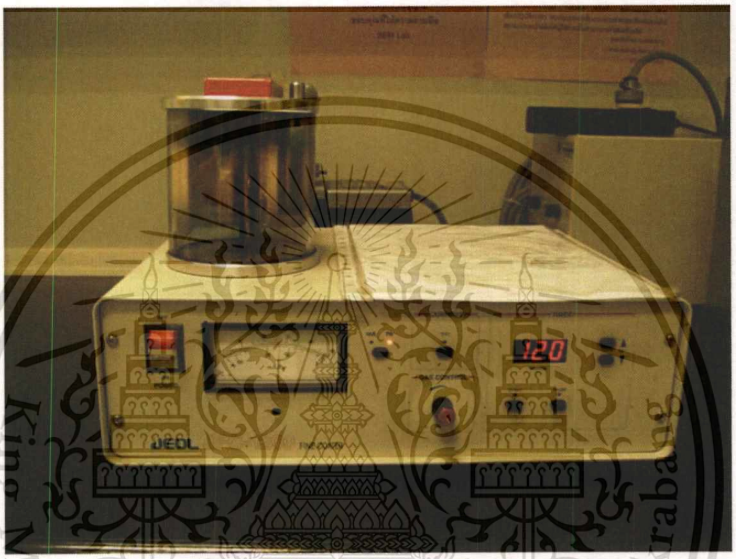

Figure 3.3 Fine coater JEOL JFC-1200

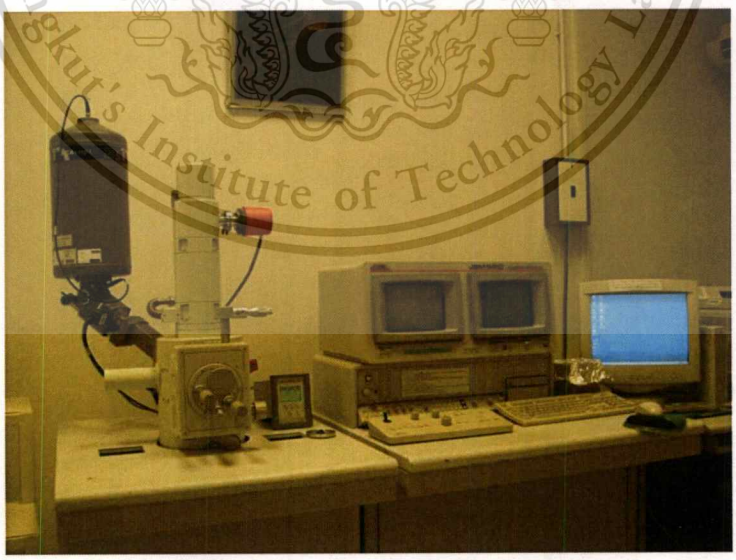

Figure 3.4 Scanning electron microscopy (SEM) JEOL JSM-5410

3.3.1.3 Surface roughness

The surface roughness analysis was performed with Dektak 150 surface profiler. Figure 3.5 shows Dektak 150 stylus profiler. The roughness average (R_a) is universally recognized (see in Figure 3.6) and international parameter of roughness and root mean square (R_q) value of roughness is corresponding to R_a. R_q has the greatest value in the optical application where it is directly related to the optical quality of a surface (see in Figure 3.7). These values were calculated according to Equations (3.2) and (3.3), respectively.

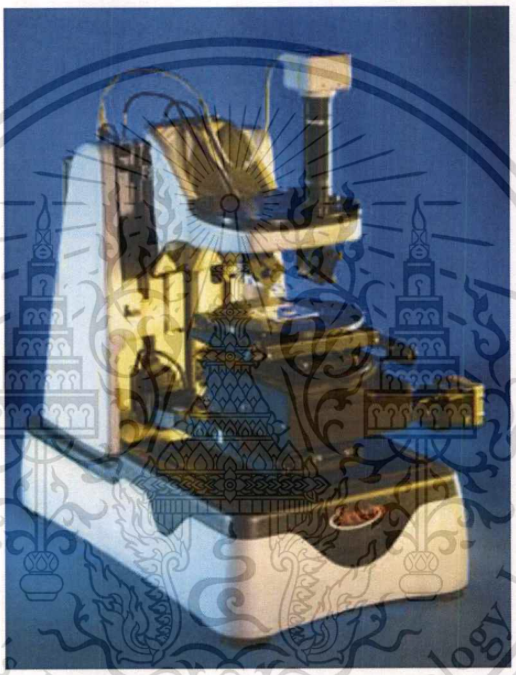

Figure 3.5 Dektak 150 stylus profiler

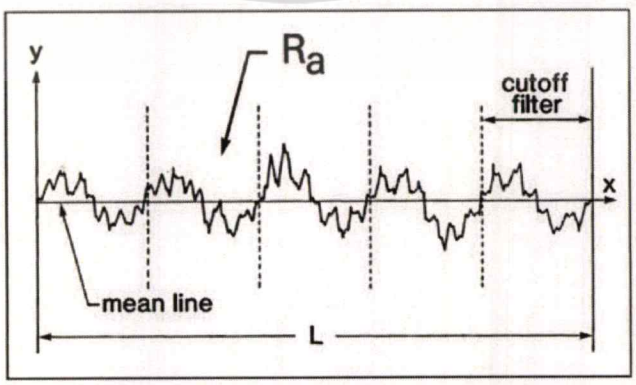

Figure 3.6 Ra Roughness Analytical Function

$$R_a = \frac{1}{L}\int_{x=0}^{x=L} |y| dx \tag{3.2}$$

R_a is the arithmetic average deviation from the mean line within the assessment length (L)

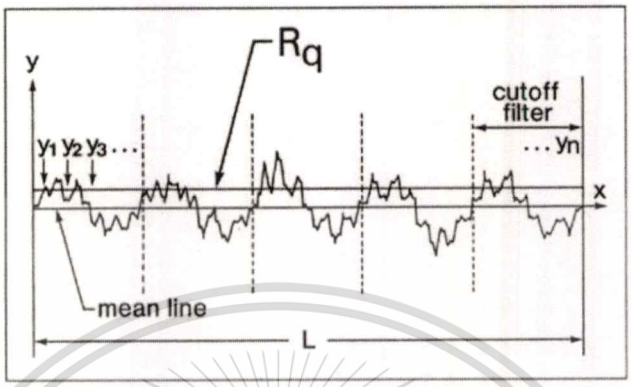

Figure 3.7 R_q Roughness Analytical Function

$$R_q = \sqrt{\frac{1}{L}\int_0^L y^2(x) dx} \tag{3.3}$$

R_q is the corresponding parameter to R_a and is the RMS value of roughness

3.3.2 Mechanical properties

3.3.2.1 Flexural test

Flexural test is used to measure material's ability to resist deformation under load. In this experiment, three-point bending was used. The specimens for flexural test were prepared according to ASTM D 790. Five specimens per sample were tested by using the Universal Testing Machine in Figure 3.8 (Instron Model 55 R4502) with the the support span of 96 mm and the cross head speed of 2.5 mm/min. The results were reported as the flexural strength and flexural modulus.

3.3.3 Thermal property

3.3.3.1 Heat Deflection Temperature test (HDT)

Thermal property was measured by using HDT/VICAT softening temperature tester (Yasuda model HD-PC) in Figure 3.9. According to ASTM D648, a rectangular bar cross section was tested in three points bending machine by applying a load at its center with a constant maximum stress of 0.455 MPa (66 psi) or 1.82 MPa (624 psi). The

dimension of specimen was 127 mm in length, 12 mm in thickness and by any width from 3 to 13 mm. The temperature was raised at the heating rate of 2 ± 0.2°C/min. The heat distortion temperature (HDT)/deflection temperature under load (DTUL) is the temperature at which the specimen deflected by 0.25 mm.

Figure 3.8 The universal testing machine Instron Model 55 R4502

Figure 3.9 HDT/VICAT softening temperature tester (Yasuda model HD-PC)

3.3.4 Adhesion Property

Adhesion testing of the top coat layer is carried out using the cross-cut and pull-off test as qualitative and quantitative measures of adhesion strength, respectively.

3.3.4.1 Cross cut test

Cross-cut test is performed according to the ASTM 3359 which makes the first cut of about 20 mm long. The test is performed by cutting through the top coat layer to the substrate in one steady motion, using just enough pressure to reach the substrate. Next, make a second cut at 90° to each other leading to a network of small squares. Brush the area again and inspect the cuts to ensure that the cut reached the substrate. Then an adhesive tape is attached onto the network and then pulled off by hand at a take-off angle of 180° with respect to the sample surface and almost with a constant force. Percent of squared millimeter surface removed from the surface network is a measure of the adhesion quality. The quality of adhesion is ranked by different numbers ranging from 0B to 5B. Excellent adhesion is assigned by 5B in which no coating could be removed from the metalized surface. By, 4B small flakes have been detached at intersections that account no more than approximately 5% of all the area, 3B small flakes have been detached along edges and at intersections of cuts that approximately 5 to 15 % of the all area is affected, 2B the coating has flaked along the edges and on the parts of the squares that approximately 35 to 65 % of the all area is affected, 0B the flaking is worse than grade 1B.

3.3.4.2 Pull-off test

Adhesion measurements were carried out using the pull-off method according to ASTM D 4541 standard specification. The general pull-off test is performed by securing a loading fixture (dolly, stud) normal to the surface of the coating with an adhesive. To do the pull-off test, the surface of the top coat was first cleaned to remove contaminations. Then cleaned dollies were stuck to the top coat by using epoxy adhesive (Sunnic epoxy) and left for 48 hr to obtain a strong bonding. The strength of adhesion was measured using the Universal Testing Machine Instron 5500 as shown in Figure 3.10. The adhesion strength is reported in terms of N/mm^2.

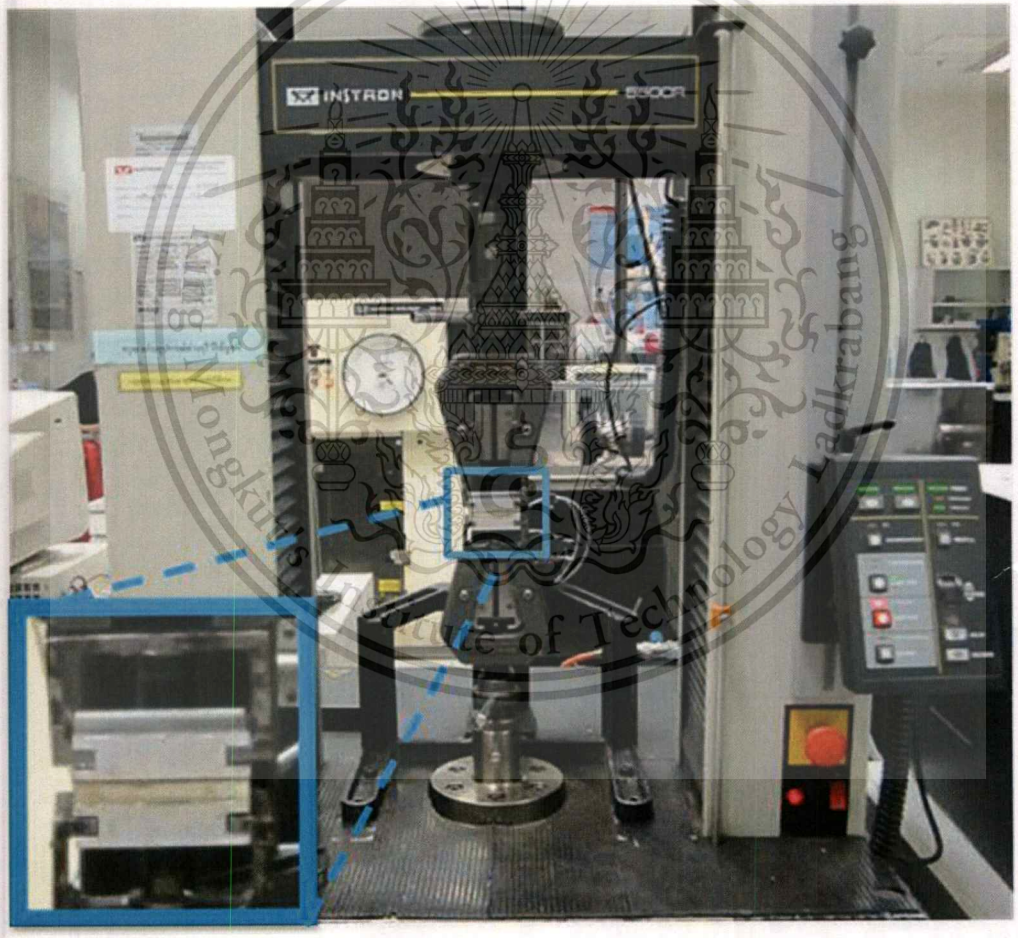

Figure 3.10 The universal testing machine Instron Model 55 R4502 (pull off test assembly)

3.3.5 Contact angle measurement

The contact angle was the angle between a liquid droplet and the surface over which it spread. The measurement of the contact angle gave an indication of the nature of the surface. In this study, the contact angle was measured by sessile drop method. For contact angle measurement the sample were cut with dimension 50 mm in width and 50 mm in length. The contact angle was measured on both sides of the drop with rame′- hart instrument in Figure 3.11, which carried out for at least 5 to 7 droplet. Then work of adhesion was calculated by drop program.

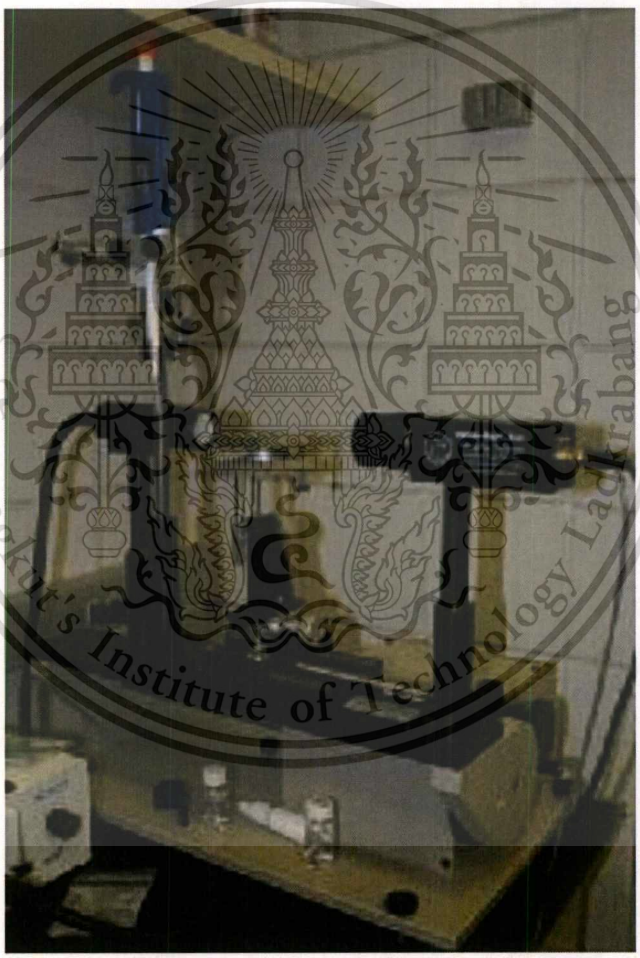

Figure 3.11 The drop with rame′- hart instrument

3.3.6 Structure analysis at the interface between coating film and polyurethane composite foam

3.3.6.1 Digital microscope

The fracture surfaces obtained by pull off test was examined by Dino-Lite shown in Figure 3.12

Figure 3.12 Digital microscope

3.3.6.2 FTIR spectroscopy

The Infrared Attenuated Total Reflectance Spectroscopy (ATR-FTIR) measurement was carried out on the samples. Single beam spectra were collected from 16 scans at resolution 4 cm^{-1} and the data was manipulated using thermo Nicolet 6700 in Figure 3.13.

Figure 3.13 The infrared attenuated total reflectance spectroscopy (thermo Nicolet 6700)

CHAPTER 4

RESULTS AND DISSCUSSIONS

4.1 Effect of processing temperature on mechanical and thermal properties and microstructure

The mold temperature is one of the most important factors that provide significant data for prediction the physical, mechanical and thermal properties of molded part. This effect was studied by several researchers for example Jackovich *et al* [23] demonstrated that mold size and processing temperature had a significant effect on the average physical and mechanical properties of polyurethane foam. In addition, Hatchett and co-worker proposed that processing temperature may be used to target the defined physical and mechanical properties of polyurethane foam without changing the composition of reactant used [18]. Moreover, Mohan *et al* [24] found that the dynamic flexural failure strength increase by 38 % when the processing temperature was increased from 25 °C to 85 °C.

This research work attempted to investigate the effect of mold temperature on mechanical, thermal and morphological properties of polyurethane foam.

4.1.1 Morphology

Not only the rigidity of the polymer matrix but also the cellular structures of the foam could the physical, mechanical and thermal properties of polyurethane foam be influenced. Thus, SEM and image processing program for calculating average cell size were used in this study to measure the cell size and cell size distribution in polyurethane matrix.

The SEM micrographs of the fracture surfaces of polyurethane processed at different processing temperatures are shown in Figure 4.1. The cell size of polyurethane foam processed at 40 °C, 50 °C and 60 °C are shown in Table 4.1. The SEM micrographs analyzed with image analysis program and the number of cell per cubic millimetre are shown in appendix B. Figure 4.2 shows cell size distribution of polyurethane. The results of microstructure studies indicated that

polyurethane foam processed at 40 °C has the most number of cells and the broadest cell size distribution. On the other hand, polyurethane foam processed at 60 °C has the least number of cells and the narrowest cell size distribution. This implies that the processing temperature influence on kinetic of foam formation. This kinetic is followed by the cream time, gel time and tack-free time. The cream time is the start of bubble rise and color of the mixture becomes cream like from dark brown due to the introduction of bubbles. Gel time is the starting point of stable network formation by intensive allophanate crosslinks and urethane. At the tack-free time, the outer surface of the foam loses it stickiness and the foam can be removed from the mold [25]. An earlier work showed the increment of processing temperature resulted in the reduction of gel time of polyurethane [1].

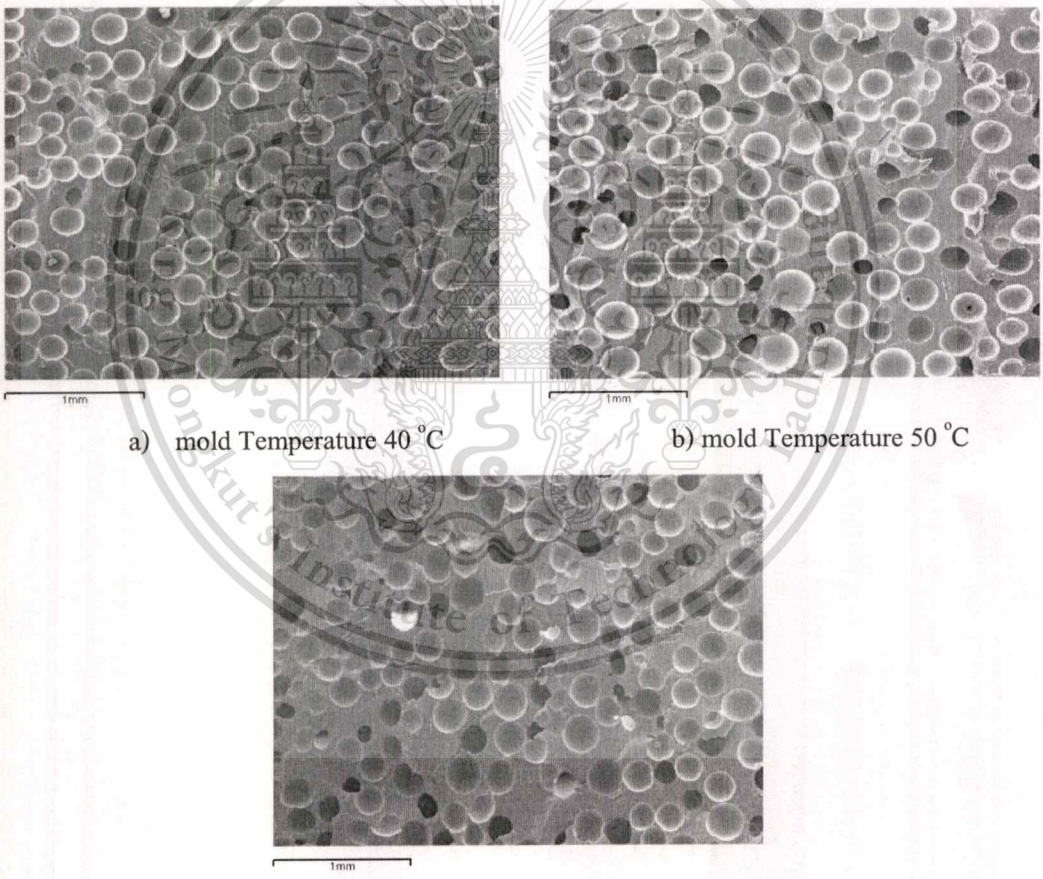

a) mold Temperature 40 °C

b) mold Temperature 50 °C

c) mold temperature 60 °C

Figure 4.1 SEM micrographs of polyurethane prepared at different processing temperature

Table 4.1 The cell size of polyurethane foam processed at 40, 50 and 60 °C

Cell size (μm)	Mold Temperature (°C)		
	40	50	60
Ave	65.38	61.65	59.25
SD	37.58	32.47	34.75

Similar result was obtained by Rungseesantivanon *et al.* [26] who found the relation between processing temperature and gel time by ranging 30-80 °C. It is shown in Equation 4.1.

$$\text{Gel time (min)} = -0.0182 * \text{Mold Temp (°C)} + 2.8684 \quad (4.1)$$

It seems that the closed cell content and cell size of polyurethane are related to processing temperature. In order to obtain the optimum processing temperature, the thermal and mechanical of sample was investigated in the next study.

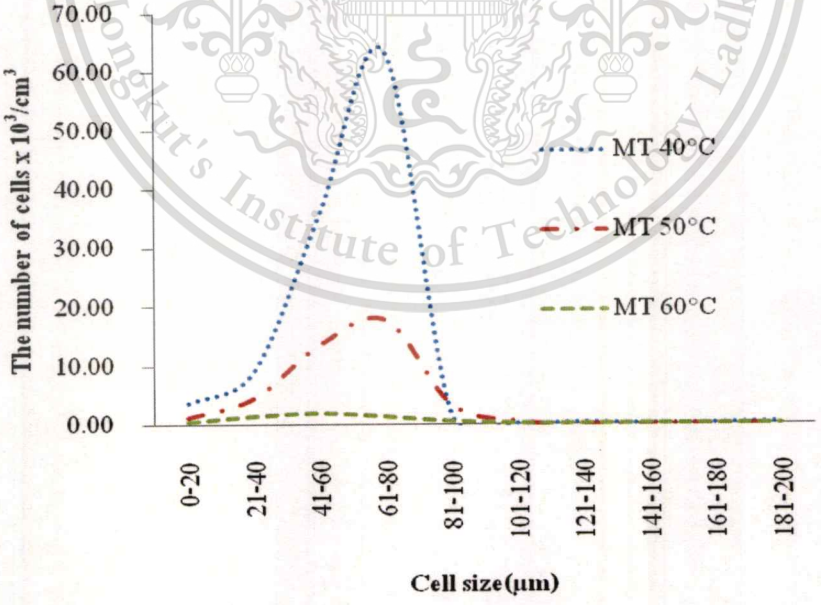

Figure 4.2 Influence of processing temperature on bubble size distribution of polyurethane from 40 °C to 60 °C

4.1.2 Effect of processing temperature on heat distortion temperature

Figure 4.3 exhibits the heat distortion temperature of polyurethane as a function of processing temperature. From the result, it can be observed that the heat distortion temperature of polyurethane processed increases with increasing processing temperature. It was found that the heat distortion temperature of polyurethane increased by 7.2 % and 9.6%, respectively, when the processing temperature was increased from 40 °C to 60 °C. It can be explained that heat distortion temperature value of polyurethane relates to cell microstructure such as cell size and cell size distribution. In Figure 4.1(a), polyurethane foam processed at 40 °C has the highest average cell size and the lowest a solid. Therefore, it has lowest heat distortion temperature value. On the other hand, Figure 4.1 (c) polyurethane foam processed at 60 °C has the lowest porosity and the highest a solid phase of matrix than others, which has higher heat resistance.

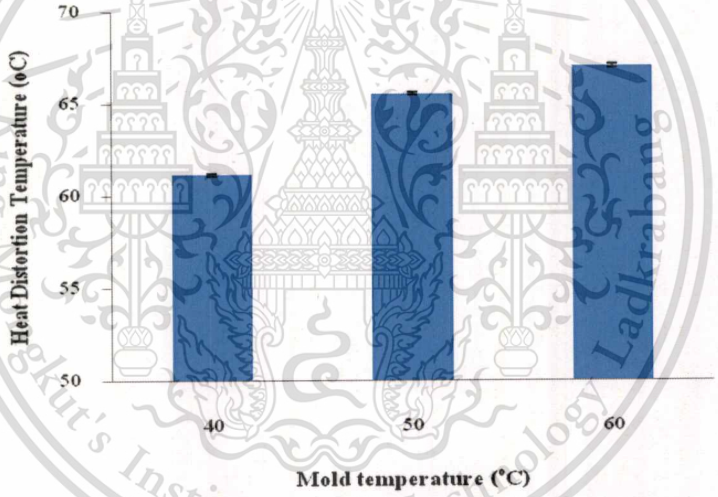

Figure 4.3 Effect of mold temperture on heat distortion temperture of polyurethane

4.1.3 Effect of processing temperature on flexural properties

Table 4.2 Flexural properties of polyurethane

mold temperature	Flexural	
(°C)	Strength (MPa)	Modulus (GPa)
40	11.42 ± 0.39	1.03 ± 0.03
50	37.37 ± 1.74	1.35 ± 0.13
60	61.23 ± 0.91	2.03 0.06

The average flexural properties as a function of processing temperature of polyurethane are shown Table 4.2. It was found that the flexural strength and modulus of polyurethane increased by 26.31 % and 32.51 %, respectively, when the processing temperature was increased from 40 °C to 60 °C. Polyurethane processed at 60 °C has significantly greater resistance to bending. Thus, there is a direct correlation between the microstructure of polyurethane foam and mechanical behavior: with the least number of sizes and narrowest cell size distribution correspond to the highest flexural properties.

In this study, it can be concluded that heat distortion temperature and flexural of polyurethane foam increase with increasing mold temperature. It is likely due to result of the effect of processing temperature that may affect the reaction chemistry resulting in changes in the polymer properties of cell structure, which could be change the mechanical and thermal properties of polyurethane [23]. Kamal *et al.* found that the higher mold temperature reduces the average number of bubbles, which this behavior is expected that the temperature effect of increasing the reaction rate [15].

4.1.4 Effect of processing temperature on adhesion property

In order to prove the effectiveness of the mold temperature on the adhesion, it is required to quantify the adhesion strength. This is conducted by measuring the adhesion strength using the pull-off test and the results are demonstrated in the Figure 4.4. From the result, it was found that the metallic coating of the polyurethane processed at 40 and 50 °C peels while metallic coating of the polyurethane processed at 60-80 °C disappear. Additionally, the contact angle results in Table 4.3 indicated that work of adhesion of polyurethane increases when the mold temperature increases. While, work of adhesion of polyurethane processed at 60, 70 and 80 °C is a similar results and maximum point.

Therefore, it can be conclusion that mold temperature at 60 °C is an appropriate temperature for using in-mold coating process in order to save energy and cost, which will be used in the next study.

Processing Temperature (°C)	Adhesion strength (MPa)	Specimen 1	Specimen 2	Specimen 3
40 °C	0.63 ± 0.128	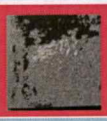		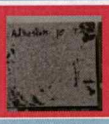
50 °C	0.21 ± 1.58			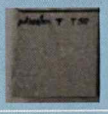
60 °C	0.09 ± 0.06	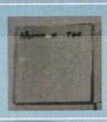	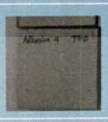	
70 °C	0.15 ± 0.01			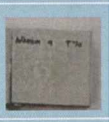
80 °C	0.057 ± 0.02			

Figure 4.4 Pull off result with various processing temperature by ranging 40 – 80 °C

Table 4.3 Contact angles and works of adhesion of polyurethane processed by ranging 40 -80 °C

Processing temperature (°C)	Contact angle (°)	Work of adhesion(mJm^{-2})
40	109±13	50±15
50	102±8	58±10
60	86±1	78±2
70	86±3	78±4
80	88±2	79±10

4.2 Investigation the optimum formula polyurethane composite for in-mold coating process

Density of polyurethane is an important parameter that influences the properties and performance of semi-rigid polyurethane foam. Moreover, the addition of glass fiber to polyurethane foam can be enhanced to provide a range of grades with high strength and stiffness.

The properties of polyurethane can be improved by reinforcements, resulting in higher modulus, strength, and heat deflection temperature under load.

In this study, it is aimed to investigate the optimum polyurethane composite for in-mold coating. Heat distortion temperature and morphological properties of polyurethane and polyurethane composites reinforced with different polyurethane density and weight percents of glass fiber were examined.

4.2.1 Density of polyurethane composite foam and foam volume expansion ratio

Table 4.4 Density of various polyurethane composite formulations

No.	Sample Name	Density (g/cm^3)	Foam volume expansion ratio
1	0.8PU	0.75	1.58
2	0.8PU10%GF	0.77	1.54
3	0.8PU20%GF	0.80	1.49
4	0.8PU30%GF	0.83	1.43
5	0.8PU40%GF	0.89	1.33
6	0.9PU	0.85	1.40
7	0.9PU10%GF	0.86	1.39
8	0.9PU20%GF	0.91	1.30
9	0.9PU30%GF	0.93	1.28
10	0.9PU40%GF	0.95	1.25
11	1.0PU	0.96	1.24
12	1.0PU10%GF	0.97	1.22
13	1.0PU20%GF	1.00	1.19
14	1.0PU30%GF	1.09	1.09
15	1.0PU40%GF	1.13	1.05

Density is one of the most important parameter to control the mechanical and thermal properties of composite foam. The apparent density data and foam volume expansion ratio of composite foams are shown in Table 4.4. The results indicated that have two parameters that affect the composite foam density and foam volume expansion ratio are

(1) Density of polyurethane matrix

The average densities of unfilled polyurethane specimen were 0.75, 0.85 and 0.96 g/cm^3 by volume/weight, which differentiate from the target density ranging from 0.8 to 1.0 g/cm^3, respectively. This is probably because of the weight lost of the reactant, while poured into the mold. In addition, the highest polyurethane density was found that had least weight lost. Furthermore, the result indicated that density of polyurethane matrix has influence composite density. It was found that the high density of polyurethane density matrix resulted in large bulk density. Moreover, foam volume expansion ratio decreased with increasing polyurethane density matrix. Since the free volume mold is constant. At higher polyurethane density matrix, the reactant has higher volume, has less free volume than lower polyurethane density matrix, the reactant has lower volume, which leads to higher foam volume expansion ratio.

(2) Glass fiber content

Composite foam densities increased with the additional amount of glass fiber. This is due to higher density of glass fiber (2.56 g/cm^3), relative to that of polyurethane matrix. While, foam volume expansion ratio decreased with increasing % glass fiber content. It is likely due to glass fiber will be hindered foam expansion. Kim *et al 2009*.found that the cell sizes of foam generally decrease as the glass fiber content increases. Because, the cells around the glass fiber are particularly small that indicated cell growth is hindered by fiber [16]. In addition, bubble rise and growth are also physically hindered by the presence of glass fiber.

4.2.2 Morphology

SEM micrographs of the fractured surface of semi rigid polyurethane foam are shown in Figure 4.5 – Figure 4.7. It can be seen that the cell size distribution of unfilled polyurethane all samples have more uniform than polyurethane composites. While, polyurethane composite, it was found that the cell size distribution is not uniform due to arrangement of glass fiber. In addition, polyurethane at higher density can be seen that cell sizes are smaller than

polyurethane at lower density. Moreover, the increase percent of glass fiber affect on cell size, which is smaller than the cell size of lower percent of glass fiber. In addition, the cell size around the glass fiber are small that implies that cell growth is hindered by the fiber.

After that, these images were analyzed with image processing program that were shown in appendix B. The cell size and cell size distribution of unfilled semi rigid polyurethane densities with ranging from 0.8 to 1.0 g/cm^3 are shown in Figure 4.8. As can be seen from the Figures, the higher density of the unfilled polyurethane, the smaller the cell size and the narrower the cell size distribution will be. This result associates with foam volume expansion. The foam volume expansion ratios were 1.58, 1.40 and 1.24, when the target polyurethane density matrixes were 0.8, 0.9 and 1.0 g/cm^3, respectively. This result can be observed that the higher density of unfilled polyurethane has lower expansion ratio. Therefore, it has the smaller the cell size. In contrast, the lower the density of unfilled polyurethane has higher expansion ratio, indicating that it has the larger cell size.

Figure 4.9 shows the cell size and cell size distribution of polyurethane composite prepared by varying density of polyurethane from 0.8 to 1.0 g/cm^3 and using glass fiber reinforcement range from 0-40%. As a result, the cell size and cell size distribution of all polyurethane composite was random. It is due to glass fiber reinforcement prepared random. Therefore, the cell growth of foam is freedom that area of free volume of mold depends on the distance between the glass fibers.

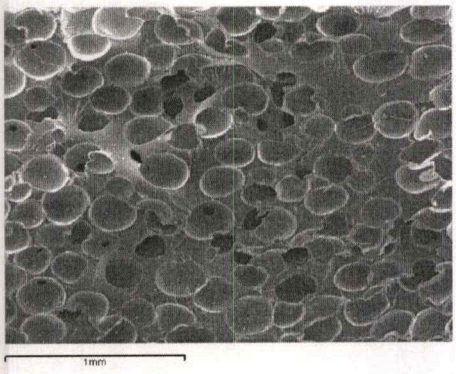

(a) 0%

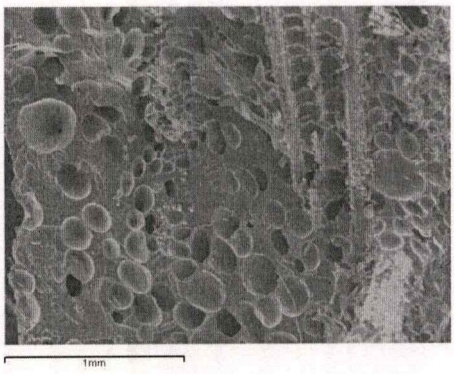

(b) 10%

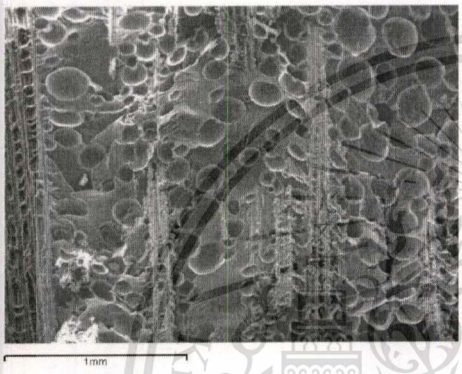

(c) 20%

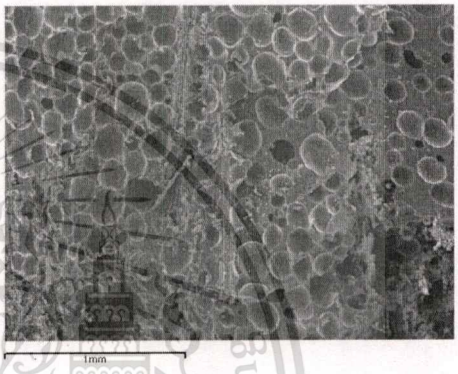

(d) 30%

(e) 40%

Figure 4.5 SEM micrographs of polyurethane density 0.8 g/cm^3 with various percentage of glass fiber

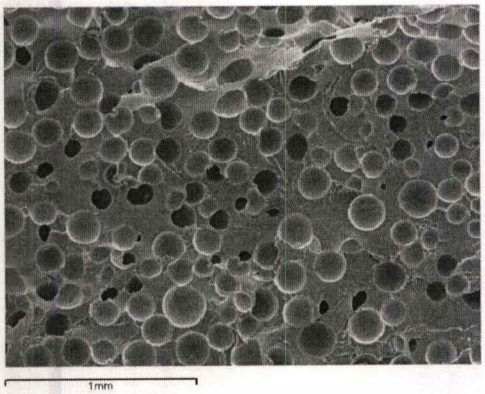

(a)0 %

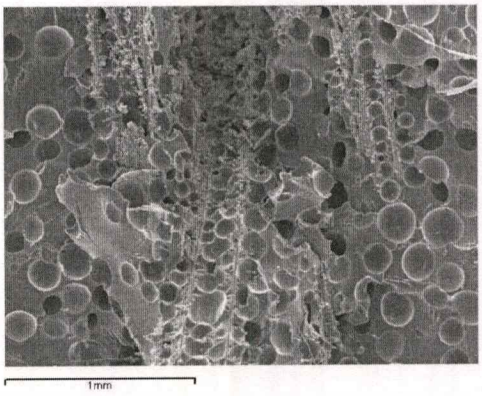

(b) 10 %

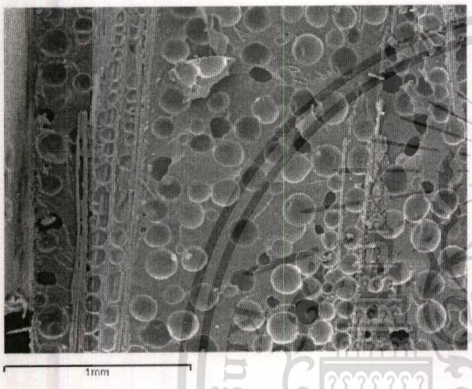

(c) 20 %

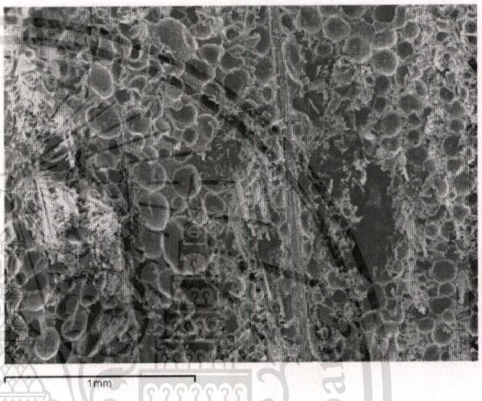

(d) 30 %

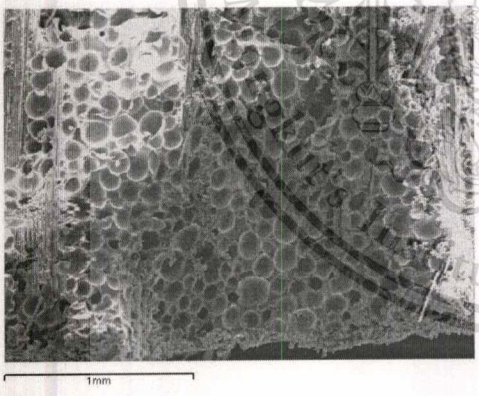

(e) 40 %

Figure 4.6 SEM micrographs of polyurethane density 0.9 g/cm^3 with various percentage of glass fiber

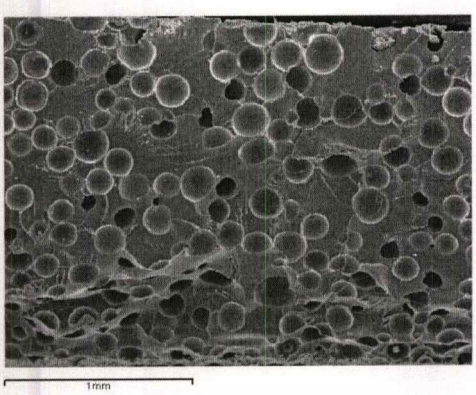

(a)0 %

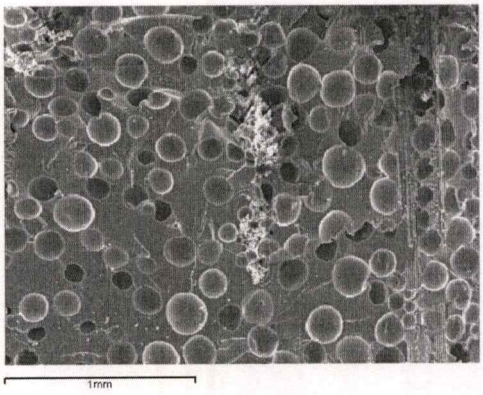

(b) 10 %

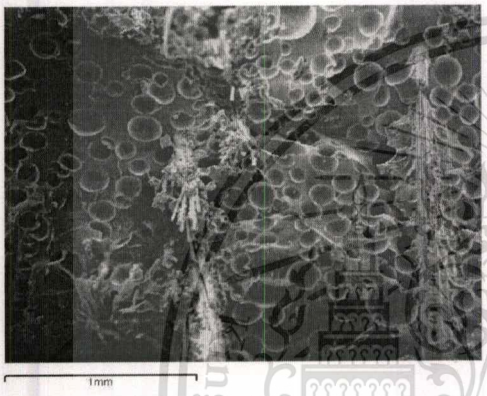

(c) 20%

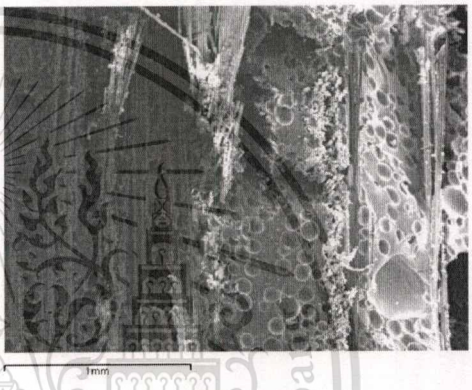

(d) 30 %

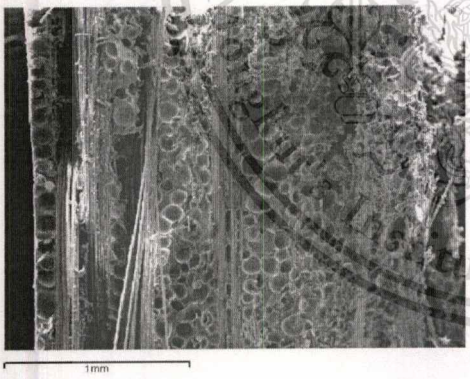

(e) 40 %

Figure 4.7 SEM micrographs of polyurethane density 1.0 g/cm^3 with various percentage of glass fiber

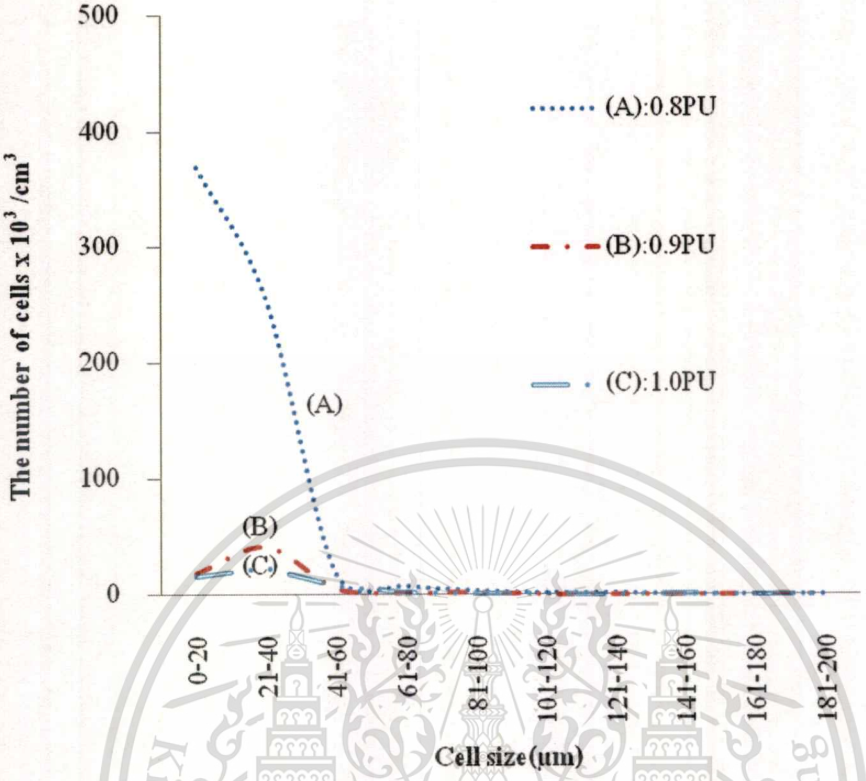

Figure 4.8 Cell size distributions of unfilled polyurethane

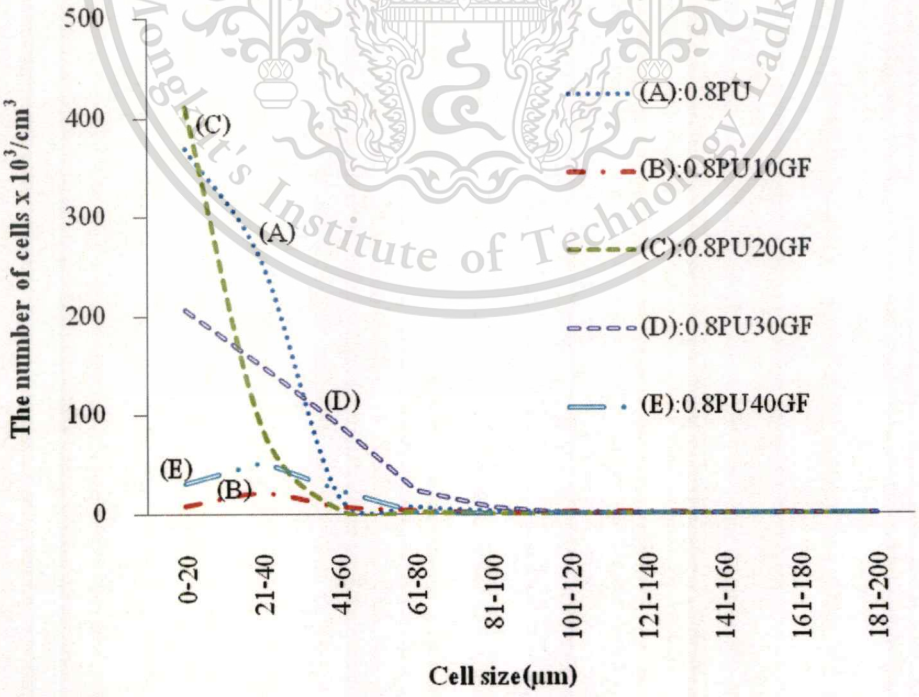

(a) Relative polyurethane density 0.8 g/cm^3

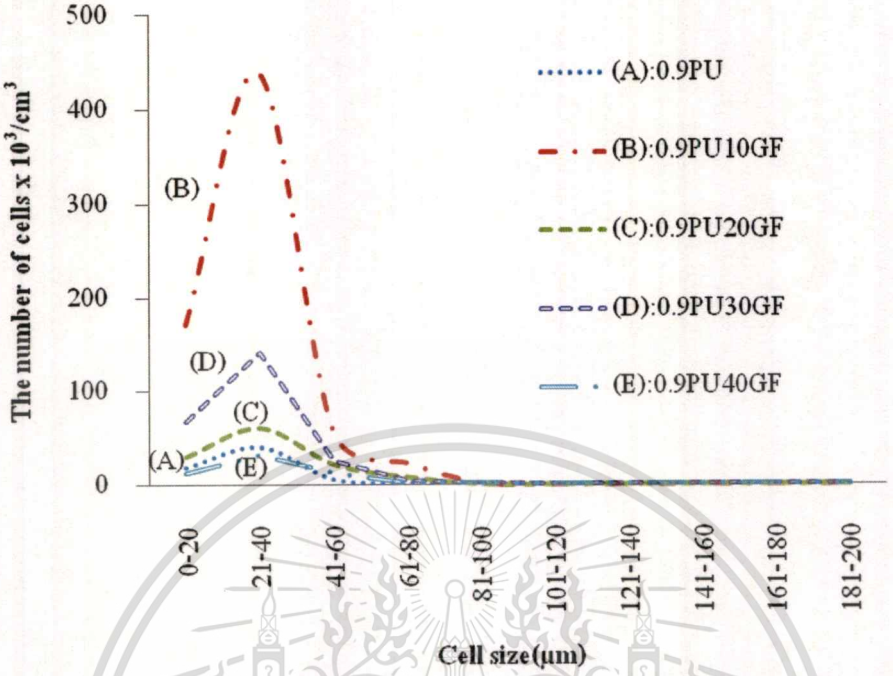

(b) Relative polyurethane density 0.9 g/cm^3

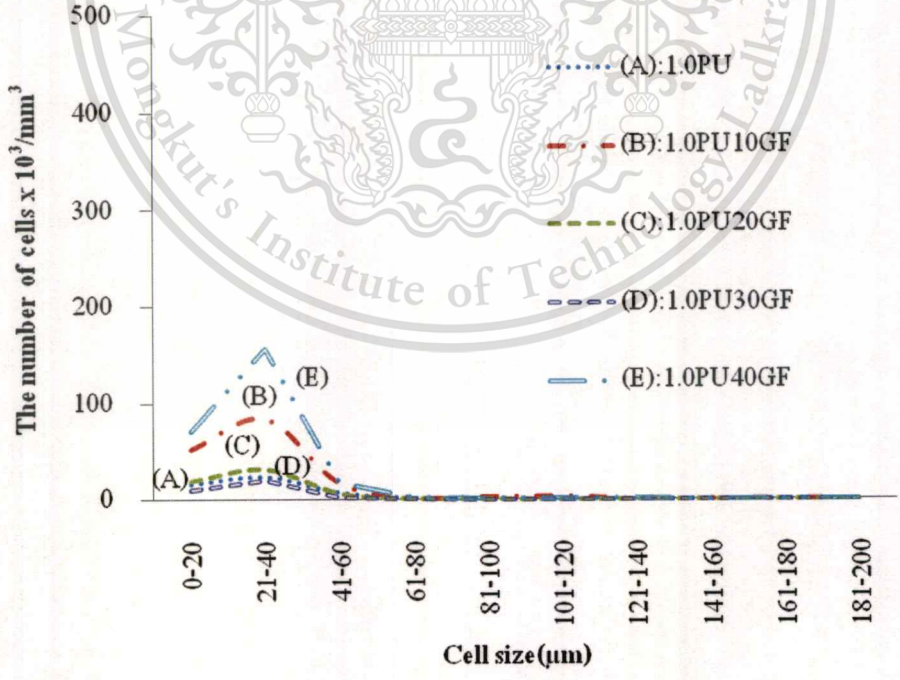

(c) Relative polyurethane density 1.0 g/cm^3

Figure 4.9 Cell size distributions of polyurethane composites

4.2.3 Effect of polyurethane composite formulation on heat distortion temperature

The effect of formulation of polyurethane composites on the heat distortion temperature was investigated by varying the polyurethane density and glass fiber content. As shown in Figure 4.10, the heat distortion temperature of unfilled polyurethane increases from 67.5 to 73.06 °C, or by 8.24%, as the target polyurethane density increases from 0.8 to 1.0 g/cm^3. At higher polyurethane density, the sample to withstand the mechanical load at elevated temperature is also enhanced. Besides, the heat distortion temperature of polyurethane composites increases with the fiber content. It can be seen that heat distortion temperature of lowest density of polyurethane 0.8 g/cm^3 containing 0% to 40 %glass fiber increases from 67.5 to 91.12 °C or 35%. The heat distortion temperature of density of polyurethane 0.9 g/cm^3 containing 0% to 40 %glass fiber increases from 69.4 to 140.9 °C or 103%. The heat distortion temperature of density of polyurethane 1.0 g/cm^3 containing 0% to 40 %glass fiber increases from 73.06 to 239.04°C or 150.41%.

The heat distortion temperature as function of polyurethane density was found that high density foams more affect by glass fiber loading than lower polyurethane density. It is due to density of polyurethane matrix related to cell structure that influenced on the properties of polyurethane composite. It can be seen that the lower polyurethane density has highest porosity, larger cell size and the boarder the cell size distribution that it can be easily to collapse, whereas higher polyurethane density has higher solid phase, the smaller cell size and the narrower the cell size distribution that it can be difficult to collapse. Therefore adding glass fiber at higher polyurethane density significantly increases heat distortion temperature than lower density. Moreover, the heat distortion temperature increases with adding amount of glass fiber. It is due to glass fiber has a high heat resistance. It was found that upper 20% glass fiber showed predominant heat distortion temperature value.

However, the optimum polyurethane composite for in-mold coating process was determined by the service temperature concretely defined at 100 °C according to the supplier. Therefore, the optimum polyurethane composite formulations consist of polyurethane matrix at densities of 0.9 and 1.0 g/cm^3 which containing 30 and 40 % glass fibers. The optimum polyurethane composite formulation used in the next study is polyurethane matrix at density of 1.0 g/cm^3 which containing 30 % glass fiber as a result of heat distortion temperature value and density.

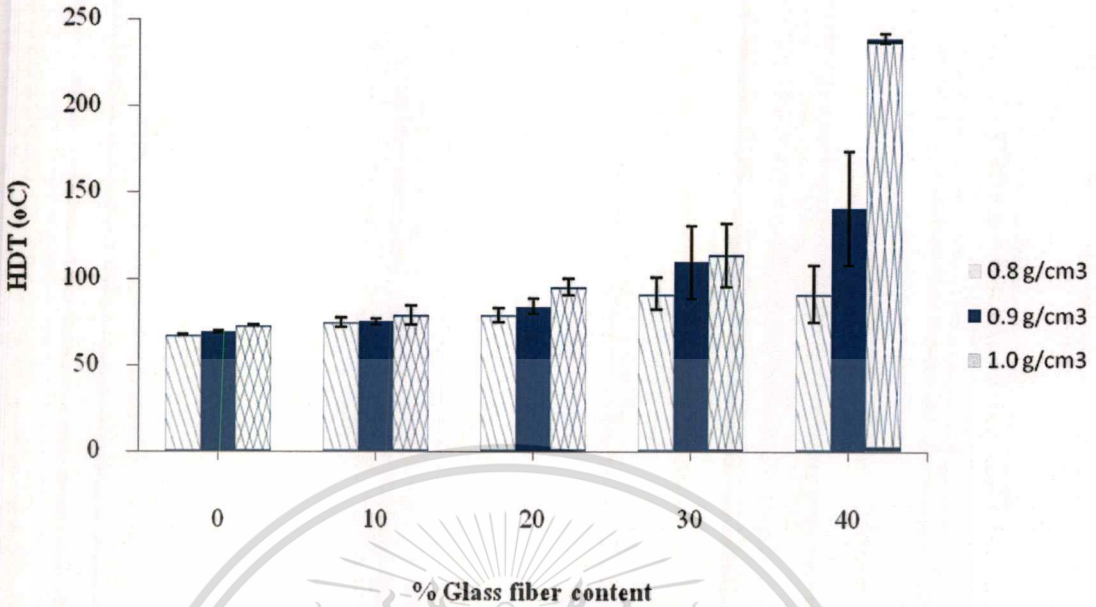

Figure 4.10 Heat distortion temperatures of polyurethane composites with various percentages of glass fiber

4.3 Investigations of the adhesion between the coating layer (PLANITTO #250) and the optimum polyurethane composite during in-mold coating with primer

The optimum polyurethane composite from previous study was prepared by conventional process (PUCS) and in-mold coating process with vinylester (IMC). After processing, each sample was coated with PLANITTO #250 from CH INDUSTRY CO., LTD and underwent the following tests:

4.3.1 Contact angle measurements

Figure 4.11 displays the appearance of water droplet on the samples. Table 4.5 shows the contact angles and adhesion works of PUCS and IMC. The results show that the contact angle of IMC sample give the lower contact angle value than PUCS sample. The decrease in contact angle value is an indication of the increase in adhesion force through the relationship between contact angle and work of adhesion. The decrease in contact angle values on the coated polyurethane composite surface can be likely ascribed to the creation of polar moieties and surface roughness. In the next study, ATR-FTIR spectroscopy and surface roughness are used to evaluate the influence of the surface modifications produced by the in mold coating on the

adhesion properties of coated polyurethane composites which will be explained in the section 4.3.2-3.

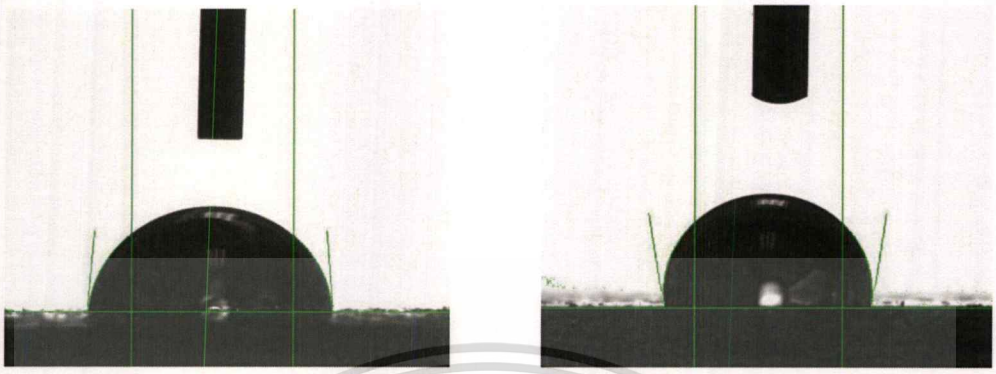

(a) In-mold coating process (b) conventional process

Figure 4.11 Dynamic contact angles (θ) of water drop on the surface of polyurethane composites prepared by different process

Table 4.5 Contact angles and adhesion works of polyurethane composite prepared conventional process and in-mold coating process.

	in-mold coating process	conventional process
Contact angle (^{o})	83 ± 6	96 ± 5
Work of adhesion(mJm^{-2})	81 ± 7	65 6

4.3.2 FTIR analysis

In order to prove the relation between contact angle and polarity the ATR-FTIR spectroscopy was used to analyze the chemical modifications produced on the polyurethane composites by the in-mold coating process (Figure 4.12 and Table 4.6). The ATR-FTIR spectrum of PUCS shows its main band at 3297.44, 2918.45, 2849.73 ,2276.57 and 1703.57 cm^{-1} which are respectively the N-H stretching of polyurethane group, C-H stretching bands of CH_2 and CH_3 groups in the polyurethane (2918.45, 2849.73 cm^{-1}) CN stretch vibration and H-bond urethane.

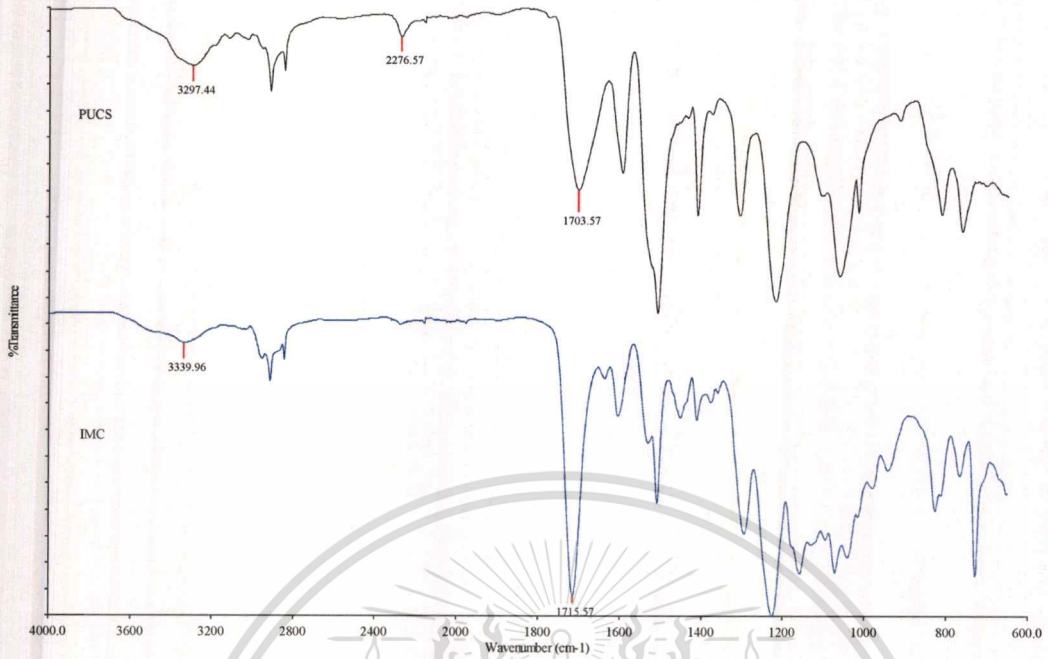

Figure 4.12 ATR-IR spectrum of polyurethane composite by conventional process and in mold coating process

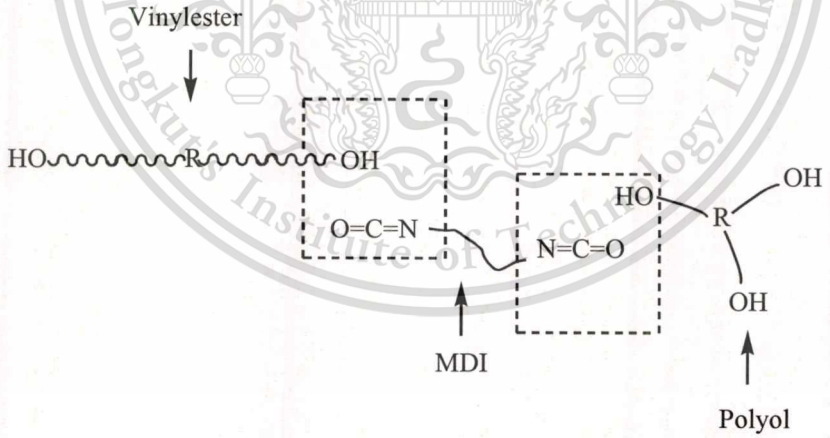

Figure 4.13 Schematic diagram of the reaction mechanism and structure of PU-VER

Table 4.6 FTIR band assignments of PUCS and IMC [9, 41]

Band	Wavenumber (cm^{-1})	
	PUCS	IMC
N-H stretching	3297.44	3339.96
CH_2 asymmetric stretching vibration	2918.45	2918.04
CH_2 symmetric stretching vibration	2849.73	2849.47
NCO asymmetric stretching vibration	2276.57	-
C=O stretching and C-O stretching vibrations of the ester group	-	1715.57
C=O stretching vibrations	1703.57	-
C-C aromatic stretching vibration	-	1638.37
C-C aromatic stretching vibration	-	1605.92
C-C aromatic stretching vibration	1596.2	-
C-C aromatic stretching vibration	-	1531.23
C-C aromatic stretching vibration	1508.9	1509.5
C-H bending vibration	-	1453.05
Amide II	1435.75	-
Amide	1411.85	1412.61
C-H bending vibration	1377.15	1377.89
Amide	-	1361.63
CH aromatic in-plane deformation	1308.43	-
CH aromatic in-plane deformation	-	1296.16
C-O-C stretching vibration	-	1159.76
C-O-C stretching vibration or C-C-O in phase	763.8	767.38

The comparison ATR-FTIR spectrum between PUCS and IMC show the N-H shifted at the wavenumbers from 3297.44 to 3339.96 cm^{-1} and intensity of the IR band of CN group in isocyanate band at 2276.57 cm^{-1} decreased. An increase in intensity of the IR band corresponding to the C=O stretching vibration was observed. It is possible to by product of the reaction between the mixture of polyurethane (isocyanate) and vinylester and it could be due to C=O stretching and C-O stretching vibrations of the ester group. Polyurethane reaction is a step growth polymerization, whereas vinylester reaction is a free radical copolymerization. The formation of isocyanate group of the reactant of polyurethane and hydroxyl group of vinylester is shown schematic in Figure 4.13. In addition, comparison of band ratio between PUCS and IMC was utilized to follow molecular level changes resulting from reaction of isocyanate group of the reactant of polyurethane and OH group of vinylester. The band ratios are summarized in Table 4.7. It can be seen that (NCO/C-H) band ratio of PUCS has more than IMC. While, (C=O/C-H) band ratio of PUCS has less than IMC. Beer and Lambert [14] suggested the intensity of the emitted radiation depends upon the concentration of the sample. From the result, the ATR-FTIR spectrum of IMC shows that the intensity of isocyanate band (NCO) at 2276.57 cm^{-1} decreases or disappears which implies isocyanate groups react with hydroxyl groups of vinylester to create another urethane linkage, increase in the intensity of the IR band corresponding to the C=O stretching vibration at 1715.57 cm^{-1}. The vinyl ester treatment modifies the polyurethane surface by creating polar moieties (C=O, C-O) which associate with decrease contact angle value. This result is in agreement with results obtained in contact angle measurement data and the adhesion strength. It can contribute to enhance wettability and increase its adhesion properties.

Table 4.7 Comparison of Band ratio of PUCS and IMC

	Area		Band ratio
PUCS	NCO	C-H	(NCO/C-H)
	17536.86	7145.48	2.45
PUCS	C=O	C-H	(C=O/C-H)
	10840.31	7145.48	1.517
IMC	NCO	C-H	(NCO/C-H)
	10045.24	5833.12	1.72
IMC	C=O	C-H	(C=O/C-H)
	16986.81	5833.12	2.91

4.3.3 Surface roughness

In order to demonstrate the feasibility of the proposed method for measuring contact angles, surface roughness tester was carried out. The surface roughness data of PUCS sample and IMC sample are depicted in Figure 4.14. Surface roughness averages of the PUCS sample and the IMC sample are shown in Table 4.8. It is observed that surface roughness of IMC sample increase its R_a and R_q about 631% and 351%, respectively in comparison with PUCS. The result indicates that surface roughness of IMC sample is rougher than PUCS sample. The higher surface roughness attribute to better mechanical interlocking at the interface. This observation accordance with contact angle measurement which suggests that polyurethane composite in-mold coated with vinyl ester by in-mold coating decrease contact angle and increase work of adhesion.

Table 4.8 Surface roughness value

Surface	R_a(μm)	R_q(μm)
IMC sample	49.90 ± 43.05	46.09 ± 54.23
PUCS sample	6.83 ± 4.53	10.20 ± 7.06

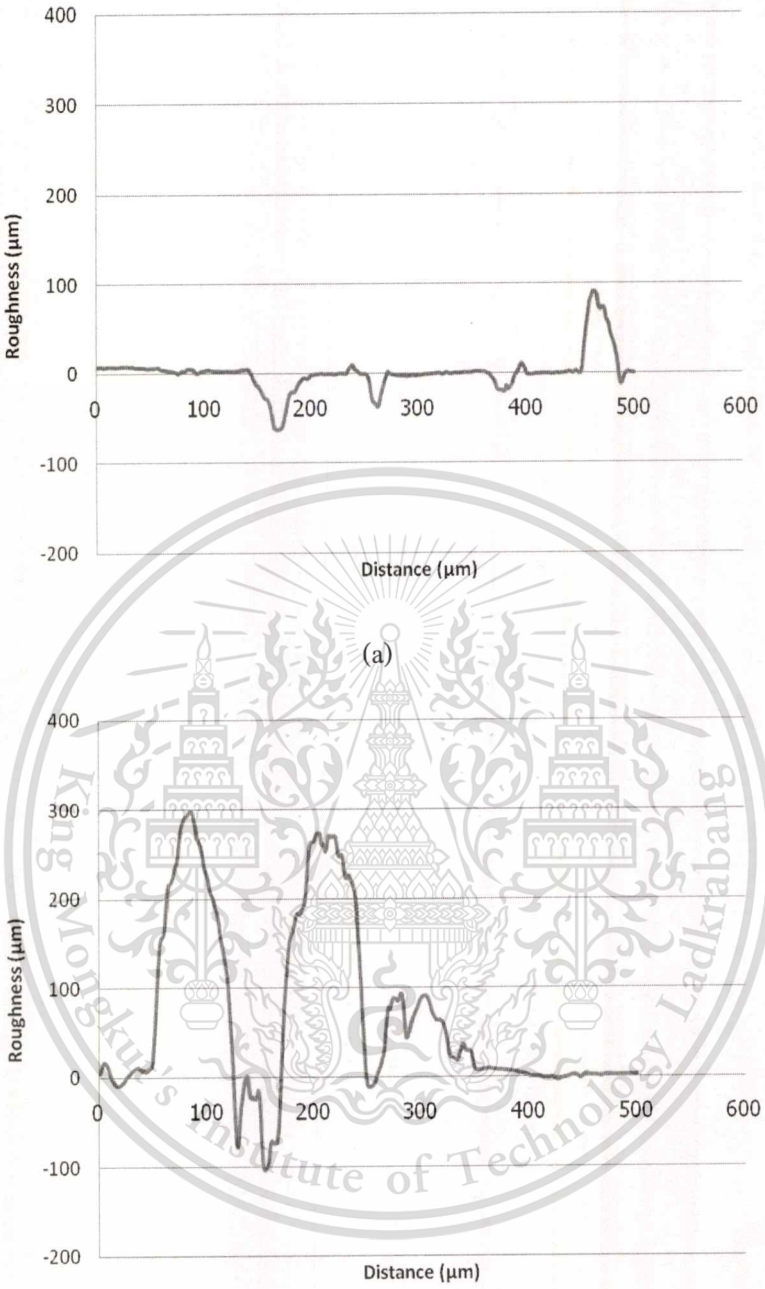

Figure 4.14 Line profile of the surface roughness for (a) conventional process (b) in-mold coating Process

4.3.4 Cross cut measurement

The samples after adhesion test by using the cutter and adhesive tape are shown in Figure 4.15.

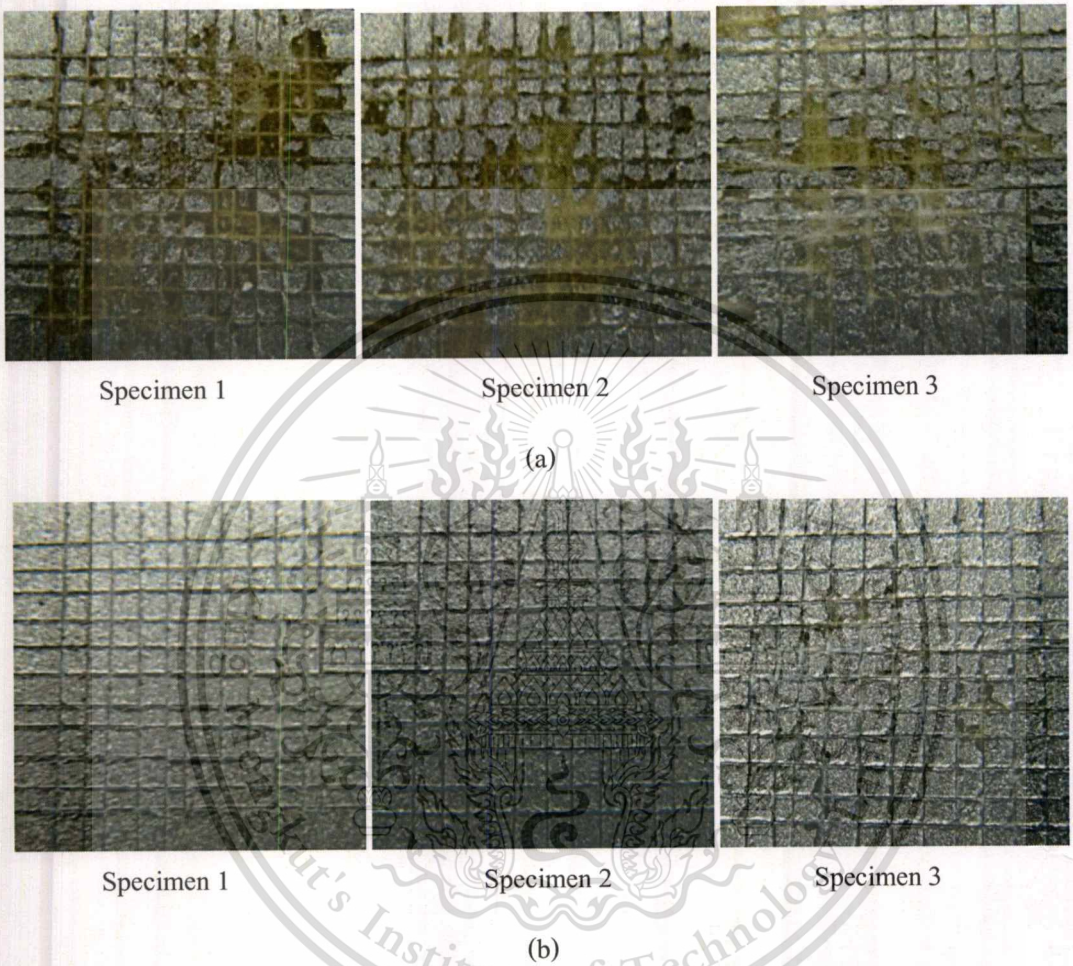

Figure 4.15 Polyurethane composites prepared by (a) conventional process, (b) in-mold coating process, after the ASTM D3359 cross cut test

It can be seen that the adhesion between the PLANITTO# 250 and the substrate is poor in case of the PUCS sample. Figure 4.15(a) shows the PLANITTO# 250 of PUCS sample has flaked in long strip along the cut edges and whole squares have been detached. Approximately 35 to 65 % of the grid is affected. On the other hand, Figure 4.15(b) exhibits that small flakes have been detached at intersection, affecting no more than approximately 5% of the area. The level of adherence of two processes is concluded in Table 4.9.

The adhesion between PLANITTO# 250 and PUCS sample was found to be poor.

On the other hand, the adhesion between PLANITTO# 250 and IMC sample was found to be very good.

Table 4.9 Evaluation of the adhesion between the PLANITTO# 250 and polyurethane composites produced by conventional and in-mold coating process

Method	Level of adherence
conventional	1B (poor)
In-mold coating	4B (very good)

4.3.5 Pull off measurement

The results of ASTM D4541 tests are summarized in Table 4.10. In case of conventional polyurethane, the average adhesion strength at which samples failed and standard deviation are 0.88 MPa and 0.28 MPa, respectively. Adhesion experiments with In-mold coated polyurethane, the average adhesion strength of 1.35 MPa and the standard deviation of 0.46 MPa. This resulted indicated that adhesion strength between polyurethane composite and PLANITTO# 250 can be improve by treating polyurethane composite with vinyl ester by in-mold coating process, which increases 53.41%.

Table 4.10 Adhesion strength of the polyurethane composite comparison between conventional process and used by in-mold coating process (in terms of MPa)

Method	Adhesion Strength
Conventional	0.88 ± 0.28
in-mold coating	1.35 ± 0.46

Both cross cut test and pull off test indicated that in-mold coating process with vinylester help improve the adhesion between the PLANITTO# 250 and polyurethane composite. This result can be explained that vinyl ester improved the wettability due to the formation of polar moieties mainly C=O and C-O and increase roughness surface of polyurethane composite.

4.3.6 Failure mode in pull out test

The fractographs of pull off test of PUCS and IMC samples are illustrated in Figure 4.16. It can be seen that the coating failure in pull out test of both specimens was a combination of adhesive (Ad) and cohesive failure (Co).

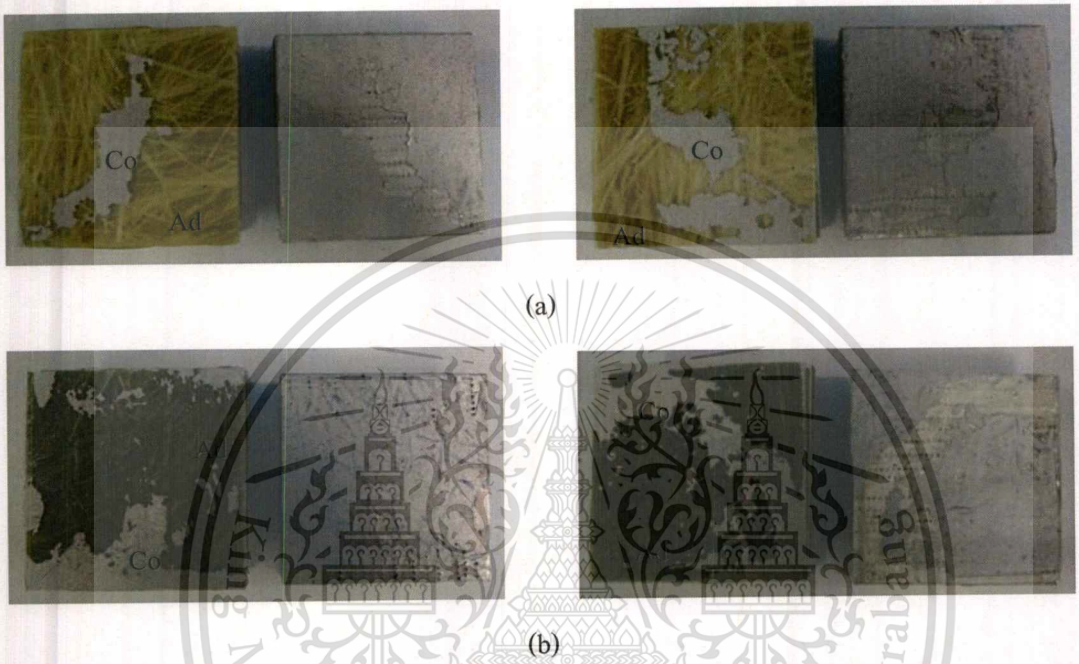

Figure 4.16 Pull off test, result of polyurethane composites prepared by (a) conventional process, (b) in-mold coating process

4.3.6.1 Digital microscope

In order to prove adhesion of IMC sample, digital microscope was used to investigate. Figure 4.17 depicts fractography by optical microscope. It can be seen that vinyl ester adhere between the coating film and substrate. It is implies that incorporation significantly increased the bonding strength of the coating, which relates to pull off result in section 4.3.5.

(a) (b)

Figure 4.17 Pull off test, result of polyurethane composites prepared by in-mold coating process (a) peeled coating film (b) IMC substrate

4.3.6.2 FTIR analysis at interface of fracture sample

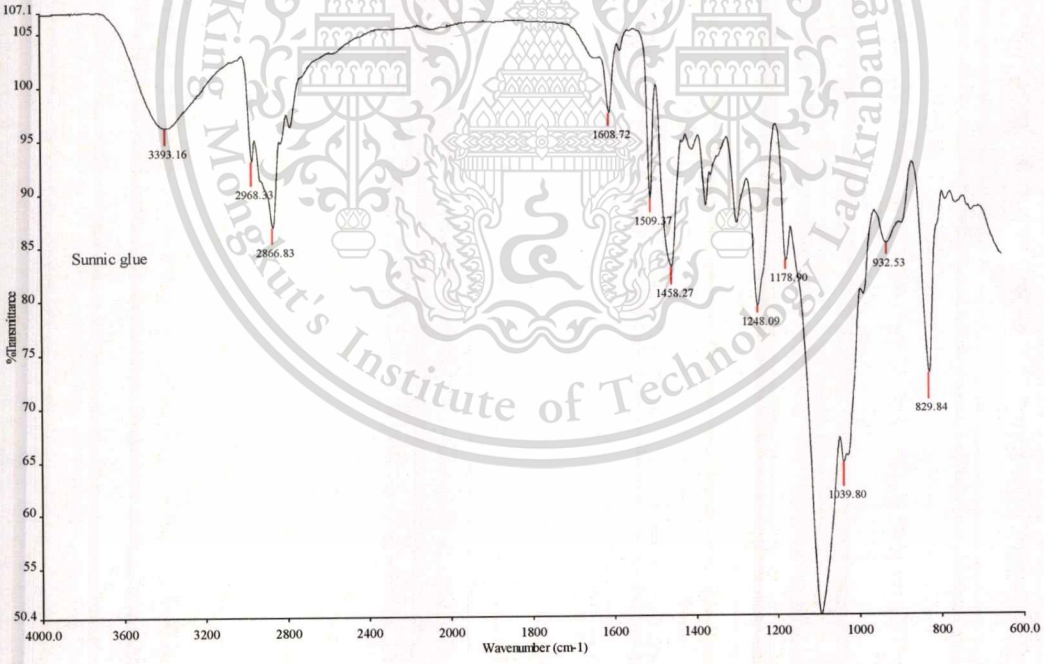

Figure 4.18 ATR-IR spectrum of Sunnic glue

Figure 4.18 shows the ATR-IR spectrum of the Sunnic glue before pull off test. Typical band correspond to N-H stretching absorption at 3393.16 cm^{-1}, C-H stretching bonds of CH_2 and CH_3 groups in the Sunnic glue (2,866.83 and 2,968.33 cm^{-1}), N-H bending absorption at 1608.72 cm^{-1}, C=C stretching band at 1509.37 cm^{-1}, C-H stretching bands at 1458.27 and

1373.64 cm^{-1}, C-H aromatic in-plane deformation band at 1298.12 cm^{-1}, C-O stretching bands at 1248.09 and 1178.90 cm^{-1}, C-O-C asymmetric stretch band at 1096.46 cm^{-1}, 1039.80 cm^{-1} and 932.53 cm^{-1} and C-O-C symmetric stretching band at 829.84 cm^{-1}.

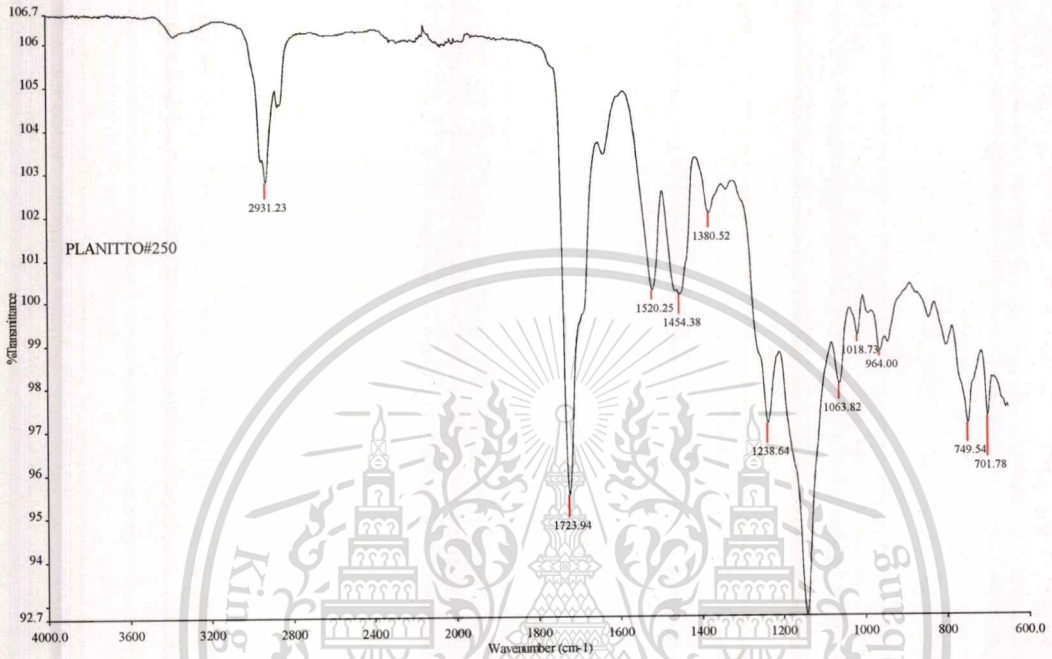

Figure 4.19 ATR-IR spectrum of PLANITTO# 250

PLANITTO# 250 is 2-component 2C1B (Acryl resin paint / Isocyanate) The ATR-IR spectrum of the metallic coating (PLANITTO# 250) is illustrated in Figure 4.19. Typical band correspond to C-H stretching adsorption band at 2931.23cm^{-1}, C=O stretching absorption at 1723.94 cm^{-1}, C=C stretching band at 1520.25 cm^{-1}, C-H stretching bands at 1454.38 and 1380.52 cm^{-1}, C-O stretching bands at 1238.64 and 1143.55 cm^{-1}, C-O-C asymmetric stretch band at 1063.82 cm^{-1}, 1018.73 cm^{-1} and 964 cm^{-1} and C-H aromatic band at 749.54 and 701.78 cm^{-1}.

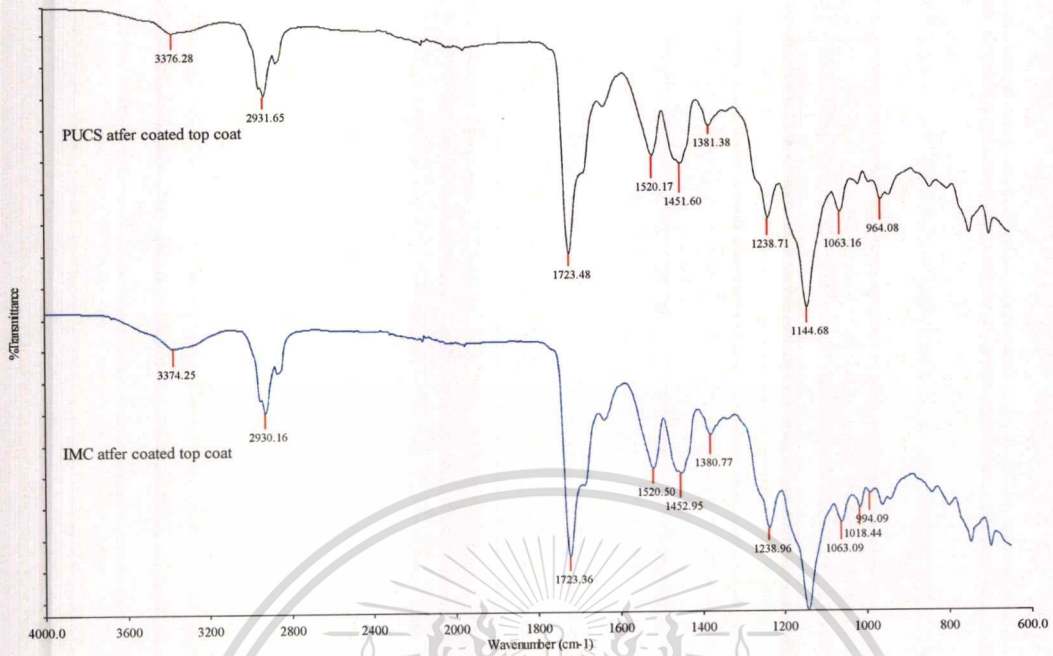

Figure 4.20 ATR-IR spectrum of IMC sample and PUCS after being coated PLANITTO# 250 (top coat)

Figure 4.20 shows typical ATR-IR spectrum of IMC sample and PUCS coated PLANITTO# 250 that is similar characteristic to PLANITTO# 250. The spectrum of IMC sample coated with top coat shows its bands at 3374.25, 2930.16, 1723.36, 1520.50, 1452.95, 1380.77, 1238.96, 1144.83, 1063.09, 1018.44 and 994.09 cm^{-1} while The spectrum of PUCS coated top coat shows its bands at 3376.28,2931.65, 1723.48, 1520.17, 1451.60, 1381.38, 1238.71, 1144.68, 1063.16 and 964.08 cm^{-1} which are respectively the N-H stretching band, C-H stretching band, C=O stretching band, C=C stretching band, C-H stretching band, C-O stretching bands and C-O-C asymmetric stretch band. The spectrum is tabulated with the key peaks identified in Table 4.11.

Table 4.11 FTIR Band Assignments of PUCS and IMC which both coated by PLANITTO# 250.

Band	Wavenumber (cm^{-1})	
	PUCS coated top coat	IMC coated top coat
N-H stretching	3376.28	3374.25
CH_2 asymmetric stretching vibration	2931.65	2930.16
CH_2 symmetric stretching vibration	2872.26	2872.02
C=O stretching vibrations	1723.48	1723.36
C-C aromatic stretching vibration	1639.16	1639.42
C-C aromatic stretching vibration	1520.17	1520.5
C-H bending vibration	1451.6	1452.95
C-H bending vibration	1381.38	1380.77
C-N-C asymmetric stretch	1144.68	1144.83
CH_2 in-plane-rock	749.43	749.36

In addition, comparison between spectrum of IMC sample (Figure 4.12) and IMC sample coated PLANITTO# 250 was found that the C=O shifted at the wavenumber from 1715.57 to 1723.36 cm^{-1}, 1227.14 to 1238.96 cm^{-1}, 1159.77 to 1144.83 $cm^{-1}$and 1073.38 to 1063.09 cm^{-1} while, bands at 1638.38 and 1605.92 cm^{-1}(C=C stretching), 1412.61 cm^{-1}(C-H stretching) and 1159.77 cm^{-1} (C=O stretching) disappear. Furthermore, spectrum of PUCS sample (see Figure 4.12) and PUCS sample coated PLANITTO# 250 was found that the C=O shifted at the wavenumber from 1703.57 to 1723.48 cm^{-1}, the C=C shifted band from 1508.90 to 1520.17 cm^{-1}, the C-O shifted band from 1219.40 to 1238.72 $cm^{-1}$and the C-O-C shifted band from 1062.90 to 1063.17 cm^{-1} while, N-H stretching band at 2276.57 cm^{-1}, C=C stretching band at 1596.20 cm^{-1}, C-H stretching bands at 1411.85 and 1308.43 cm^{-1} and C-O bands at 1219.40 cm^{-1}disappear.

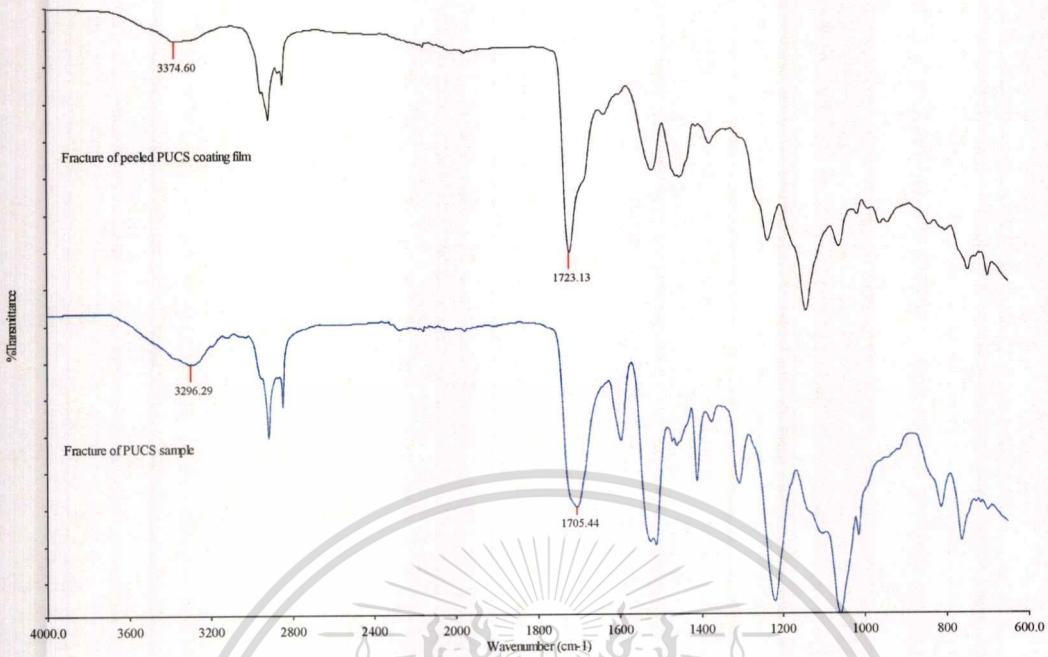

Figure 4.21 ATR-IR spectrum of failed surface of polyurethane composite by conventional process

To properly assess the failure of pull off test, the ATR-IR spectrum of the failure surface after pull off test is carried out and compared to the ATR-IR spectrum of the PUCS sample (see Figure 4.12) and the PUCS after coated the top coat before pull off test (see Figure 4.20). From the result, it can be seen that the ATR-IR spectrum of the fracture of peeled PUCS coating film is similar to the spectrum of PUCS coated top coat (see Figure 4.20). While, the ATR-IR spectrum of the fracture of PUCS sample corresponds to the PUCS sample (see Figure 4.12).

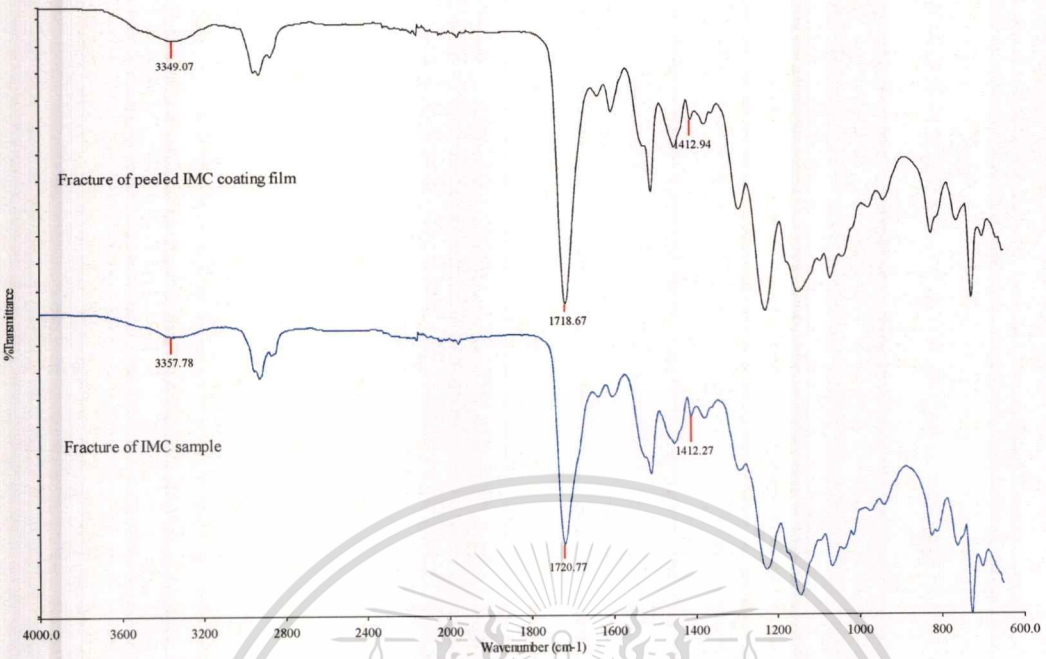

Figure 4.22 ATR-IR spectrum of failed surface of polyurethane composite by in-mold coating process

In order to confirm cause increase adhesion strength between IMC sample and top coat which compared with adhesion strength between PUCS sample and top coat, the ATR-IR spectrum of the failed surface of IMC coated top coat and sample (see Figure 4.22) compared to the ATR-IR spectrum of surface of PUCS coated top coat film and sample the failed (see Figure 4.21). It can be observed that the spectrum of the fracture of peeled IMC coating film shows the amide band at wavenumber 1412.94 cm^{-1} [41]. While, the spectrum of the fracture of peeled PUCS coating film disappears. This implies that adhesion strength between polyurethane composite in-mold coated by in-mold coating process with vinylester and PLANITTO#250 has more than the adhesion between polyurethane by conventional process and PLANITTO# 250 which is due to reaction between isocyanate of polyurethane and hydroxyl group of vinyester.

CHAPTER 5

CONCLUSIONS AND SUGGESTIONS

5.1 Conclusions

In-mold coating process is used to improve surface of a part. This research presents to investigate the adhesion of polyurethane composite in-mold coated with vinyl ester by in-mold coating process, which include investigation the optimum processing temperature and formula polyurethane composite for in-mold coating process. The results show that the optimum processing temperature is 60 °C while the optimum polyurethane composite formulation consists of polyurethane matrix at density of 1.0 g/cm^3 which containing 30 % glass fiber. Subsequently, the optimum polyurethane composite by conventional process and by in-mold coating process have been analyzed via contact angle, ATR- FTIR analysis and roughness surface. The contact angle result exhibits that the contact angle of polyurethane composite in-mold coated give the lower contact angle value than conventional polyurethane composite, which relates to increase work of adhesion. Furthermore, the vinyl ester treatment modifies the polyurethane surface by creating polar moieties (C=O, C-O) which contributes to enhance wettability and increase adhesion properties. In addition, the surface roughness of polyurethane composite in-mold coated is rougher than conventional polyurethane composite, which the higher surface roughness attributes to better mechanical interlocking at the interface.

Afterwards, the adhesion of polyurethane composite by conventional process and by in-mold coating process /top coat (PLANITO#250 (2-component 2C1B) have been evaluated by cross cut and pull off measurement. The cross cut result shows that the adhesion between top coat and conventional polyurethane composite is poor. On the other hand, the adhesion between top coat and polyurethane composite in-mold coated is very good. The result of pull off test indicates that adhesion strength between polyurethane composite and top coat can be improve by treating polyurethane composite with vinyl ester by in-mold coating process, which increases 53.41%. In

addition, from ATR- FTIR analysis, it is proposed that some of amide groups of polyurethane are attached on fracture of peeled IMC coating film, while fracture of peeled PUCS coating film disappears, implying vinylester can be improve adhesion between polyurethane composite and PLANITO#250.

From a combination of all the studied carried out, it seems that the adhesion of polyurethane composite in-mold coated is better than polyurethane composite by conventional process. Finally, it may be concluded that polyurethane composite in-mold coated with vinyl ester has the potential to apply for improving interfacial adhesion between polyurethane composite and PLANITO#250.

5.2 Suggestions

Although this work was finished, it was only the first step of the study polyurethane composite in-mold coated vinyl ester by using in-mold coating process. There are some suggestions to this work to improve some point as follow:

1. The other type of glass fiber reinforcements such as A, S and ECR or glass fiber mat or natural fiber should be investigated.

2. The other primer type for using in in-mold coating such as PLANITTO#543 CONDUCTIVE PRIMER. (Chlorinated poly propylene/Excellent conductivity, Good adhesion on PP) and DELICON SURFACERMD200LB. (Polyester/ Melamine /Low temperature baking) should be test.

3. Using film insert provides a class A surface part. Films such as polyvinalinedifloride /acrylic, polyester, ionomer, and ASA have been used.

4. The viscosity effect of the vinyl ester should be investigated because it may be affect on adhesion property.

REFERENCES

[1] Christopher W. Macosko, **Rim: Fundamentals of Reaction Injection Molding**, Hanser, 1989

[2] George Woods. **The ICI Polyurethane Book.** 2nd ed", 1990

[3] Zuyev, K.S., Processing studies in reactive in-mold coating for thermoplastic substrate, Ph.D. Dissertation, the Ohio State University, 2004

[4] Chen, Xu, Mathematical Modeling of the In-Mold Coating Process for Injection Molded Thermoplastic Parts, Ph.D. Dissertation, the Ohio State University, 2004

[5] Gunter Oertel. **Polyurethane Handbook.**, Hanser /Gardner Publications, 1993

[6] Lardrock.H .a .**Handbook of Plastic Foams Types, Properties Manufacture and Applications**. ,United States of America by Noycs ,

[7] B. Remillard,T. Vu-Khanh, and B. Fisa* "Reaction Injection Molding of Mica Reinforced Polyurethane" **Polymer Composites,** Vol. 7,1986, pp 395-403

[8] F.R. Jones. **Hand book of Polymer – Fibre Composite**. 1st ed", 1994

[9] Daniel Klemper and Kurt C.Frish, **Hand book of polymeric Foams and Foam Technology.** Hanser, 1991

[10] Ling Li, Xiudong Sun, and L. James Lee. "Low Temperature Cure of Vinyl Ester Resins." **Polym,Eng. Sci.** , Vol. 39,1999. pp. 646-661

[11] Posen Chiu. "In-Mold Coating of Composites Manufactured with the Resin Infusion between Double Flexible Tooling Process by Means of Co-Infusion" M.S. Project, the Florida state University College of Engineering, 2004

[12] Kanthamas Thaworn "Study and development of EVA-based encapsulant for solar-cell", King Mongkut's Institute of Technology Ladkrabang 2007.

[13] Specialchem4polymers, "Adhesion Theory" [Online]. Available: http://www.specialchem4adhesives.com/resources/adhesionguide/

REFERENCES (CONT.)

[14] B. Stuart., Infrared Spectroscopy : Fundamentals and Applications, John Wiley and sons Ltd, 2004 pp.57-58

[15] M. R. Kamal,* P. Singh, and Q. Samak. "Microstructure and Mechanical Behavior of Reinforced Reaction Injection Molded (RRIM) Polyurethane." **Polym, Eng. Sci**,Vol. 27, 1987. pp. 1258-1264

[16] S.H.kim, H.C. Park, H.M. Jeong and B.K.Kim "Glass fiber reinforced rigid polyurethane foams." **Journal of Materials Science**, Vol. 45, 2010. pp 2675–2680

[17] Takemori "Towards an Understanding of the Heat Distortion Temperature of Thermoplastics." **Polym, Eng. Sci**, Vol 19, 1979. pp. 1104-1109

[18] D.W. Hatchett, D.W., Kinyanjui, J.M and Sapochak, L. "FTIR Analysis of Chemical Gradients in Thermally Processed Molded Polyurethane Foam." **Journal of Cellular Plastic**.Vol. 43, 2007. pp. 183-195

[19] Esmaeilnezhad E, Rezaei* M, and Razavi M K. "The Effect of Alternative Blowing Agent on Microstructure and Mechanical Characteristics of Rigid Polyurethane Foam." **Iranian Polymer Journal**. Vol 18, 2009. pp. 569-579

[20] Z G Yang, B Zhao, S L Qin, Z F Hu, Z K Jin and J H Wang. "Study on the Mechanical Properties of Hybrid Reinforced Rigid Polyurethane Composite Foam." **Journal of Applied Polymer Science.** Vol. 92, 2004. pp. 1493-1500

[21] S. Mojtaba Mirabedini, Hamid Rahimi, Sh. Hamedifar and S. Mohsen Mohseni. "Microwave Irradiation of Polypropylene surface: a study on wettability and adhesion." **Journal of Adhesion and Adhesive**, Vol. 24, 2004. pp. 163-170

[22] A. Shojaei, R. Fathi, N. Sheikh. "Adhesion modification of polyethylenes for metallization using radiation-induced grafting of vinyl monomers." **Surface and Coatings Technology**, Vol. 201, 2007. pp. 7519-7529.

REFERENCES (CONT.)

[23] D Jackovich, B O'Toole, M C Hawkins and L Sapochak. "Temperature and Mold Size Effects on Physical and Mechanical Properties of a Polyurethane Foam." **Journal of Cellular Plastics**, Vol. 41, 2005. pp. 153–168

[24] R. B. Mohan, B.J. O'Toole, J.Malipica, D.W. Hatchett, G. Kodippili and J.M. Kinyanjul. " Effect of Processing Temperaure on ReCrete Polyurethane Foam." **Journal of Cellular Plastic**.Vol. 44, 2008. pp. 327-345

[25] H.Lim, S.H.kim and B.K.Kim. "Effect of silicon surfactant in rigid polyurethane foam." **eXPRESS Polyner Letters**, Vol.2, 2008.pp.192-100

[26] W. Rungseesantivanon, T. Yamwong, B. Hararak and D.Thanomjitr, **Development of Composite Processing for Automotive Parts**, National metal and materials technology center, Plastics Tech Lab, Thailand, 2006

[27] M. Thirumal, Dipak Khastgir, Nikhil K. Singha, B. S. Manjunath and Y. P. Naik. "Effect of Foam Density on the Properties of Water Blown Rigid Polyurethane Foam." **Journal of Applied Polymer Science**, Vol. 108, 2008. pp. 1810–1817

[28] M. C. Silva, J. A. Takahashi, D. Chaussy, M. N. Blegacem and G. G. Silva. "Composite of Rigid Polyurethane Foam and Cellulose Fiber Residue." **Journal of Applied Polymer Science**, Vol. 117, 2010. pp. 3665–3672

[29] Shang-Han Wu, Feng-Yih Wang, Chen-Chi. M. Ma), Wen-Chi Chang, Chun-Ting Kuo, Hsu-Chiang Kuan, Wei-Jen Chen. "Mechanical, thermal and morphological properties of glass fiber and carbon fiber reinforced polyamide-6 and polyamide-6rclay nanocomposites." **Materials Letters**, 49, 2001. pp. 327–333

[30] Y. Zhang and D. J. Hourston. "Rigid Interpenetrating Polymer Network Foams Prepared from Rosin-Based Polyurethane and an Epoxy Resin." **Journal of Applied Polymer Science**, Vol. 69, 1998. pp. 271–281

[31] Saran Poshyachida, The Fracture properties of highly–crosslinked polyurethane composites, M.S. Dissertation, the University of Manchester 1988

REFERENCES (CONT.)

[32] 1995 C.D. Snyder, "Materials for Reaction Injection Molding (RIM) Processing", Composites 2001 Convention and Trade Show, 3-6 October (2001).

[33] Herman F.Mark, Norbert M. Bikales and Charles G. Overberger, **Encyclopedia of polymer science and engineering**,2nd ed., Vol.3 Wiley-Interscience,New York, 1985. pp. 476-518

[34] J R Svendsen, G M Kontogeorgis, S kiil, C E Weinell and M GrΦnlund. "Adhesion between coating layers based on epoxy and silicone." **Journal of Colloid and Interface Science**, Vol. 316, 2007. pp. 678-686

[35] J. Van Den Brand, S. Van Gils, P.C.J. Beentjes, H. Terryn, V. Sivel and J.H.W. De Wit. "Improving the adhesion between epoxy coatings and aluminium substrates." **Progress in Organic Coatings**, Vol. 51, 2004. pp. 339–350

[36] J.K.F Tait, G.Davies, R. McIntyre and J.Yarwood. "FTIR-ATR studies of interfacial interactions in epoxy resin/polymer laminate structures." **Vibrational spectroscopy**, Vol.15, 1997. pp. 79–89

[37] L. H. Fan, C.P. HU and S.K. Ying. "Mechanical Properties of Hand-Cast and Reaction Injection Molded Polyurethane and Vinyl ester Resin Interpenetrating Polymer Networks." **Polym, Eng. Sci**, Vol 37, 1997. pp. 338-345

[38] N. V. Bhat and D.J. Upadhyay. "Plasma-Induced Surface Modification and Adhesion Enhancement of Polypropylene Surface." **Journal of Applied Polymer Science**, Vol. 86, 2002. pp. 925–936

[39] Long Lin. "Measurement of the Adhesion Strength of paint" Department of Colour & Polymer Chemistry. University of Leeds.

[40] "Deflection Temperature Testing of Plastics" [Online]. Available: http://www.matweb.com/reference/deflection-temperature.aspx

[41] Nair, B. R.; Gregoriou, V. G.; Hammond, P. T. "FT-IR studies of side chain liquid crystalline thermoplastic elastomers". **Polymer 2000**, 41, pp. 2961-2970.

Appendices

Appendix A

Determining the Composition of Polyurethane Composites

The calculation of reactants and glass fiber content used in preparing unfilled polyurethanes and polyurethane composites as follows:

1. Unfilled polyurethane

For example of unfilled polyurethane density is 0.8 g/cm^3 (0.8PU) after demold

1.1 Calculate the volume of the mold (V)

$$V = (\text{width}) \times (\text{length}) \times (\text{depth})$$

$$= (297\text{mm}) \times (420\text{mm}) \times (5\text{mm})$$

$$= (29.7\text{cm}) \times (42.0\text{cm}) \times (0.5\text{cm})$$

$$= 624\ \text{cm}^3$$

1.2 Calculate the weight of unfilled polyurethane

$$M_{PU} = \rho_{PU} \times V$$

$$= (0.8\ \text{g/cm}^3) \times (624\ \text{cm}^3)$$

$$= 499.20\ \text{g}$$

1.3 Calculate the weight of polyol and isocyanate

The raito of polyol and isocyanate is 1:2 by weight

Therefore, the raito of polyol and polyurethane is 1:3 by weight

The weight of polyol is calculated as follow:

$$M_{Polyol} = (1/3) \times M_{PU}$$

$$= (1/3) \times (499.20\ \text{g})$$

$$= 166.40\ \text{g}$$

The weight of isocyanate is calculated as follow:

$$M_{isocyanate} = (2/3) \times M_{PU}$$

$$= (2/3) \times (499.20\ g)$$

$$= 332.80\ g$$

2. Polyurethane composite

For example of polyurethane with relative polyurethane density is 0.8 g/cm^3 and 10 % glass fiber content (0.8PU10%GF)

2.1 Calculate the volume of the mold (V)

$$V = (width) \times (length) \times (depth)$$

$$= (297mm) \times (420mm) \times (5mm)$$

$$= (29.7cm) \times (42.0cm) \times (0.5cm)$$

$$= 624\ cm^3$$

1.4 Calculate the weight of mold at density is 0.8 g/cm^3

$$M_{mold} = \rho_{PU} \times V$$

$$= (0.8\ g/cm^3) \times (624\ cm^3)$$

$$= 499.20\ g$$

1.5 Calculate the weight of 10 % glass fiber content

$$M_{GF} = M_{mold} \times (\%\ glass\ fiber\ content)/\ 100$$

$$= 499.20 \times 10/100\ g$$

$$= 49.92\ g$$

While $V_{GF} = M_{GF}/\rho_{GF}$

$$= 49.92\ /2.5\ \ cm^3$$

$$= 19.97\ cm^3$$

1.6 Calculate the weight of polyol and isocyanate by free volume of mold

Free volume mold = $V_{mold} - V_{GF}$

$= 624 - 19.97\ cm^3$

$= 604.03\ cm^3$

$M_{PU} = \rho_{PU}$ x free volume mold

$= (0.8\ g/cm^3) \times (604.03\ cm^3)$

$= 483.23\ g$

The raito of polyol and isocyanate is 1:2 by weight

Therefore, the raito of polyol and polyurethane is 1:3 by weight

The weight of polyol is calculated as follow:

$M_{Polyol} = (1/3) \times M_{PU}$

$= (1/3) \times (483.23\ g)$

$= 161.08\ g$

The weight of isocyanate is calculated as follow:

$M_{isocyanate} = (2/3) \times M_{PU}$

$= (2/3) \times (483.23\ g)$

$= 322.15\ g$

Table A-1 The composition of polyurethane composites table

No.	Sample name	Polyol (g)	Isocyanate (g)	Glass fiber (g)
1	0.8PU	166.40	332.80	0
2	0.8PU10%GF	161.08	322.15	49.92
3	0.8PU20%GF	155.75	311.50	99.84
4	0.8PU30%GF	150.43	300.85	149.76
5	0.8PU40%GF	145.10	290.20	199.68
6	0.9PU	187.20	374.40	0
7	0.9PU10%GF	180.46	360.92	56.16
8	0.9PU20%GF	173.72	347.44	112.32
9	0.9PU30%GF	166.98	333.96	168.48
10	0.9PU40%GF	160.24	320.49	224.64
11	1.0PU	208.00	416.00	0
12	1.0PU10%GF	199.68	399.36	62.4
13	1.0PU20%GF	191.36	382.72	124.8
14	1.0PU30%GF	183.04	366.08	187.2
15	1.0PU40%GF	174.72	349.44	249.6

Appendix B

Polyurethane Properties

Bubble Size Distribution of Polyurethane Foam

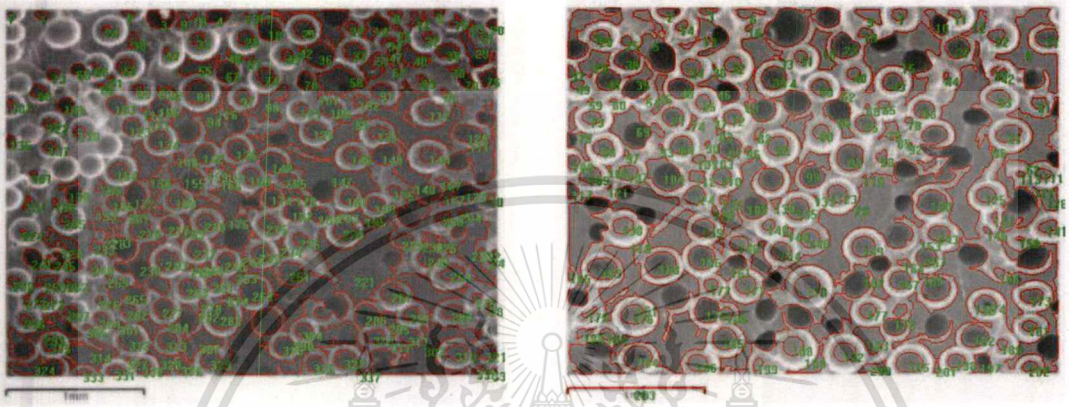

a) mold temperature 40 °C

b) mold temperature 50 °C

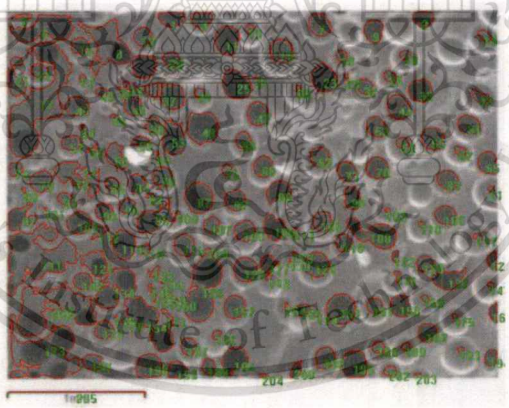

c) mold temperature 60 °C

Figure B.1 SEM micrographs analyzed with image analysis program of polyurethane prepared at different processing temperature

Calculating the number of cell and expansion ratio

The number of cells was calculated as follow

$$n = \left(\frac{n_b}{l^2}\right)^{\frac{3}{2}} x10^5 x\varphi$$

While

$$\varphi = \frac{\rho_p}{\rho_f}$$

n = The number of cell per cubic centimetre

n_b = The number of cell in area lxl

l = The length (mm)

φ = Expansion ratio

ρ_p = The polyurethane density before expansion (g/cm^3)

ρ_f = The polyurethane density after expansion (g/cm^3)

For example of the number of cell and expansion ratio of polyurethane processed at 40 °C that the cell size range of 0 -20 μm is shown in the next.

- Expansion ratio of polyurethane foam

$$\varphi = \frac{\left(\frac{1}{3}x1.10\right)+\left(\frac{2}{3}x1.23\right)}{0.98}$$

φ = 1.20

- The number of cell per cubic centimetre

$$n = \left(\frac{13}{2.5^2}\right)^{\frac{3}{2}} x10^{3} x1.20$$

$n = 3.60.x10^3$ cells per cubic centimetre

Table B.1 The number of cell size of polyurethane prepared at different processing temperature

Cell size (μm)	Mold Temperature (°C)					
	40		50		60	
	Nunber of cell in area (mm^2)	Nunber of cell x 10^3 per cm^3	Nunber of cell in area (mm^2)	Nunber of cell x 10^3 per cm^3	Nunber of cell in area (mm^2)	Nunber of cell x 10^3 per cm^3
0-20	13	3.60	7	1.21	6	0.39
21-40	24	9.03	17	4.58	21	1.36
41-60	60	35.69	35	13.52	29	1.87
61-80	88	63.40	42	17.77	20	1.29
81-100	7	1.42	14	3.42	7	0.45
101-120	1	0.08	4	0.52	2	0.13
121-140	2	0.22	0	0.00	1	0.06
141-160	0	0.00	0	0.00	1	0.06
161-180	1	0.08	1	0.07	0	0.00
181-200	2	0.22	0	0.00	0	0.00
Ave	65.38	40.60	61.65	31.60	59.25	3.83
SD	37.58	17.69	32.47	12.08	34.75	2.25

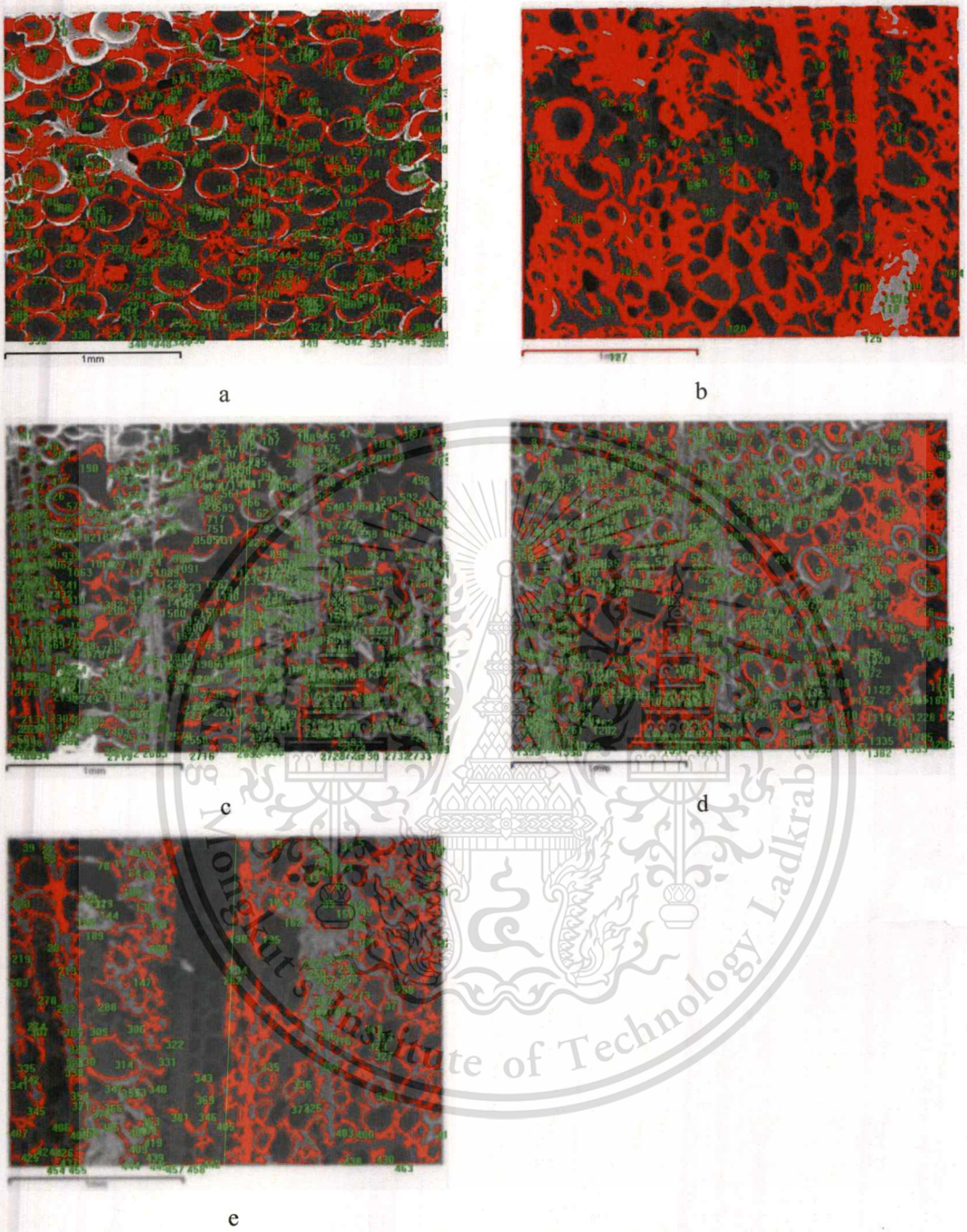

Figure B.2 SEM micrographs analyzed with image analysis program of polyurethane density 0.8g/cm^3 with % glass fiber content: (a) 0%, (b) 10%, (c) 20%, (d) 30%, (e) 40 %

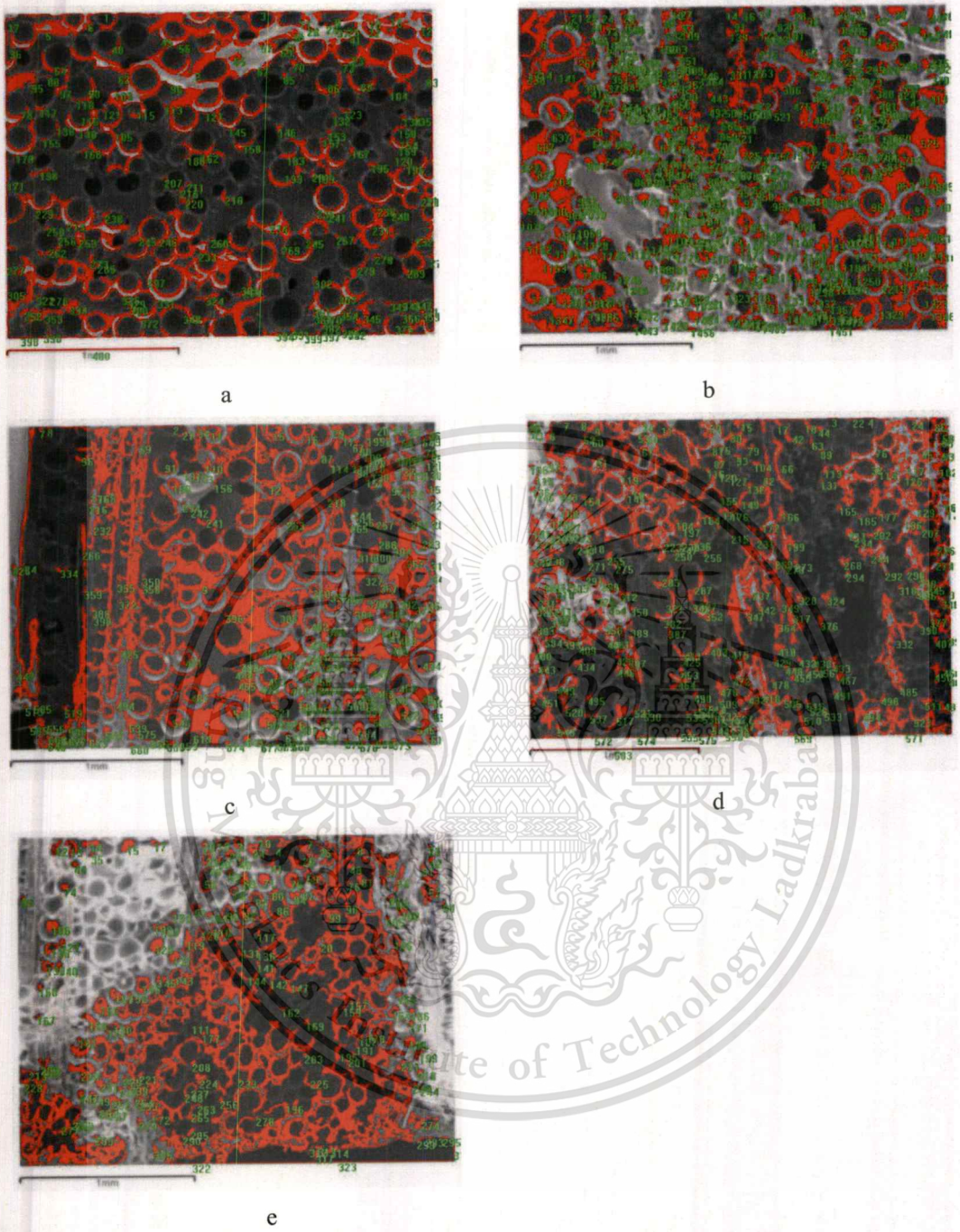

Figure B.3 SEM micrographs analyzed with image analysis program of polyurethane density 0.9 g/cm^3 with % glass fiber content: (a) 0%, (b) 10%, (c) 20%, (d) 30%, (e) 40 %

Figure B.4 SEM micrographs analyzed with image analysis program of polyurethane density 1.0 g/cm^3 with % glass fiber content: (a) 0%, (b) 10%, (c) 20%, (d) 30%, (e) 40 %

Table B.2 The number of cell size of polyurethane density 0.8 g/cm^3 with % glass fiber content: 0-40% (The number of cell size /mm^2)

Cell size (μm)	% Glass fiber content				
	0	10	20	30	40
0-20	237	19	265	167	48
21-40	185	36	94	135	67
41-60	31	18	13	96	40
61-80	18	10	7	40	6
81-100	10	1	2	17	2
101-120	6	5	1	2	0
121-140	6	5	0	0	0
141-160	1	0	0	2	0
161-180	1	2	0	1	0
181-200	1	0	0	0	0
Ave	41.00	57.60	34.80	39	35.32
SD	46.18	13.48	45.37	39.67	22.14

Table B.3 The number of cell size of polyurethane density 0.8 g/cm^3 with % glass fiber content: 0-40% (The number of cell size x 10^3 /cm^3)

Cell size (μm)	% Glass fiber content				
	0	10	20	30	40
0-20	369.22	8.09	411.28	206.17	31.71
21-40	254.69	21.72	86.58	148.85	52.34
41-60	17.62	7.38	4.56	89.47	24.41
61-80	7.57	3.23	1.95	24.41	1.40
81-100	3.31	0.14	0.27	6.47	0.27
101-120	1.42	1.14	0.10	0.27	0.00
121-140	1.42	1.14	0.00	0.00	0.00
141-160	0.15	0.01	0.03	0.35	0.00
161-180	0.15	0.24	0.00	0.07	0.00
181-200	0.15	0.00	0.00	0.00	0.00
Ave	65.57	4.31	50.47	47.61	11.01
SD	132.74	6.82	129.61	75.01	18.65

Table B.4 The number of cell size of polyurethane density 0.9 g/cm^3 with % glass fiber content: 0-40% (The number of cell size /mm^2)

Cell size (μm)	% Glass fiber content				
	0	10	20	30	40
0-20	33	148	47	80	26
21-40	57	276	74	130	48
41-60	14	71	37	42	26
61-80	7	39	19	12	7
81-100	7	7	3	6	7
101-120	2	2	1	2	0
121-140	1	0	1	3	0
141-160	0	2	0	0	1
161-180	0	0	0	0	0
181-200	1	1	0	0	0
Ave	49.85	37.35	41.63	41.67	46.29
SD	16.30	49.25	21.90	30.22	15.81

Table B.5 The number of cell size of polyurethane density 0.9 g/cm^3 with % glass fiber content: 0-40% (The number of cell size x 10^3 /cm^3)

Cell size (μm)	% Glass fiber content				
	0	10	20	30	40
0-20	18.18	171.42	30.30	67.83	12.94
21-40	40.55	438.39	61.20	141.21	32.03
41-60	5.12	56.52	21.85	25.88	12.94
61-80	1.63	23.12	7.90	4.11	1.77
81-100	1.77	1.77	0.49	1.40	1.77
101-120	0.27	0.27	0.10	0.27	0.00
121-140	0.10	0.00	0.10	0.50	0.00
141-160	0.00	0.27	0.00	0.00	0.10
161-180	0.00	0.00	0.00	0.00	0.00
181-200	0.10	0.10	0.00	0.00	0.00
Ave	6.77	69.18	12.19	24.12	6.15
SD	13.12	140.41	20.32	46.44	10.48

Table B.6 The number of cell size of polyurethane density 1.0 g/cm^3 with % glass fiber content: 0-40 % (The number of cell size /mm^2)

Cell size (μm)	% Glass fiber content				
	0	10	20	30	40
0-20	30	67	35	21	82
21-40	39	92	48	35	139
41-60	18	32	17	7	32
61-80	7	8	6	4	7
81-100	5	9	4	1	3
101-120	2	10	1	1	3
121-140	0	2	0	0	2
141-160	2	1	0	1	1
161-180	0	1	1	0	0
181-200	0	1	0	0	0
Ave	48.63	48.55	45.08	43.81	40.2
SD	13.91	23.48	15.61	12.21	31.17

Table B.7 The number of cell size of polyurethane density 1.0 g/cm^3 with % glass fiber content:

0-40 % (The number of cell size x 10^3 /cm^3)

Cell size (μm)	% Glass fiber content				
	0	10	20	30	40
0-20	15.98	52.16	19.37	9.36	70.71
21-40	23.23	83.49	31.71	19.75	156.07
41-60	7.28	17.00	6.47	1.77	17.26
61-80	1.77	2.29	1.40	0.76	1.77
81-100	1.10	2.70	0.86	0.10	0.50
101-120	0.27	3.12	0.10	0.10	0.50
121-140	0.00	0.27	0.00	0.00	0.27
141-160	0.27	0.10	0.00	0.10	0.10
161-180	0.00	0.10	0.10	0.00	0.00
181-200	0.00	0.10	0.00	0.00	0.00
Ave	4.99	16.13	6.00	3.19	24.72
SD	8.19	28.67	10.88	6.49	51.15

Contact angle measurement

Table B.8 Contact angles of polyurethane processed by ranging 40-80 °C.

Contact angle					
No.	Mold temp (°C)				
	40	50	60	70	80
1	125.5	106.3	86	88.9	90.1
2	119.1	95.7	84.5	81.9	86.3
3	104.4	99.2	87.9	83.8	90.1
4	95.6	113.1	85.9	89	87.8
5	98.8	93.8	85.1	85.5	86.9
Ave	109	102	86	86	88
SD	13	8	1	3	2

Work of adhesion

Table B.9 Work of adhesion of polyurethane processed by ranging 40-80 °C.

Work of adhesion (mJm^{-2})					
No.	Mold temp (°C)				
	40	50	60	70	80
1	125.5	106.3	86	88.9	90.1
2	119.1	95.7	84.5	81.9	86.3
3	104.4	99.2	87.9	83.8	90.1
4	95.6	113.1	85.9	89	87.8
5	98.8	93.8	85.1	85.5	86.9
Ave	109	102	86	86	88
SD	13	8	1	3	2

Density of Polyurethane and Polyurethane Composites

Table B.10 The density of polyurethane density 0.8 g/cm^3 with % glass fiber content: 0-40%

No	% Glass fiber content				
	0	10	20	30	40
1	0.79	0.79	0.82	0.81	0.90
2	0.75	0.76	0.74	0.85	0.89
3	0.78	0.75	0.86	0.82	0.85
4	0.75	0.78	0.78	0.84	0.89
5	0.70	0.77	0.80	0.83	0.92
Ave.	0.75	0.77	0.80	0.83	0.89
SD.	0.04	0.02	0.04	0.02	0.03

Table B.11 The density of polyurethane density 0.9 g/cm^3 with % glass fiber content: 0-40%

No	% Glass fiber content				
	0	10	20	30	40
1	0.86	0.86	0.90	0.92	0.94
2	0.81	0.87	0.91	0.90	0.99
3	0.86	0.83	0.90	0.94	0.94
4	0.87	0.86	0.93	0.91	0.92
5	0.86	0.86	0.91	0.95	0.96
Ave.	0.85	0.86	0.91	0.93	0.95
SD.	0.03	0.02	0.01	0.02	0.03

Table B.12 The density of polyurethane density 1.0 g/cm^3 with % glass fiber content: 0-40%

No	% Glass fiber content				
	0	10	20	30	40
1	0.97	1.00	0.99	1.07	1.13
2	0.96	0.98	1.00	1.15	1.10
3	0.96	1.00	0.99	1.08	1.19
4	0.96	0.97	1.03	1.05	1.09
5	0.94	0.93	0.99	1.09	1.15
Ave.	0.96	0.97	1.00	1.09	1.13
SD.	0.01	0.03	0.02	0.04	0.04

Mechanical properties of Polyurethane Foam

Table B.13 The flexural strength of polyurethane prepared at different processing temperature

Flexural strength			
No.	Mold temperature (°C)		
	40	50	60
1	43.49	46.65	62.68
2	43.4	47.2	62.25
3	46.17	49.37	60.35
4	49.17	46.94	61.08
5	43.47	47.58	59.96
Ave.	45.14	47.55	61.26
SD.	2.54	1.07	1.18

Table B.14 The flexural modulus of polyurethane prepared at different processing temperature

Flexural modulus			
No.	Mold temperature (°C)		
	40	50	60
1	1.33	1.39	2.11
2	1.32	1.43	2.07
3	1.51	1.49	1.99
4	1.37	1.43	2.00
5	1.31	1.44	1.96
Ave.	1.37	1.44	2.03
SD.	0.08	0.04	0.06

Thermal property of Polyurethane Foam

Table B.15 The heat distortion temperature of polyurethane prepared at different processing temperature

Heat distortion temperature			
No.	Mold temperature (°C)		
	40	50	60
1	61.1	65.5	67.2
2	61.2	65.9	66.9
3	62.8	65.6	67
4	61.2	65.4	65.9
5	59.8	65.5	67.1
Ave.	61.22	65.58	66.82
SD.	1.06	0.19	0.53

Table B.16 The heat distortion temperature of polyurethane composite prepared at polyurethane density 0.8 g/cm^3 with glass fiber content: 0-40%

Heat distortion temperature					
No.	% Glass fiber content				
	0	10	20	30	40
1	67.1	74	81	81.6	74.2
2	67.3	76.1	76.8	85	75.4
3	67.3	76.5	85.2	88.8	91.2
4	67.90	70.60	76.50	98.60	104.10
5	67.9	76.9	76.1	103.4	110.7
Ave.	67.50	74.82	79.12	91.48	91.12
SD.	0.33	2.34	3.52	8.24	14.73

Table B.17 The heat distortion temperature of polyurethane composite prepared at polyurethane density 0.9 g/cm^3 with glass fiber content: 0-40%

Heat distortion temperature					
No.	% Glass fiber content				
	0	10	20	30	40
1	68.5	73.9	78.3	87.2	141.6
2	68.6	73.9	81.6	101	100.7
3	69.80	74.80	84.80	103.50	184.90
4	70.10	76.80	87.30	114.30	158.70
5	70.20	77.60	88.60	142.60	118.60
Ave.	69.44	75.4	84.12	109.72	140.9
SD.	0.74	1.53	4.21	20.76	33.04

Table B.18 The heat distortion temperature of polyurethane composite prepared at polyurethane density 1.0 g/cm^3 with glass fiber content: 0-40%

Heat distortion temperature					
No.	% Glass fiber content				
	0	10	20	30	40
1	73.3	74.6	88.7	99.3	236
2	73.1	75.5	92	99.8	237.1
3	72.50	76.70	96.60	104.10	241.90
4	73.10	79.60	99.50	125.10	238.40
5	73.30	88.60	100.50	140.70	241.80
Ave.	73.06	79.00	95.46	113.8	239.04
SD.	0.29	5.09	5.02	18.38	2.70

Contact angle measurement

Table B.19 Contact angles of polyurethane composite prepared conventional process and in-mold coating process.

No.	in-mold coating process	conventional process
1	79.19	99.22
2	76.1	101.04
3	84.22	99.01
4	87.65	90.47
5	90.26	92.52
Ave	83	96
SD	6	5

Work of adhesion

Table B.20 Work of adhesion of polyurethane composite prepared conventional process and in-mold coating process.

No.	in-mold coating process	conventional process
1	86.45	61.14
2	90.29	58.86
3	80.13	61.4
4	75.79	72.2
5	72.43	69.6
Ave	81	65
SD	7	6

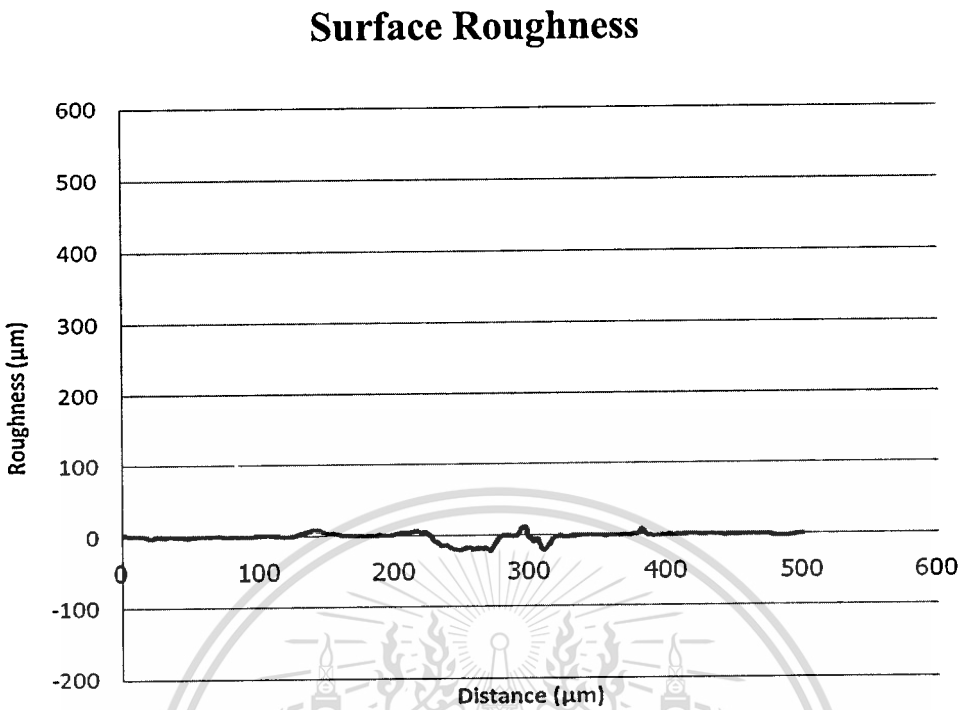

Figure B.5 Roughness surface of sample PUCS 1

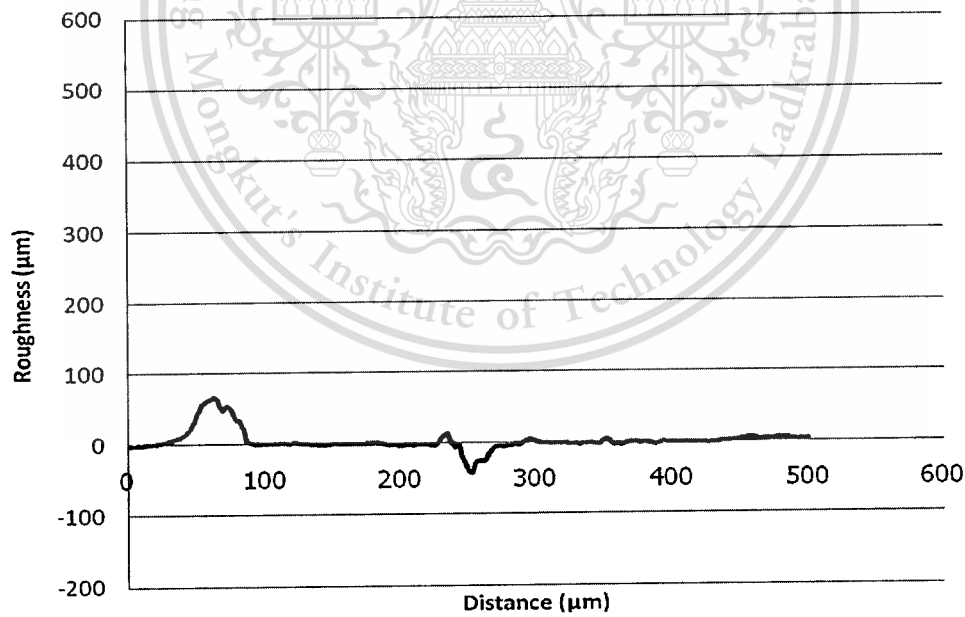

Figure B.6 Roughness surface of sample PUCS 2

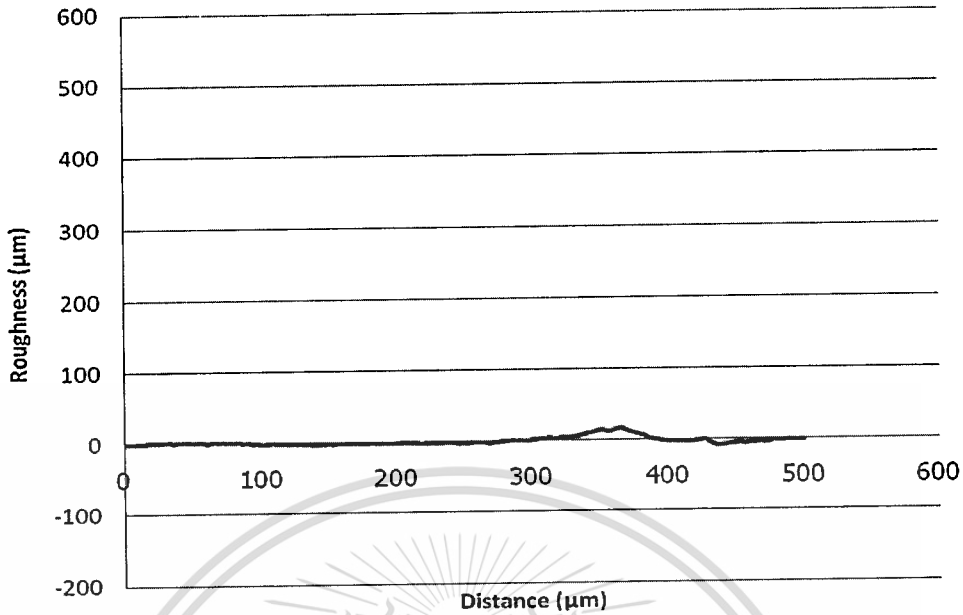

Figure B.7 Roughness surface of sample PUCS 3

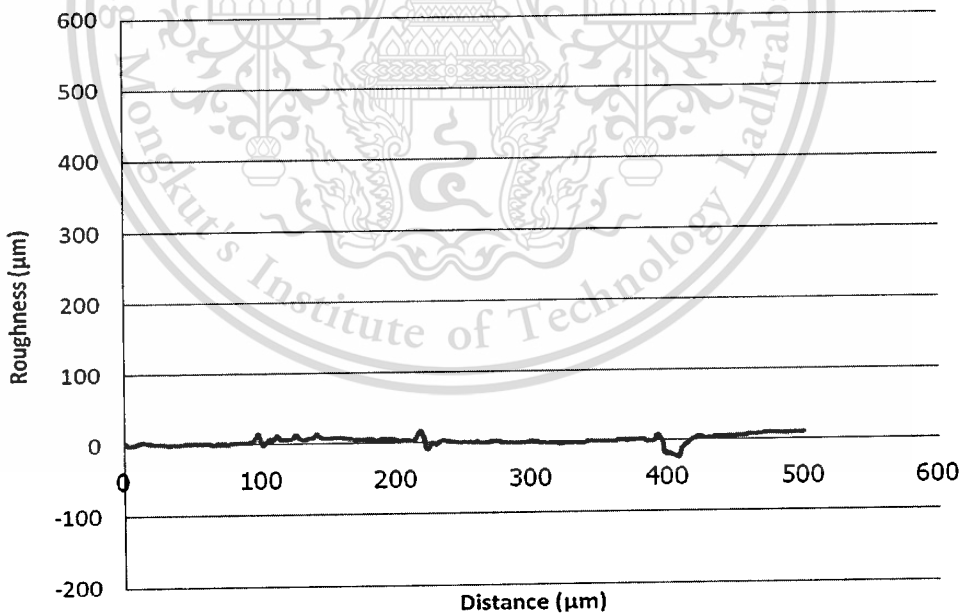

Figure B.8 Roughness surface of sample PUCS 4

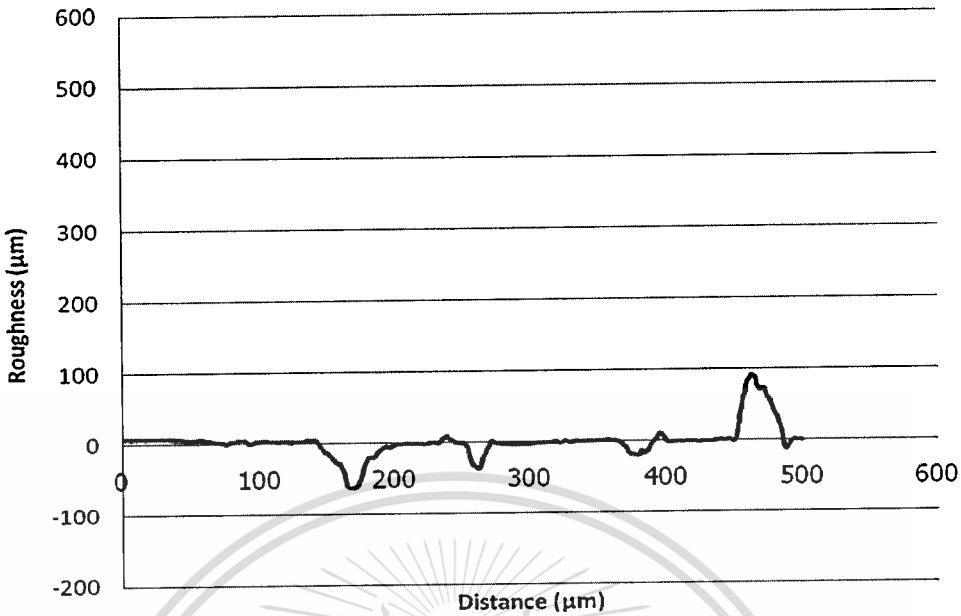

Figure B.9 Roughness surface of sample PUCS 5

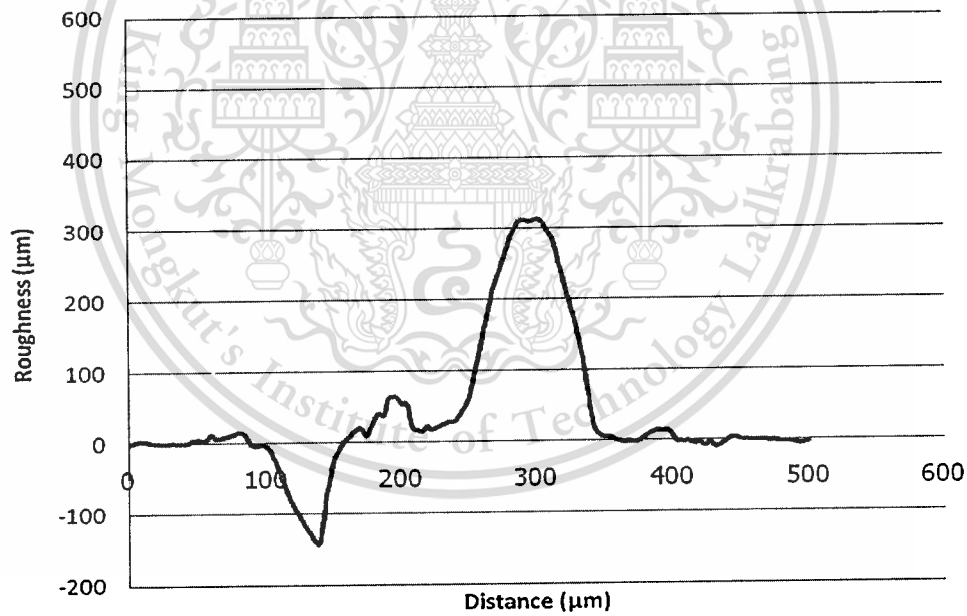

Figure B.10 Roughness surface of sample IMC 1

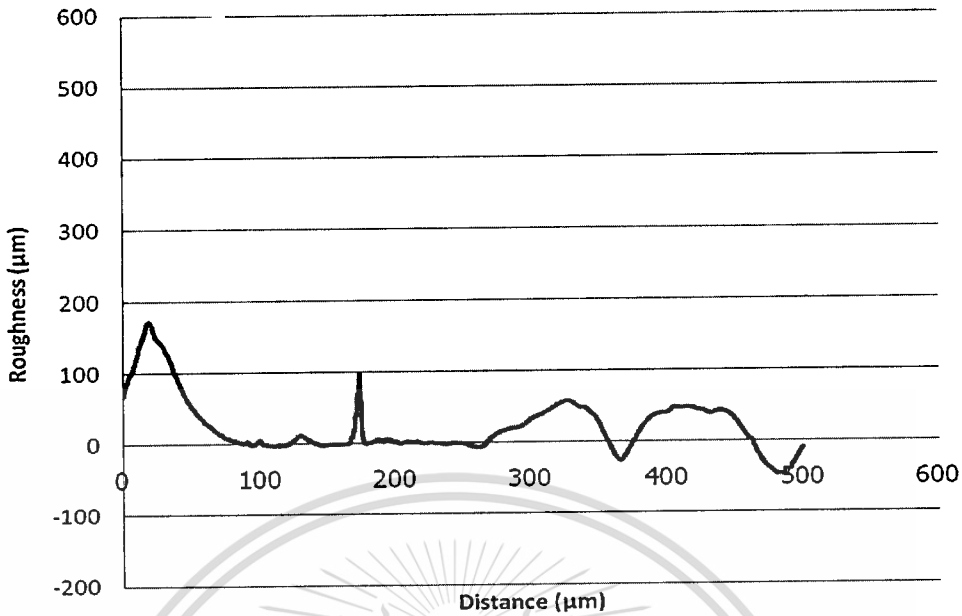

Figure B.11 Roughness surface of sample IMC 2

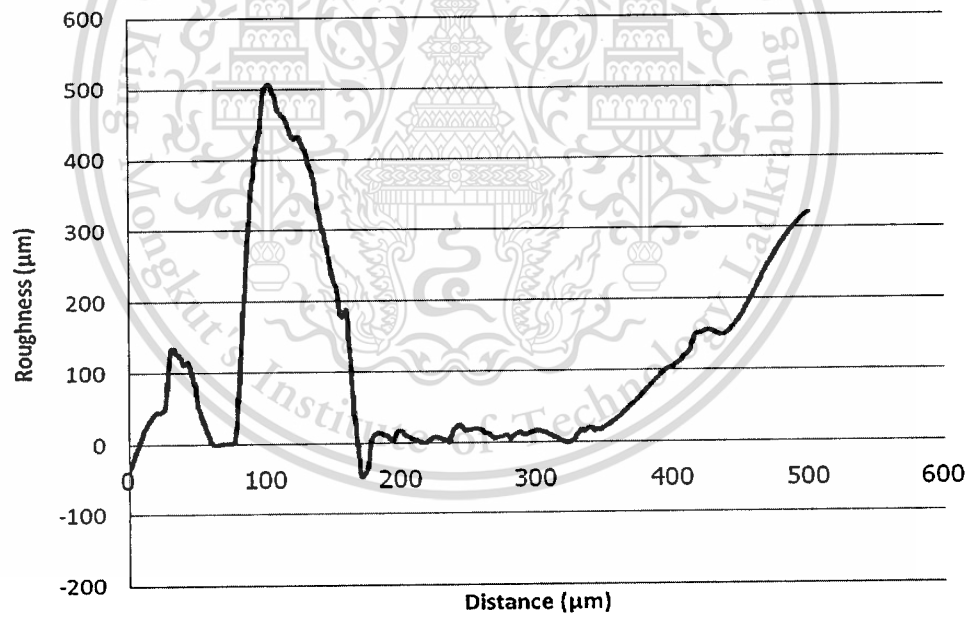

Figure B.12 Roughness surface of sample IMC 3

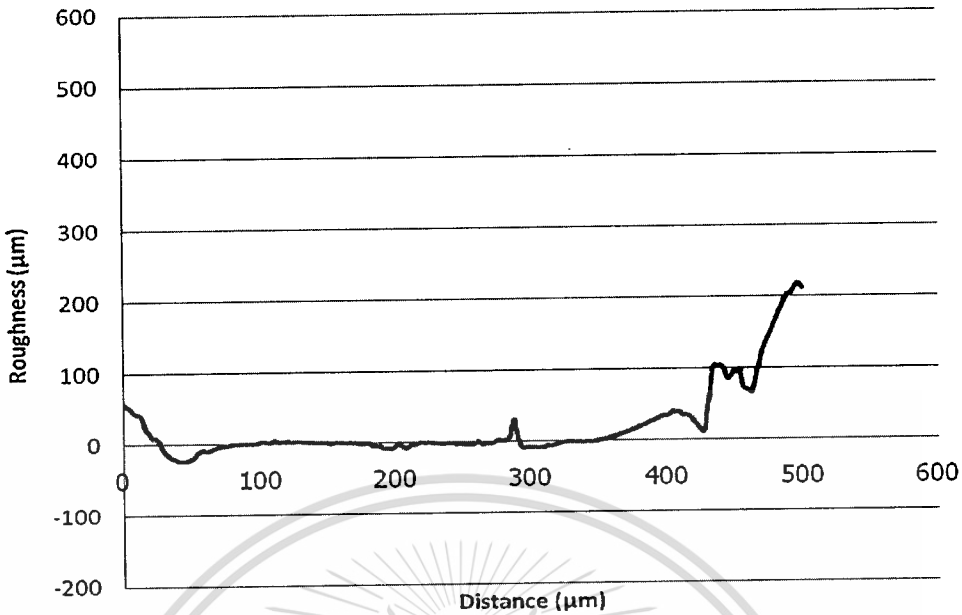

Figure B.13 Roughness surface of sample IMC 4

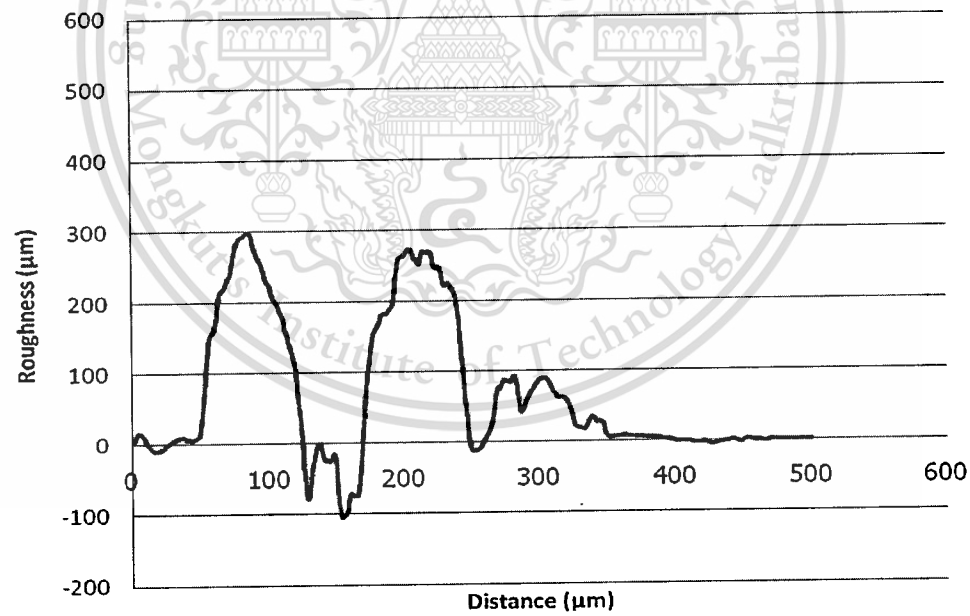

Figure B.14 Roughness surface of sample IMC 5

Table B.21 Surface roughness of polyurethane composite prepared conventional process and in-mold coating process.

No	in-mold coating process		conventional process	
	R_a	R_q	R_a	R_q
1	74.69	10.32	4.20	6.24
2	30.53	36.87	10.07	14.83
3	112.05	139.17	3.08	4.47
4	27.90	39.02	3.62	5.11
5	4.33	5.05	13.17	20.37
Ave	49.90	46.09	6.83	10.20
SD	43.05	54.23	4.53	7.06

Adhesion Strength

Table B.22 Adhesion strength of polyurethane composite prepared conventional process and in-mold coating process.

No.	in-mold coating process	conventional process
1	1.22	1.32
2	1.31	0.88
3	1.86	0.55
4	0.68	0.82
5	1.68	0.81
Ave	1.35	0.88
SD	0.46	0.28

FTIR (Comparison of Band Ratio of PUCS and IMC)

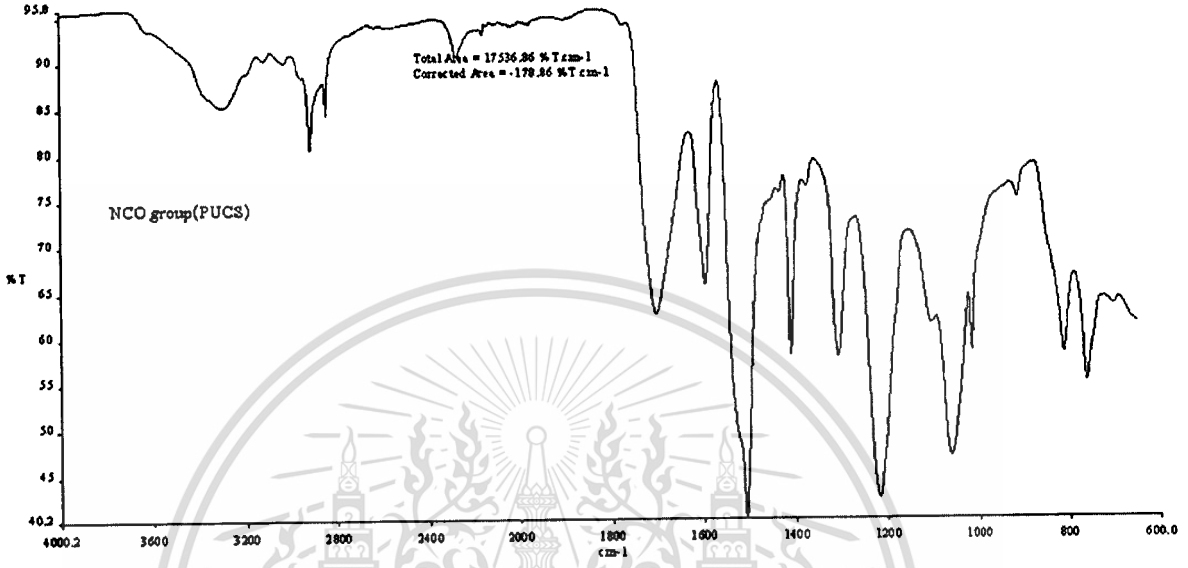

Figure B.15 Area of NCO group of PUCS FT-IR spectrum

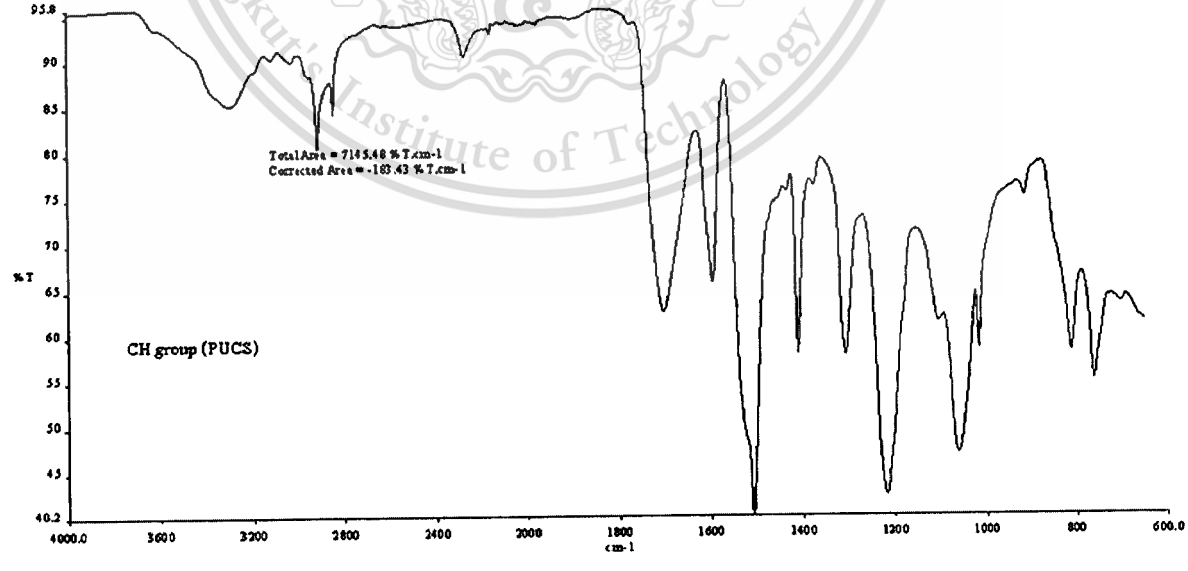

Figure B.16 Area of CH group of PUCS FT-IR spectrum

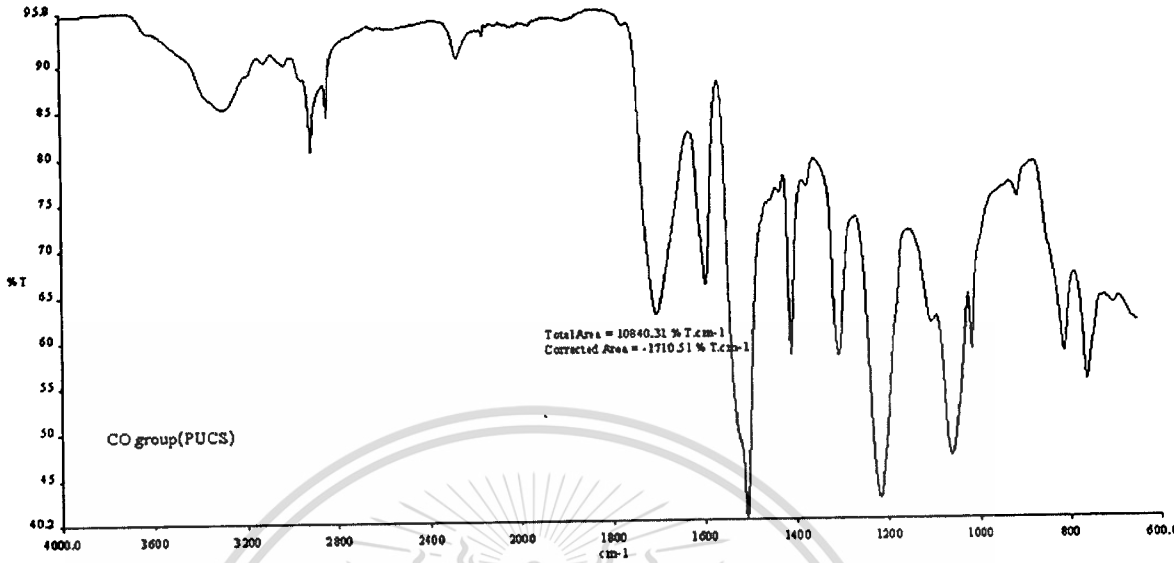

Figure B.17 Area of CO group of PUCS FT-IR spectrum

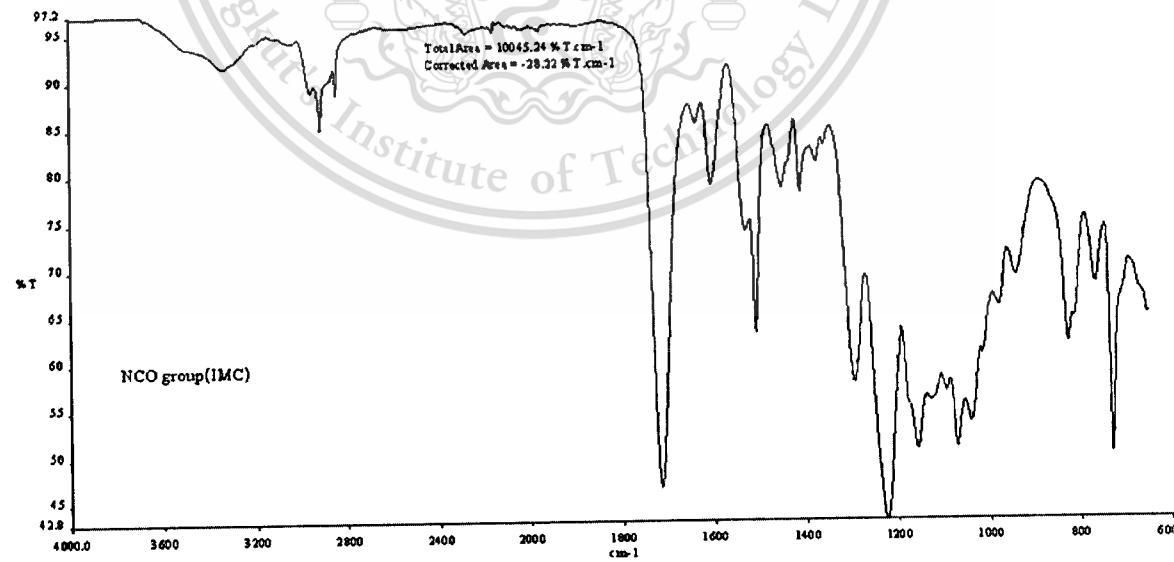

Figure B.18 Area of NCO group of IMC FT-IR spectrum

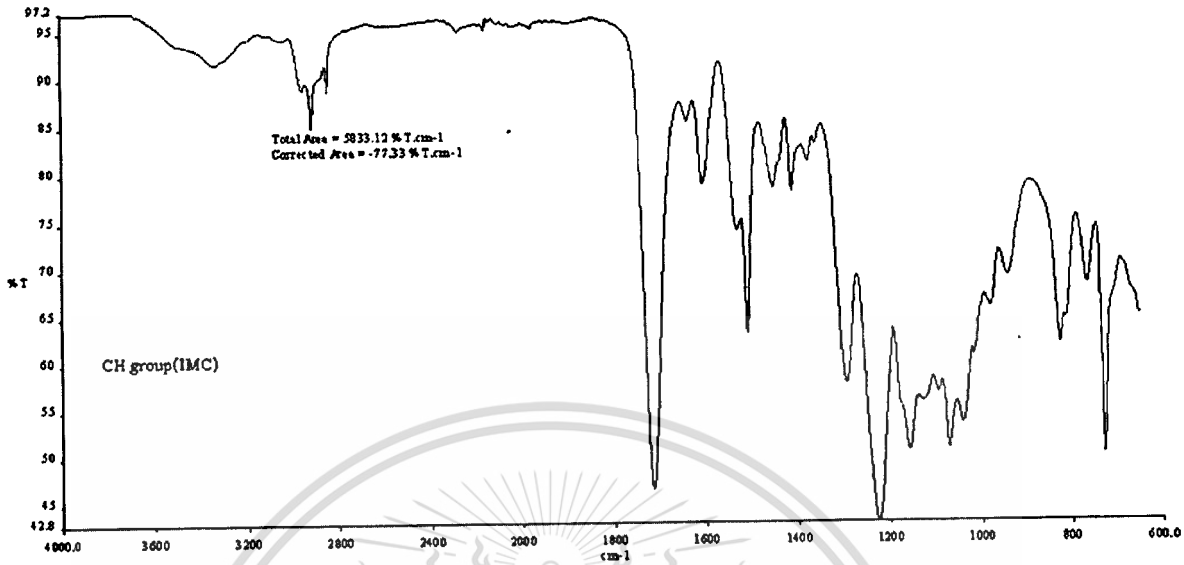

Figure B.19 Area of CH group of IMC FT-IR spectrum

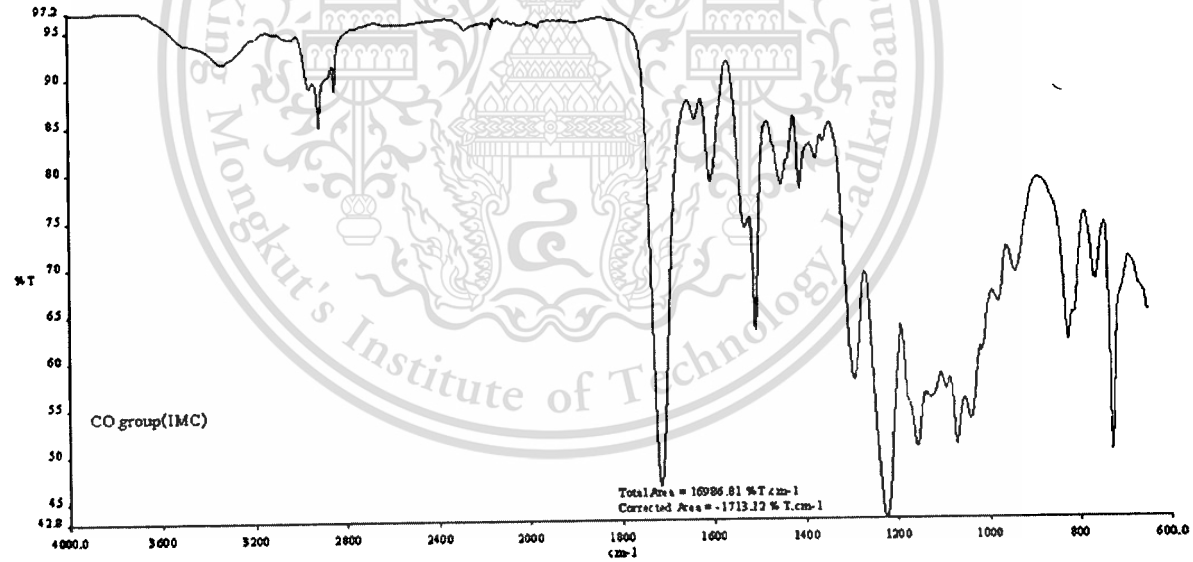

Figure B.20 Area of CO group of IMC FT-IR spectrum

BIOGRAPHY

Name:	Miss Natcha Prakymoramas
Date of Birth:	January 1, 1984
Place of Birth:	Bangkok, Thailand
Education:	
2000-2004	B. Eng. in Department of Tool and Material Engineering,, King Mongkut's University of Technology Thonburi (KMUTT)
Scholarships:	
2007-2009	Full scholarship for study in the master degree from National Science and Technology Development Agency (NSTDA)
Work experience:	
2005-2011	National Metal and Materials Technology Center